CONTRIBUTION TO LASER MILLING PROCESS PARAMETERS SELECTION FOR PROCESS PLANNING OPERATIONS

Daniel TEIXIDOR EZPELETA

Dipòsit legal: Gi. 1532-2013
http://hdl.handle.net/10803/124506

Universitat de Girona

DOCTORAL THESIS

Contribution to laser milling process parameters selection for process planning operations

Daniel Teixidor Ezpeleta

2013

Universitat de Girona

DOCTORAL THESIS

Contribution to laser milling process parameters selection for process planning operations

Daniel Teixidor Ezpeleta

2013

Programa de turisme, dret i empresa

Supervisors: Joaquim de Ciurana i Gay

Inés Ferrer Real

A thesis submitted in partial fulfillment of the requirements for the degree of doctor by the University of Girona

als que m'estimo

Acknowledgements

First of all, I express my sincere gratitude to my supervisors, Quim de Ciurana and Inés Ferrer for his enthusiastic interest, encouragement and bright guidance in this work. Gràcies Quim per tots aquests anys, per tantes converes sobre la feina i tantes altres coses, saps que ets més que un jefe.

I also, wish to thank ASCAMM Technology Centre for their extensive support: Laura Puigpinós, Xavier Plantà, Agustí Chico, Joan Guasch i Benjamin Cavallini. Gràcies per facilitar-me accés a les instal·lacions i a la màquina i ajudar-me amb moltes de les experimentacions. Gràcies per la beca de recerca que m'ha permès treballar amb vosaltres aquests quatre anys i per l'oportunitat de treballar en d'altres projectes com el MADE4U. Gràcies sobretot a en Pol Paluzie, per les estones invertides davant la màquina.

Many thanks to Tugrul Özel for his guidance during my stage in New Jersey. Thank you for make me feel like home, for the conversations about laser and for the essential contributions in this thesis.

I am also grateful to Ciro Rodríguez for hosting me in Monterrey. Gracias por las platicas compartidas y por las inestimable contribuciones en el trabajo.

Thank you also to Thanongsak Thepsonthi and Francisco Orozco for the contribution in the chapter 4. Thank you also to Nicola Milesi and Massimo Scalmana for being my travelling companions during the stays in USA and Mexico. Grazie.

In all these years of work in GREP, Product, Process and Production Engineering Research Group, in the University of Girona have been very edifying for me. I also wish to thank my research group colleagues: María Luisa García-Romeu, Rudi de Castro, Martí Casadesús, Isabel Bagudanch. Sobretot als matxos; a en Francesc Tauler per ser tan gran, a en Jordi Delgado i en Jordi Grabalosa per portar-ho a un nivell superior i a en Guillem Quintana, perquè la seva lírica sempre m'ha servit d'exemple. També a l'Elisa Vázquez per la seva complicitat, a la Jèssica Gomar i sobretot, sobretot a la Lídia Serenó per compartir amb mi

més hores que amb ningú. També a en Xevi Gòmez per continuar-hi essent, a l'Anna Ymbern, Guillem Vallicrosa, Bernardo Providência, Andrea Rota i Daniel Takanori. No em vull deixar en Jordi Vicens per les classes magistrals al taller ni a la Cristina Miàs pels cafès on solucionar el món. He après moltes coses i he passat molt bones estones amb tots vosaltres. Moltes Gràcies!

I could never thank my family enough. Gràcies papa, mama i Isaac, vosaltres m'ho heu donat tot i m'heu donat un model a seguir.

I, finalment, gràcies a la Mireia, per tantes i tantes coses. Només amb un somriure fas que tot tingui sentit.

Summary Resum Resumen

Els processos de mecanitzat no tradicionals van aparèixer per donar resposta a la creixent demana del mercat productiu. A la necessitat de productes d'alta qualitat en el menor temps possible s'hi afegeixen noves demandes com nous materials exòtics, dissenys amb geometries innovadores així com dimensions molt petites. El mecanitzat làser és un procés no tradicional que presenta un seguit d'avantatges únics que el fan adequat per donar solució a aquestes demandes. Tot i això, el mecanitzat làser és un procés complex. El tipus de làser, la combinació dels paràmetres de procés, el material i la configuració, entre d'altres variables, poden afectar l'execució del procés.

Aquesta tesi pretén ampliar el coneixement sobre el fresat làser, establint relacions entre els paràmetres de procés i els aspectes rellevants de procés (qualitat, precisió dimensional i productivitat).

Los procesos de mecanizado no tradicionales aparecieron para dar respuesta a la demanda creciente del mercado productivo. A la necesidad de productos de alta calidad en el menor tiempo posible se unen nuevas demandas como nuevos materiales exóticos, diseños con geometrías innovadoras así como dimensiones muy pequeñas. El mecanizado láser es un proceso no tradicional que presenta unas ventajas únicas que lo hacen adecuado para dar solución a estas demandas. Pese a ello, el mecanizado láser es un proceso complejo. El tipo de láser, la combinación de parámetros de proceso, el material y la configuración, entre otras variables, pueden afectar la ejecución del proceso.

Esta tesis pretende ampliar el conocimiento sobre el fresado láser, estableciendo relaciones entre los parámetros de proceso y los aspectos relevantes del proceso (calidad, precisión dimensional y productividad).

Nontraditional manufacturing processes (NTM) appeared to answer the growing demands of market productivity. Needs of higher quality products in less time and new demands such as new exotic work materials, innovative geometric designs as well as much smaller dimensions justify laser processes insight. Laser machining is a NTM which presents several unique advantages in material processing that makes it suitable to solve these demands. However, laser machining is a complex process, because the type of laser, the combination of process parameters, the material and the configuration of the process among other variables, could affect the performance of the process.

This thesis focuses on increasing knowledge about the laser milling, establishing relationships between the process parameters and the key process aspects (quality, dimensional accuracy and productivity).

Contents

List of symbols

a	Absorptance
Cp	Specific heat [J/kgK]
CS	Cutting Speed [mm/s]
Lm	Latent heat [J/kg]
Ox	Overlapping between passes
Oy	Overlapping between adjacent pulses
P	Laser Power [W]
PF	Pulse Frequency [Hz]
PI	Pulse Intensity [W/m^2]
PPP	Peak Pulse Power [W/s]
SR	Scanning Rate [pulse/mm]
SS	Scanning Speed [mm/s]
$\mathbf{T_0}$	Initial/Room Temperature [K]
$\mathbf{T_m}$	Melting Temperature [K]
$\mathbf{T_v}$	Vaporization Temperature [K]
λ	wavelength [m]
Ø	Laser spot size [mm]
ρ	Density [kg/m^3]
μ	dynamic viscosity [Ns/m^2]
τ	Pulse duration [s]
Φ	Fluence [J/cm^2]

List of acronyms

AI	Artificial Intelligence
AJM	Abrasive Jet Machining
ANOVA	Analysis of Variance
ASCAMM	Associació Catalana d'Empreses de Motlles i Matrius
ASME	American Society of Mechanical Engineers
CAPP	Computer Aided Process Planning
CFRP	Carbon Fibre Reinforced Plastic
CIRP	College International pour la Recherche en Productique
CNC	Computer Numerical Control
COP	Cyclo Olefin Polymer
CW	Continuous Wave
DFA	Design For Assembly
DFE	Design For the Environment (Eco-Design)
DFM	Design For Manufacturing
DFMA	Design For Manufacturing and Assembly
DMLS	Direct Metal Laser Sintering
DFSS	Design For Six Sigma
EDM	Electrical Discharge Machining
GA	Genetic Algorithms
GREP	Grup de Recerca en Enginyeria de Producte, Procés i Producció
HAZ	Heat Affected Zone
HSM	High Speed Machining, High Speed Milling
IR	Infra-Red
IREBID	International Research Exchange for Biomedical Devices Design
ISF	Incremental Sheet Forming

kNN	k-Nearest-Neighbours
LCA	Life Cycle Analysis
LM	Laser Machining/Milling
MAE	Mean Absolute Error
MARL	Manufacturing and Automotive Research Laboratory
MEMS	Microelectromechanical Systems
MRR	Material Removal Rate
Nd:YAG	Neodymium-Doped Yttrium Aluminium Garnet
NIR	Near Infra-Red
NSGA-II	Non-Dominating Sorting Algorithm
NTM	Nontraditional Manufacturing Process
PC	Polycarbonate
PCL	Polycaprolactone
PDLA	Polymer d-lactic acid
PDMS	Polydimethylsiloxane
PET	Polyethylene terephtalhate
PMMA	Polymethylmethacrylate
PP	Polypropylene
PPC	Production Planning Control
PS	polystyrene
PSO	Particle Sworm Optimization
PVC	polyvinylchloride
SEM	Scanning Electron Microscope
SMA	Shape Memory Alloy
SS	Stainless Steel
TECNIPLAD	Caracterització de tecnologies innovadores per a la planificació detallada dels processos
UdG	University of Girona
UM	Ultrasonic Machining
UV	Ultraviolet

Chapter 1. Introduction

Chapter 1 presents the general domain of the Thesis, establishes the historical and conceptual frame and exposes the interest, motivation and objectives persecuted in this work.

1.1 Historical and conceptual framework

The demands of the market, which is increasingly competitive and demanding, are growing every day without giving respite to manufacturing companies. Needs of higher quality products in less time and new demands like new exotic work materials, innovative geometric designs as well as much smaller dimensions. These, were putting lot of pressure on capabilities of conventional machining processes to manufacture the components with desired tolerances economically. This led to the development and establishment of new manufacturing processes in the industry as efficient and economic alternatives to conventional ones. These technologies are called nontraditional manufacturing processes (NTM). Abrasive jet machining (AJM), ultrasonic machining (UM), Electro discharge machining (EDM) or Laser machining (LM) are some of these processes. With development in the NTM processes, currently there are often the first choice and not an alternative to conventional processes for certain technical requirements. Unlike conventional processes these are characterized by:

- Material removal may occur with chip formation or even no chip formation may take place.
- There may not be a physical tool present.
- The tool does not need to be harder than the work piece material.
- Mostly NTM processes do not necessarily use mechanical energy to provide material removal. They use different energy domains to provide machining. (electrothermal energy, electrochemical, chemical)

Laser, an acronym for light amplification by stimulated emission of radiation, is surely one of the greatest innovations of 20th century. Its constant evolution has been writing new chapters in the field of science and technology. Laser is essentially a coherent, convergent and monochromatic beam of electromagnetic radiation with wavelength ranging from ultra-violet to infrared.

Laser has wide applications because of a unique combination of properties. These are a spatial and temporal coherence (phase and amplitude are unique), low divergence (parallel to the optical axis), high continuous or pulsed power density and monochromaticity. The applications vary from common (bar code scanner, audio recording, printer) to futuristic (3D holography) and are applied to many fields like metrology, entertainment, medical diagnostics and surgery/therapy and optical communication/computation.

Accordingly, several series of lasers capable of delivering a wide variety of wavelength, energy, temporal/spectral distribution and efficiency have been developed over the last several decades. Laser can deliver very low (mW) to extremely high (1–100kW) focused power with a precise spot size and pulse time on to any kind of substrate through any medium.

The first theoretical foundation of Laser was established by Albert Einstein in the article Quantum Theory of Radiation in 1917. Einstein predicted the possibility of stimulating the electrons to emit light at a specific wavelength. It was not until 1960 that Mainman developed a ruby laser for the first time. The laser emitted a red light in the near-invisible spectrum, with a pulse of 10 kW. Altough, Maiman's work consisted in a letter of 300 words it was enough to reproduce the same experiment in other laboratories. Thus, this was followed by much basic development of lasers from 1962 to 1968. Almost all important types of lasers including semiconductor lasers, Nd:YAG lasers, CO2 gas lasers, dye lasers and other gas lasers were invented in this era (Dutta Majumdar et al., 2010).

The first experiment in laser materials processing which was subsequently to evolve into a significant industrial process was conducted in May 1967 when Peter Houldcroft used an oxygen assist gas to cut 1mm thick steel sheet with a focused CO 2 laser beam (Sullivan et al., 1967). This laser was operational in the Services Electronic Research Laboratory

(SERL) in Harlow, UK only two years after Patel had demonstrated lasing action from the CO2 molecule. The laser was of the slow flow type, consisting of 5 discharge sections, making a total length of 10m. A maximum output power of 300W at 100Hz was available. The laser had been developed for military applications but potential industrial applications were also being considered. Figure 1 presents an early commercial version of the SERL laser. These first experiments probably mark the start of laser materials processing as it is known it today.

After 1968, the existing lasers were designed and fabricated with better reliability and durability. By mid 1970s more reliable lasers were made available for truly practical applications for several materials in the industrial applications such as cutting, welding, drilling and marking. The first commercially available laser systems with a recognizable configuration comparable to a range of equipment available today started to appear. During the 1980s and early 1990s the lasers were explored for surface related applications such as heat treatment, cladding, alloying, glazing and thin film deposition.

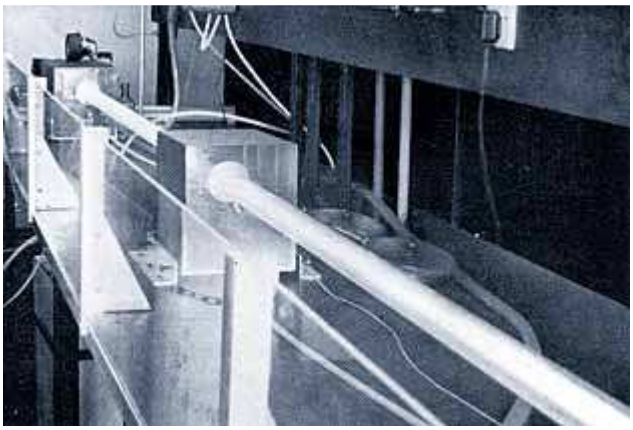

Figure 1: Early commercial version of SERL laser 1967. (Hilton, 2002)

The increasing demand of laser in material processing can be attributed to several unique advantages. Laser can be applied to a wide range of materials (metals and non-metals, soft and difficult-to-machine) and allows the production of parts with complex shapes without expensive tooling. Being a non contact material removal process compared with other conventional mechanical processes, laser machining (milling) removes much less material, involves highly localized heat input to the workpiece, minimizes distortion, and offers no tool wear. Therefore, the process is not limited by constraints such as maximum tool force, buildup edge formation or tool chatter. It is an ablation operation causing vaporization of material as a result of interaction between a laser beam and the workpiece being machined.

From the application point of view, laser material processing can be broadly divided into four major categories, namely, forming (manufacturing of near net-shape or finished products), joining (welding, brazing, etc.), machining (cutting, drilling, etc.) and surface engineering (processing confined only to the near-surface region). Figure 2 presents this classification showing some representative examples from each category of application.

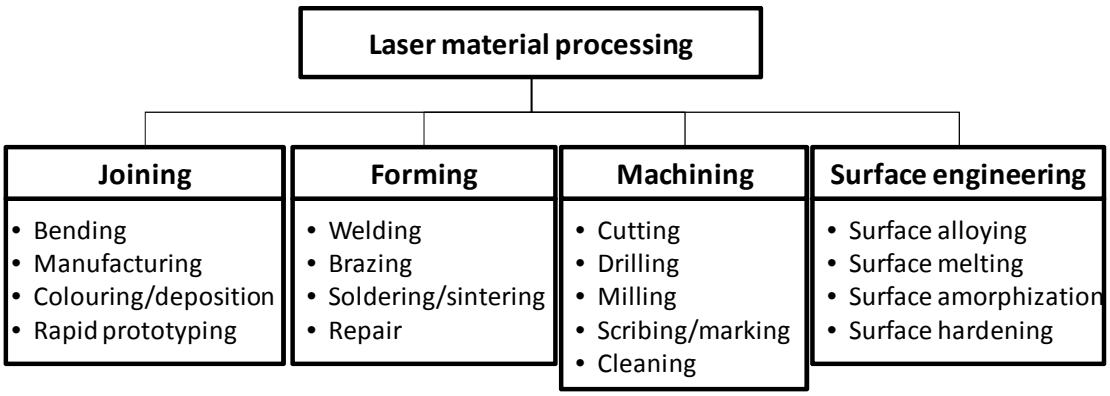

Figure 2: Laser material processing classification from the application point of view. (adapted from Dutta Majumdar et al., 2010)

Obviously, depending on the application the process will involve only heating (without melting/vaporizing), melting (no vaporizing) or vaporizing. Thus, the laser power density and interaction/pulse time are so selected in each process that the material concerned undergoes the desired degree of heating and phase transition. Processes like bending and surface which rely on surface heating without surface melting require low power density. On the other hand, surface melting, glazing, cladding, welding and cutting that involve melting require high power density. Similarly, cutting, drilling, milling and similar machining operations remove material as vapor; hence need delivery of a substantially high power density within a very short interaction/pulse time.

Laser ablation occurs only when the substrate material absorbs strongly the wavelength of the transmitted radiation. Therefore, the removal of material during laser machining is affected by the characteristics of the laser beam and the workpiece but is mainly determined by the way that both interact. Wavelength is one of the major factors that affects the laser process, but rarely can be modified without changing the laser type. Laser radiation can be continuous or controlled and modulated in an order sequence of pulses with predetermined pulse duration (length), repetition rate (pulse frequency), laser speed (scanning speed) and laser power. This, combined with a very small focusing spot increases the energy density (fluence) and power density (intensity) in the laser-material interaction zone. This explains why laser milling can successfully process materials that are difficult to machine using conventional methods. Material parameters like surface finishing, surface coating, and the thermal conductivity lead to more or less effective laser machining. The laser radiation absorption mechanism will be affected for all these parameters. Although, when a particular wavelength of light is transmitted through a material, its absorption is a function of the material path length and independent of the incident intensity, for very high intensities, non-linear effects take place and become a factor for stronger energy absorption.

Hence, we find ourselves in front of a sea consisting of different laser types with many characteristics and process parameters, and multiple processes that can be applied to a wide variety of materials. This results into an infinite combinatorial almost impossible to control

and implement successfully. Clearly, much research is needed to lead and optimize this process.

Professor Bill Steen (Steen, 2010) affirmed that since the invention of the laser in 1960, we have entered into a new industrial revolution, based on the use of coherent optical energy. If we subscribe to this idea and we think in how this technology progressed in the last decades, it is difficult to see what will be the limits and when will stop its evolution.

1.2 Interest and motivation

This Thesis is carried out on one hand, in the frame of the Research Group on Product, Process and Production Engineering (GREP) main research lines and on the other hand, in the context of ASCAMM Technology Centre research interests.

1st of February, 2006 University of Girona, UdG and ASCAMM Foundation signed a scientific collaboration agreement in the field of investigation and formation of researchers in innovative manufacturing technologies.

GREP, Research Group on Product, Process and Production Engineering (GREP, 2013) was set up in 1998 by University of Girona faculty members. The group is currently carrying out research on aspects related to the fields of the product, the process and the production. GREP research interest focuses along the following lines:

- Process and productivity improvement: high speed machining (HSM), grinding, sheet metal folding, precision control and surface roughness, machine sensor systems, process monitoring, diagnostics and control.
- Planning, organization and control of processes: computer-aided process planning (CAPP) systems, production planning control (PPC) systems and the integration of both.
- Quality: total quality management and assurance standards (ISO 9001), environmental standards (ISO 14001), health and safety, Lean Manufacturing, etc.
- Product design: specifications, design for manufacturing (DFM), design for assembly (DFA), design for manufacturing and assembly (DFMA), design for the environment (DFE) or eco-design, and design for six sigma (DFSS) systems.
- Environmentally sensitive production: control, reduction and management of environmental impact, life-cycle analysis (LCA), reuse, recycling and recovery of components, surplus materials, chips, waste and residues of the productive process.

ASCAMM Technology Centre (ASCAMM, 2013) is located in Cerdanyola del Vallès (Barcelona). Was founded in 1987 by the Catalan Association of Dies and Moulds Makers and turned into a non-profit foundation in 1996 with the mission of helping industrial businesses to improve their competitiveness by technological innovation and knowledge transfer in the fields of industrial design and production, especially for plastic, metal and light alloy products and tooling.

This thesis is developed in the context of two funded projects; TECNIPLAD and IREBID.

TECNIPLAD, Description of innovative technologies for detailed process planning (DPI2009 - 9852 PN de Diseño y Producción Industrial), is funded by the Ministry of Science and Innovation of Spain. The main goal of this project is to understand better processes such as Electrical Discharge Machining (EDM), Laser Milling (LM), Direct Metal Laser Sintering (DMLS) and Incremental Sheet Forming (ISF).

IREBID, International Research Exchange for Biomedical Devices Design and Prototyping (FP7-PEOPLE-2009-IRSES-247476), is supported by the European commission. The main objective of the exchange programmed is to create and reinforce synergies between applied investigation fields of engineering and medicine in order to develop new solutions for the healthcare sector.

In the context of this IREBID project two exchange stays were done. In 2011 a stay of 6 months was done at the Department of of Industrial and Systems Engineering of the Rutgers University in New Jersey (USA) in order to acquire knowledge about the laser micro-machining of transparent polymers. In 2013 another stay of 3 months was done at the Center for Innovation in Design and Technology of the Tecnológico de Monterrey in Monterrey (Mexico) working in analytical and modelling tools.

This thesis has been developed with a PhD scholarship BR-GR1 from the University of Girona.

This thesis focuses on increasing knowledge about the laser milling, establishing relationships between the process parameters and the key process aspects (quality, dimensional accuracy and productivity).

1.3 Objectives

The objectives of this Thesis were established considering the lack of knowledge of this non-traditional process and trends of the nowadays metal removal sector.

The main objective of this thesis is to increase the existing knowledge in the laser milling process, evaluating and defining the parameters involved to improve the process based on the analysis of qualitative and geometrical properties of the final product. This should help to design process methodology in the laser manufacturing as a process suitable for the manufacture of parts where the final qualities do not differ from traditional technologies.

Although laser milling is a very complex process, the operators select the process conditions based on the experience acquired or the standards proposed by the machine supplier. This usually results in higher costs and production times due to testing and repetitions.

There are many published works on the process but, a better establishment of the relationship between the inputs (process parameters, geometries, materials) and outputs (objective functions as surface roughness, dimensional accuracy, processing) is needed. Such knowledge must be more practical for use in planning detail by operators and companies.

This thesis aims to develop studies and experiments needed to reach a level of knowledge of the process. In addition to develop tools for planning and selection of the laser process conditions.

More specifically, the objectives of the thesis are:

- Describe the information needed to improve the laser micro-machining process in the production of microshapes and to develop a suitable AI model for the modelization of this industrial task.

- Provide the insight for improving dimensional and surface quality in the laser milling micro-manufacturing process by optimizing process parameters.

- Investigate the feasibility of utilizing a nanosecond laser to ablate micro-channels in a transparent PMMA-polymer substrate.

- Study the capability of a nanosecond Nd:YAG laser to produce micro-cavities with preset dimensions. Understand the effect of laser milling parameters on the desired dimensional quality.

- Investigate the characteristics of fiber laser cutting of stainless steel 316L-based cylindrical stents. The effect of laser cutting parameters on the cutting quality for fixed gas type and gas pressure was investigated.

- Analyze the influence of key process parameters as scanning speed, pulse intensity and pulse repetition rate on the dimensional precision, surface quality and productivity on different process configurations (2.5D and 3D laser milling).

- Study of the effect of the process on different materials. The laser technology is able to manufacture a wide range of materials, even materials impossible to manufacture

with the conventional processes. However, the materials have different response to the laser beam radiation.

- Development of intelligent selection of parameters for process planning. The development of AI models and genetic algorithms should allow the selection of the optimum process parameters for the laser milling of a feature with its specific quality and dimensional requirements.

- Development of mathematical models and algorithms to predict the process response.

- Focus and test the process in biomedical applications. Laser milling is more conducive to the machining of small dimensions at the meso or micro scale. The objective is to perform experiments related and applicable to production sectors of consumer goods in small or low batch, as in the medical sector.

Achieving the objectives established will permit the laser systems operators to improve the parameters selection optimizing the productivity while ensuring quality requirements.

1.4 Thesis structure

The Thesis is organized as follows:

Chapter 1 presents the general domain of the Thesis, establishes the historical and conceptual framework and exposes the interest, motivation and objectives persecuted in this work.

Chapter 2 reviews the fundamentals of laser material interaction, the laser processing of different materials and the laser processing parameters. Finally, the laser configurations are exposed. The main research works on these topics are reviewed.

Chapter 3 presents an experimental study of the process parameters on quality and productivity responses on the machining of micro-channels on hardened steel. Different machine learning techniques are tested to build high accuracy models.

Chapter 4 presents experimental models to study the relation between process parameters and quality characteristics. Different decision tools and multi-objective optimization models are developed.

Chapter 5 presents investigations on the effects of nanosecond laser processing parameters on depth, width and MRR of microchannels fabricated from PMMA polymer. Mathematical

modeling for predicting microchannel profile was developed and validated with experimental results.

Chapter 6 presents a multi-objective optimization (NSGA-II) of the laser milling process of micro-cavities for the manufacturing of drug eluting stents (DES). Experiments on SS316L are carried out as a work material. The dimensional accuracy is the main response studied.

Chapter 7 presents an experimental study of fiber laser cutting of 316L stainless steel thin sheets. The applicability for the manufacturing of cardiovascular stents is studied.

Chapters 3 to 7 present the work done in the form of published or submitted articles. The first article (chapter 3) presents a study of the process parameters effect on the laser milling in 2.5D on a metallic material. The second article (chapter 4) presents different optimization tools for the previous investigation in order to provide prediction tools to the machine operators. The next article (chapter 5) presents a similar study in a completely different material, a transparent polymer. The fourth article (chapter 5) studies the dimensional accuracy of the laser milling process in 3D micro-geometries. Finally the last article (chapter 7) presents an applied case of the laser machining process.

Finally, Chapter 8 presents conclusions and outlook.

Chapter 2. State of the art

Chapter 2 reviews the fundamentals of laser material interaction, with special attention to the laser ablation process. The laser processing of the different materials; metals, polymers and ceramics are explained. The laser processing parameters are presented although the process also depends on the material characteristics and the way both interact. After that, the laser configurations are exposed. The laser drilling and its different approaches are introduced first. Then, the 2D laser machining or laser cutting and the laser milling are explained. The main research works on these topics are reviewed.

2.1 Introduction

The use of lasers in materials processing, machining, diagnostics, and medical applications is a rapidly growing area of research. Laser-based material processing has been used in thermal processing, shock processing, surface treatment, cleaning of surfaces, welding, melting and polishing, scribing, cutting, milling as well as micro-machining of basic geometric features on a variety of materials. Lasers can provide unique solutions in materials processing, offer the ability to manufacture otherwise unattainable devices, and yield cost-effective solutions to complex manufacturing processes.

Further developments in the pulsed laser techniques and systems have increased the applicability of the laser milling technology in the production systems. Hence, laser milling technology has become a viable alternative to conventional methods for producing complex

and micro features on difficult-to-process materials and is being employed increasingly in industry because of its known advantages.

Laser machining can be applied to a wide range of materials (metals and non-metals, soft and difficult-to-machine) and allows the production of parts with complex shapes without expensive tooling. Being a non contact material removal process compared with other conventional mechanical processes, laser machining removes much less material, involves highly localized heat input to the workpiece, minimizes distortion, and offers no tool wear. Therefore, the process is not limited by constraints such as maximum tool force, buildup edge formation or tool chatter. Otherwise this process presents low energy efficiency from production rate point of view and the difficulty to achieve good dimensional precision.

The removal of material during laser milling is affected by the characteristics of the laser beam and the workpiece but is mainly determined by the way that both interact [Pham et al., 2002]. The wavelength, the laser power, and pulse duration are the major factors that affect laser milling and rarely can be modified without changing the laser type with a few exception (e.g. Q-switching can provide the harmonics of the main wavelength). Laser ablation occurs only when the substrate material absorbs strongly the wavelength of the transmitted radiation. Hence, the surface finishing, surface coating, and the thermal conductivity are parameters which will lead to more or less effective laser machining. The process parameters which can be controlled and modified in order to obtain optimal machining results are the selection of the repetition rate of the pulses (frequency), the scanning speed, and the pulse intensity which in turn significantly affects the quality of the micro-feature created and also the material removal rate.

Lasers are usually categorized as two groups: continuous wave (CW) and pulsed lasers. Conventional CW and pulsed laser ablation is used in many fields, such as material processing, ablation, etching, rapid prototyping, micro-fluidics, and medical applications.

Pulsed lasers achieve much higher intensities than CW lasers and are the preferred solution for the fabrication of micro-sized structures. Long-pulsed (nanosecond, ns), short-pulsed (picoseconds, ps) and ultrashort-pulsed (femtosecond, fs) lasers that are commonly used for repairing, trimming, marking, scribing, texturing, welding, ablation, cutting, and drilling are presented in the Table 1.

Table 1: Most common lasers. [Koç et al., 2011]

Laser Type	Wavelength (nm)	Power (W)	Pulse Energy (mJ)	Fluence (J/cm^2)	Pulse Duration	Repetition Rate
Q-switched	1064	1–35 W	8 mJ	—	5–100 ns	1–400 kHz
Nd:YAG	532	0.5–20 W	5 mJ	—	5–70 ns	1–300 kHz
	355	0.2–10 W	3 mJ	—	5–50 ns	15–300 kHz
	266	0.5–3 W	<1 mJ	—	5–30 ns	15–300 kHz
Ti:sapphire	800 (central)	0.5–2 W	0.25–0.9 mJ	—	100–150 fs	1–5 kHz
	(700–980)	—	—	—	—	—
Excimer-	—	—	—	—	10–20 ns	5–10 Hz
XeF	351	—	—	1.8–9.1	—	—
XeCl	308	—	—	1.2–9.8	—	—
KrF	248	—	—	0.9–9.8	—	—
ArF	193	—	—	0.7–4.0	—	

2.2 Laser material interactions

Laser radiation is essentially electromagnetic waves. When the electromagnetic radiation is incident on the surface of a material, various phenomena that occur include reflection, refraction, absorption, scattering, and transmission. The most important phenomena in the laser processing of materials is the absorption of the radiation.

Absorption of light can be explained as the interaction of the electromagnetic radiation with the electrons of the material and it depends on both the wavelength of the material and the spectral absorptivity characteristics of the material being machined. The absorption of laser radiation in the material is generally expressed by the Beer-Lambert law:

$$I(z) = I_0^{-az} \tag{1}$$

Thus, once inside the material, absorption causes the intensity of the light to decay with depth at a rate determined by the material's absorption coefficient a. In general, absorption is a function of wavelength and temperature, but for constant a, intensity decays exponentially with depth.

The laser energy absorbed by the material during laser-material interaction is converted into heat by degradation of the ordered and localized primary excitation energy. The conversion of light energy into heat and its subsequent conduction into the material establishes the temperature distributions in the material. Depending on the magnitude of the temperature rise, various physical effects in the material include heating, melting, and vaporization of the material. Furthermore, the ionization of vapor during laser irradiation may lead to

generation of plasma. These effects of laser material interaction are schematically presented in Figure 3.

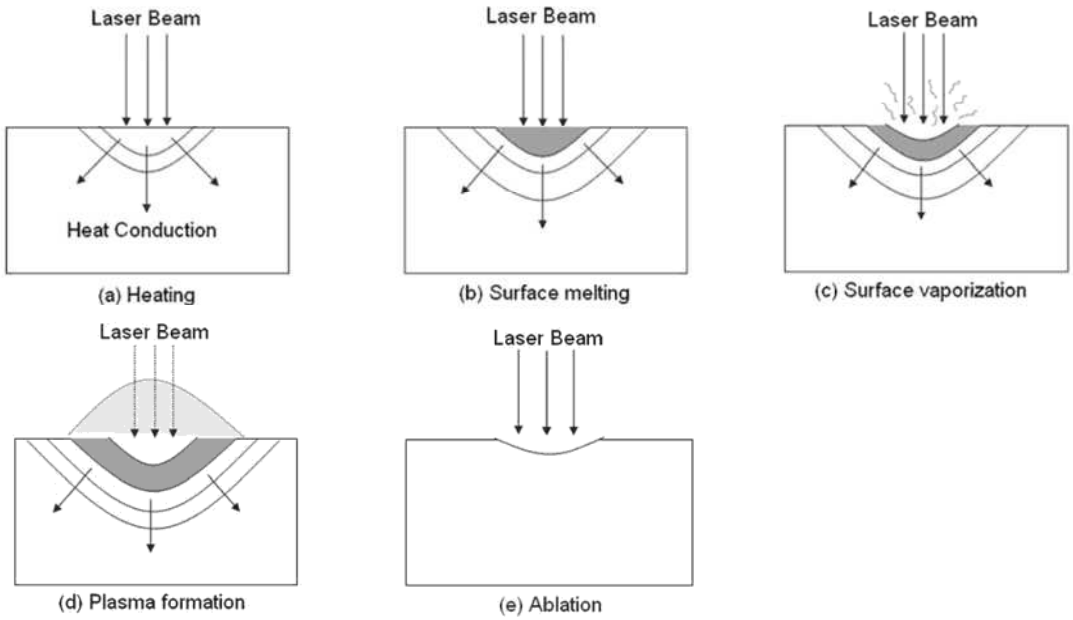

Figure 3: Laser material interaction [Dahorte et al,. 2008].

Laser ablation is the removal of material from a substrate by direct absorption of laser energy. The onset of ablation occurs above a threshold fluence, which will depend on the absorption mechanism, particular material properties, microstructure, morphology, the presence of defects, and on laser parameters such as wavelength and pulse duration. The laser-material interaction during ablation is complex and involves interplay between the photothermal (vibration heating) and photochemical (bond breaking) processes.

At low fluences, photothermal mechanisms for ablation include material evaporation and sublimation. The absorbed laser energy gets converted into thermal energy in the material. The subsequent temperature rise at the surface may facilitate the material removal due to generation of thermal stresses. When the incident laser energy is sufficiently large, the temperature at the surface exceeds the boiling point causing rapid vaporization. These thermal mechanisms can be understood as thermodynamic phase changes in response to the high temperatures.

When the excitation time is shorter than the thermalization time in the material, non-thermal, photochemical ablation mechanisms can occur. In photoachemical ablation, the energy of the incident photon causes the direct bond breaking of the molecular chains in the organic materials resulting in material removal by molecular fragmentation without significant thermal damage. The photon energy must be greater than the bond energy.

The laser's temporal pulse length can have a significant effect on the dynamics of the ablation process. In general, as the pulse length is shortened, energy is more rapidly

deposited into the material leading to a more rapid material ejection. The volume of material that is directly excited by the laser has less time to transfer energy to the surrounding material before being ejected. Therefore, the ablated volume becomes more precisely defined by the laser's spatial profile and optical penetration depth, and the remaining material has less residual energy, which reduces the HAZ.

2.3 Laser processing of materials

As explained, the laser absorption mechanisms depend on the type of material. The different characteristics of absorption, reflectivity, and thermal diffusion and conductivity of different kinds of materials affects the laser machining process. Hence, depending on the material, the use of a laser system with the adequate wavelength and the selection of the optimum set of process parameters will be essential. Here are explained how are the interaction between the laser systems and the different materials.

2.3.1 Laser processing of metals and alloys

When radiation interacts with metals, the energy absorbed raises the temperature level. The laser beam heats, melts and vaporizes the metal (metal sublimation). However, due the high ablation threshold of metals and their high reflectivity at most common laser wavelengths, the energy absorbed may not be sufficient to achieve the softening of the material to substantially affect the process of removal of the material. The use of short-pulsed lasers with proper choice of laser parameters may still achieve thermal softening in highly reflective metals.

Several authors used lasers systems to machine steel [Ciurana et al., 2009; Teixidor et al., 2013, Dhara et al, 2007 and Bartolo et al., 2006], copper [Bustillo et al., 2008], aluminium [Dubey et al., 2008 and Dobrev et al., 2006] and other metals. Heyl et al. [2001] and Dumitru et al. [2005] machined hardmetals with a UV laser and a femtosecond laser respectively presenting favorable experimental results. Some other authors reported favorable results on machining different metals using a femtosecond Ti:sapphire laser [Chichkov et al., 1996; Nedialkov et al., 2007 and Cheng et al., 2009]

2.3.2 Laser processing of polymers

Polymers are the materials of choice for disposable lab-on-chip devices (in special the microfluidic systems) because of their ease and low cost of manufacture, widely tunable properties, biocompatibility, and optical transparency. Polymers exhibit strong absorption in the UV and deep infrared (IR) wavelengths, but weak absorption at visible wavelengths.

However, the reaction to lasers is somewhat different in polymers, compared to that seen in metals. It is believed that UV produces a cooler excitation in polymers. On the other hand, IR causes the most molecular vibration and material change through thermal process. However, the properties of most polymers are very strong functions of temperature. This implies that even slight changes in temperature can have strong effect on machining and localized laser heating can be used effectively for increasing the productivity and the product characteristics. At UV wavelengths (200-400nm), the material removal mechanism in polymers is generally thermal evaporation. Below 400 nm, the polymeric material is removed typically by chemical ablation. Various UV lasers [Suriyage et al., 2004; Waddle et al., 2006 and Roberts et al., 1997] and IR CO2 lasers [Romoli et al., 2011; Klank et al., 2002 and Snakenburg et al., 2004] have been used for machining microfluidic channels of polymer materials.

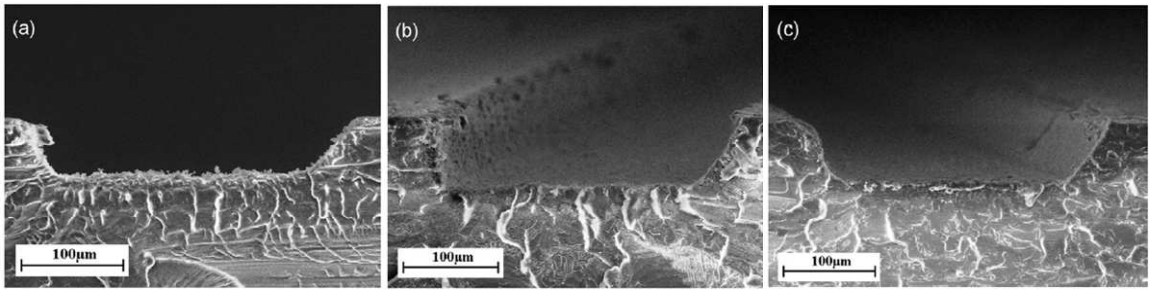

Figure 4: Multi scan micro-channels ablated with a femtosecond laser in (a) PMMA, (b) PS, and (c) COP [Suriano et al., 2011]

On the other hand, polymers can be machined by ultra-short laser pulses (Figure 4). Femtosecond laser pulses provide a unique micromachining tool as they can modify transparent materials at wavelengths at which they are normally transparent, by depositing energy through high-order non-linear absorption processes, inducing optical breakdown. [Malek et al., 2006]. Several authors used femtosecond (Ti:sapphire) lasers to machine polymer materials [Gomez et al., 2005; Suriano et al., 2011 and Marco et al., 2010]

2.3.3 Laser processing of ceramics

Laser machining of ceramics is mostly challenging due to their brittleness and large scattering exhibited at common laser wavelengths, which restrict energy absorption. A combination of short pulse and short wavelength usually presents best results (Karnakis, 2006). High hardness and thermal stability, low electrical conductivity along with high wear resistance have made structural ceramics such as alumina (Al2O3), silicon nitride (Si3N4), silicon carbide (SiC), and magnesia (MgO) useful for several applications in aerospace, electronics, automotive, medical, and semiconductor industries. Figure 5 presented results in aluminum titanate. Samant et al. [2009a, 2009b and 2010] presented results machining alumina (Al2O3), silicon nitride (Si3N4), silicon carbide (SiC), and magnesia (MgO) in one

dimension machining (drilling), two dimensions machining (cutting) and three dimensions machining (milling) with a millisecond pulsed Nd:YAG laser (1064 nm wavelength).

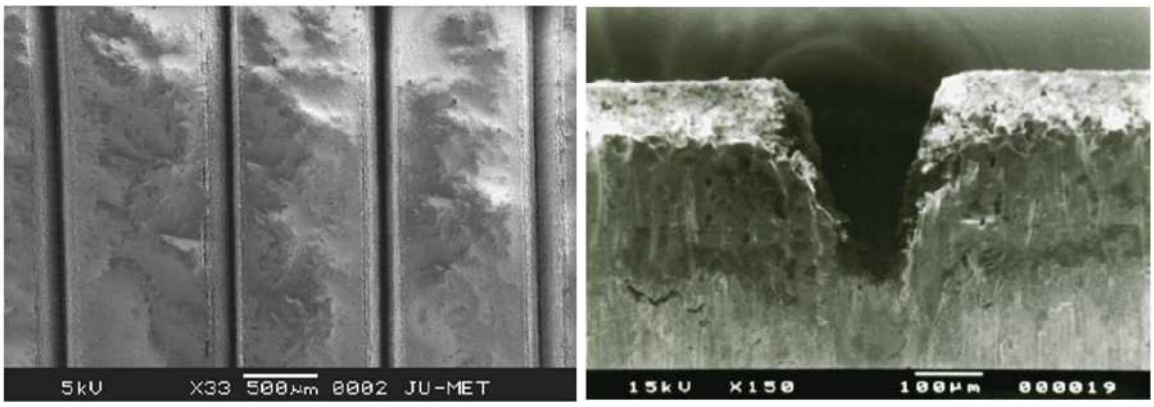

Figure 5: Micro-groove of aluminum titanate machined with a Nd:YAG laser [Dhupal et al., 2007].

Gilbert et al. [2007] generated a series of lines and pockets on the surface of the AlN using Nd:YAG lasers of UV and near IR wavelengths. The near IR laser presented better material removal rates but, if smaller features were desired, the UV laser would be preferred. Other authors used Nd:YAG laser to machine grooves and cavities in alumina and aluminum titanate [Dhupal et al., 2007; Wang et al., 2007 and Tsai et al., 2003]

2.3.3.1 CVD Diamond

Synthetic CVD diamond (allotropic form of carbon may be though as a type of ceramic) is an attractive material, since it has various applications such as IR optical applications, detectors, sensors, and thermal management systems. Among all materials, diamond is the most difficult one to be machined because of its hardness and inertness, and, like glass, it is highly transparent over a broad range of the optical spectrum. Diamond can be ablated by two ways: If the laser radiation is highly absorbed in diamond or by the mechanism of laser-induced graphitization. Various authors have been used femtosecond (Ti:sapphire) lasers [Komlenok et al., 2011 and Kononenko et al., 2009] and nanosecond Nd:YAG lasers [Kononenko et al., 2005 and Butler-smith et al., 2013] for machining of diamond.

2.3.3.2 Silicon

Being a semiconductor, silicon has a widespread application in many applications in electronic devices and microelectromechanical system and thin-film applications [Ngoi et al., 2001]. Laser etching of silicon permits a wide variety of structures to be made, since it is independent of the crystal plane orientation unlike wet etching. Although the laser machining of silicon has no been much investigated some authors used femtosecond lasers [Tsai et al., 2002; Ngoi et al., 2001 and Amer et al., 2005] and UV lasers [Greuters et al., 2002 and Karnakis, 2006] for machining silicon.

2.3.3.3 Glass

Glass is an amorphous (non-crystalline) ceramic material. Micro-machining of hard and brittle glasses finds applications in biochemistry, biomedicine, lab-on-chip devices, sensors, and Bio-MEMS devices. One of the difficulties is the brittleness and poor thermal properties of most glasses, making the fabrication of finely machined features a challenging task with a risk of laser-induced microcracking and other laser-induced collateral damage such as debris and poor surface quality. The absorption of light by some glasses can have a very nonlinear behavior. However, since glass is monopaque, absorption occurs largely within the volume of the material, rather than on the surface.

Glasses exhibit strong optical absorption at deep UV and IR wavelengths with much weaker absorption at visible and near-infrared wavelengths. Thus, one way to laser machine glass is to use short wavelengths as nanosecond pulsed excimer laser at 355 nm to machine fused silica among others [Niino et al., 2004 and Bohme et al., 2006]. The other way is to use laser with ultra-short pulse duration which can modify transparent materials at wavelengths at which they are normally transparent, by depositing energy through high-order non-linear absorption processes, inducing optical breakdown. Many authors used femtosecond lasers (Ti:sapphire) to machine fused silica (Streltsov et al., 2002; Vishnubhatla et al., 2009; Will et al., 2002 and Ben-Yakar et al., 2002), borosilicate glass (Cai et al., 2007; Eaton et al., 2005 and Giridhar et al., 2004) among other glass materials (Cheng et al., 2008; Davis et al., 1996 and Florea et al., 2003). Other authors [Nikumb et al., 2005 and Karnakis, 2006] conducted comparative studies machining glass bulk materials using different type of pulsed lasers, UV and femtosecond.

2.3.4 Laser processing of composites

The use of carbon fibre reinforced plastic CFRP materials in aerospace, automotive and marine industries is rapidly growing due to their lighter weight and superior performance. Therefore, CFRP composites have become major structural materials and are considered as substitutes for metals in many weight-critical components. There is however challenges in laser processing of CFRP where the goal is to minimize or eliminate excessive HAZ in the polymer matrix and to maintain a high processing speed. The properties of conventional materials such as metals, ceramics and polymers are assumed as isotropic so that the machining quality is the same in all directions. However CFRP composite material is laminated with different fibre orientation bound together in a polymer matrix according to its application. Each constituent retains its own chemical, physical and mechanical properties and therefore poses a challenge in laser processing due to the large differences of material properties of the two constituents at elevated temperatures. Anisotropic heat conduction at different fibre orientation directions is another problem that characterizes the HAZ. Although the use of lasers for composites machining has not been much studied, some authors studied the drilling of holes in CFRP materials with UV lasers (Li et al., 2008; Li et

al., 2010 and Yung et al., 2002) and femtosecond lasers (Wang et al., 2012). Riveiro et al. (Riveiro et al., 2012) studied laser cutting of CFRP material using a CO2 laser and reported the experimental results.

2.4 Laser processing parameters

There are several key parameters influencing laser ablation and directly affecting the energy working on materials. Larger reduction in laser power or increases in cutting speed will result in incomplete penetration of the cut zone, or poor quality ablation. There are several research works which deal with how process parameters affect the quality of the resultant surfaces or geometrical features using experimental analysis tools. Several authors [Ciurana et al., 2009; Bartolo et al., 2006 and Cicala et al., 2008] studied the influence of process parameters (pulse intensity, scanning speed, pulse frequency) on the quality of the final part and the material removal rate in order to establish the relations between them and to identify the optimum set of these process parameters.

2.4.1 Pulse duration

The effect of pulse duration (also called pulse width) on feature quality is significant in laser ablation. Chichkov et al. [1996] investigated laser ablation of different materials with femtosecond, picoseconds and nanosecond laser. The Figure 6 presents clearly the difference between the different pulse duration laser machining. Several authors [Petkov et al., 2008; Karnakis, 2006 and Jandeleit et al., 1998] developed similar studies evaluating the effect of the pulse duration on the targets. So it is obvious, that there are different interaction mechanisms of light and matter when applying laser pulses of different timescales.

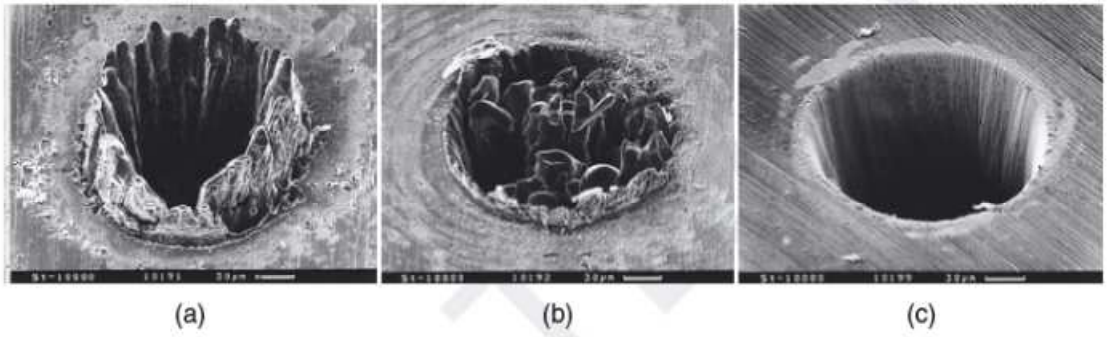

Figure 6: Laser ablation with (a) nanosecond pulse, (b) picosecond pulse, and (c) femtosecond pulse [Chichckov et al., 1996].

Continuous wave (CW) lasers emit laser radiation with a laser power that continuously depends on the pump power. CW lasers are used for applications which require a thermal

impact, e.g. welding or melt cutting. Pulsed systems with long laser pulses (~1ms) are used when higher power densities are required on short timescales, e.g. for micro welding.

Short laser pulses (pulse duration 1 ns to 1us) is a reduction of thermal impact on the material. Material removal requires an energy density above the ablation threshold. A short laser pulse with an energy density above the ablation threshold is absorbed by the material and a part of this material is transformed into an expanding plasma plume within several picoseconds. Short laser pulses are generated through resonator q-switching. Due to the high peak power, q-switched solid state lasers allow for efficient frequency conversion and therefore they can deliver visible or UV wavelengths.

Ultrashort laser pulses are defined as pulses with pulse duration below 10 ps. In contradiction to short laser pulses, the energy is deposited in a time period shorter than the relaxation time between the electron system and the lattice. The vaporization and plasma formation take place much faster than the heat conduction occurs. This leads to a decrease in thermal impact and allows material processing without thermally affecting the surrounding material when processing at moderate fluences.

2.4.2 Pulse repetition rate

The repetition rate (or pulse frequency) defines the number of pulses per second used for machining. The scanning speed can be scaled by the repetition rate. Thermal impact occurs by increasing the repetition rate even for ultrashort laser pulses.

When the energy is sufficient, every pulse makes an effect on the workpiece. If the pulse rates were low, the energy would leave the thermal zone and would be of no use. If the residual heat were retained by a rapid repetition rate (limiting the time for thermal conduction) the thermal effect on the work material would be more efficient. On the other hand, a pulsed laser has an upper limit in pulse repetition.

The thermal impact is caused by two different factors. The first is heat accumulation. Increasing the repetition rate leads to a reduction of time for heat diffusion into the workpiece. With higher repetition rates, the heat put into the material cannot be transferred out of the interaction zone. Hence, the temperature of the workpiece rises. This effect leads to a formation of molten material also when applying ultrashort laser pulses. The second cause of thermal impact is particle shielding. Due to the short interval between two subsequent pulses, ablated airborne particles are located in the region of the laser radiation. The subsequent laser pulse interacts with these particles and leads to plasma ignition above the workpiece. The plasma forms an additional heat source close to the workpiece surface. The impact of these two effects strongly depends on the laser fluence, the thermal conductivity of the processed material as well the size and geometry of the ablated structures. Both effects appear at repetition rates above 100 kHz for metals.

2.4.3 Wavelength

The selection of the optimum laser wavelengths is influenced by the minimum feature size and the optical properties of the work material. As is presented in the Figure 7 the characteristics of absorption, reflectivity, and thermal diffusion of the materials are different for each laser wavelength [Lee et al., 2007]. For instance, aluminium is highly reflective. However, copper and steel have better absorption at UV wavelengths. Polymers and Glasses exhibit strong absorption at UV and deep infrared wavelengths, but with weak absorption at visible and near infrared wavelengths. Therefore, the same result can be achieved with much less laser power when using green radiation instead of IR radiation. Even after taking the conversion efficiency into account, the energy balance is still superior for converted laser systems. However, due to the complexity of the conversion technology, cost efficiency plays an important role in determining the required wavelength.

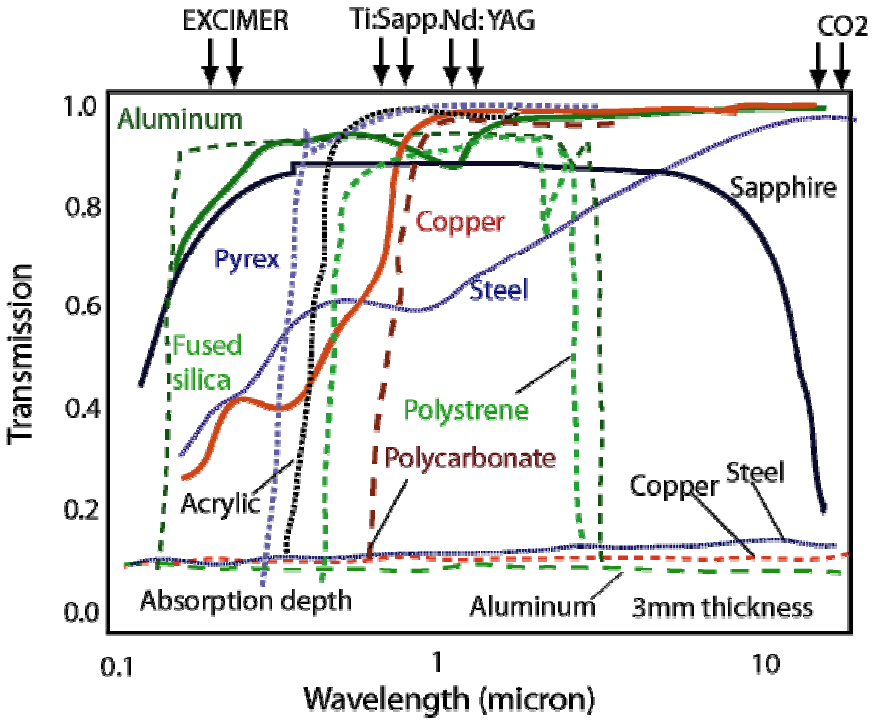

Figure 7: The relationship between wavelength and transmission for some materials [Lee et al., 2007].

2.4.4 Beam quality

The beam quality (M^2) is a property of the laser system. It is essentially a measure of how tightly a laser beam can be focused under certain conditions. The spatial intensity distribution of laser radiation mainly depends on the laser source. Depending on the design of the resonator, different transverse modes can be emitted. The best possible beam quality is achieved for a diffraction-limited Gaussian, which corresponds to $M^2 = 1$. This value is closely approached ($M^2 \leq 1.1$) by many lasers, in particular by solid-state bulk lasers operating on a single transverse mode and by fiber lasers based on single-mode fibers.

High beam quality is desired to decrease the spot size as well as to increase the working distance which is required in many laser material processes (cutting, drilling, and marking). An additional motivation for high beam quality is its well defined intensity distribution in the focal plane for using beam shaping elements.

2.4.5 Laser power

A major processing control parameter is the on-target laser power (W). The controlled variation of this parameter could enable processing advantages where different functional properties of the exposed base material are realized by mere consequence of the irradiation conditions.

In laser material processing, the power can be controlled either internally to the laser using the inherent excitation and light amplification characteristics to advantage, or externally by use of a light valve and modulator.

With the advent of the all solid state laser and with particular care in the design of thermal management, it is now possible for lasers to vary the laser power without incurring much loss in pulse-to-pulse stability. In fact, the current generation of pulsed have the capability to create any pulse amplitude profile and controllably alter it on a pulse to pulse level. Depending on the application the laser power can be represented in terms of fluence (J/m2) or pulse energy (J).

2.4.5.1 Pulse energy

The pulse energy (J) is simply the total optical energy content of a pulse, i.e., the integral of its optical power over time. For single pulses, e.g. from a Q-switched laser, the pulse energy may be measured e.g. with a pyroelectric device. For regular pulse trains, the pulse energy is often calculated by dividing the average power (measured e.g. with a powermeter) by the pulse repetition rate.

Typical pulse energies from Q-switched lasers range from microjoules to millijoules, and for large systems to multiple joules or even kilojoules. Mode-locked lasers achieve much lower pulse energies (picojoules, nanojoules or sometimes several microjoules) due to their high pulse repetition rates and sometimes due to limiting nonlinear effects in the laser resonator. Much higher energies of ultrashort pulses can be achieved by amplifying pulses at a lower repetition rate, as obtained e.g. with a pulse picker or a regenerative amplifier. Some authors focused their research on the effects of the pulse energy on the quality of the machined cavities [Boardatchev et al., 2003,; Yousef et al., 2003 and Ngoi et al., 2001].

2.4.5.2 Fluence

The fluence (J/m2) is the most important parameter affecting the ablation result, using short and ultrashort laser pulses. The fluence is defined as the energy density on the workpiece. The fluence is calculated dividing the pulse energy by the spot size. The fluence determines the ablation diameter and depth as well as the thermal impact. The ablation depth and the square of the ablation diameter are proportional to the logarithm of the fluence.

2.4.5.3 Peak power

The peak power of a pulse is the maximum occurring power. Due to the short pulse durations, peak powers can become very high even for moderately energetic pulses. The peak power is calculated by dividing the pulse energy by the pulse duration. The peak power must be able to soften the workpiece, but must not be strong enough to cause direction ablation. There exist optimal values of laser beam intensity such that extremely localized material softening will occur.

2.4.6 Pulse overlap

The pulse overlap describes the spatial overlap between two subsequent laser pulses. It is not a parameter of the laser system itself, but depends on parameters of the process:

$$O = 1 - \frac{v_{rel}}{\emptyset PF} \quad (2)$$

Where the v_{rel} is the relative speed between laser spot and workpiece (Scanning speed), PF is the pulse repetition rate and Ø is the focal diameter. Samant et al. [2010] developed the calculation of this parameter and its incidence in the process. In experimental studies a pulse overlap of around 75% has been determined to be appropriate. Higher pulse overlap often shows a significant decrease of quality due thermal effects.

2.5 Laser drilling

Drilling has been one of the first applications in laser machining. The common industrial applications of laser drilling include cooling holes in aircraft turbine blades, optical apertures, flow orifices, and apertures for electron beam instruments [Knowles et al., 2007]. Laser drilling is an established application for lasers in the field of micro-fabrication. Application examples are broad varying in quality, processing time, costs, and other conditions.

Laser drilling is a noncontact, precise, and reproducible technique that can be used to form small diameter and high-aspect ratio holes in a wide variety of materials. The advantages of laser drilling include the ability to drill holes in difficult-to-machine materials such as superalloys, ceramics, and composites without high tool wear rate normally associated with conventional machining of these materials. In laser drilling, the high intensity, stationary laser beam is focused onto the surface at power densities sufficient to heat, melt, and subsequently eject the material in both liquid and vapor phases. There are four approaches to laser drilling, namely, single pulse, percussion, trepanning, and helical drilling [Sugioka et al., 2010]. These are shown in Figure 8.

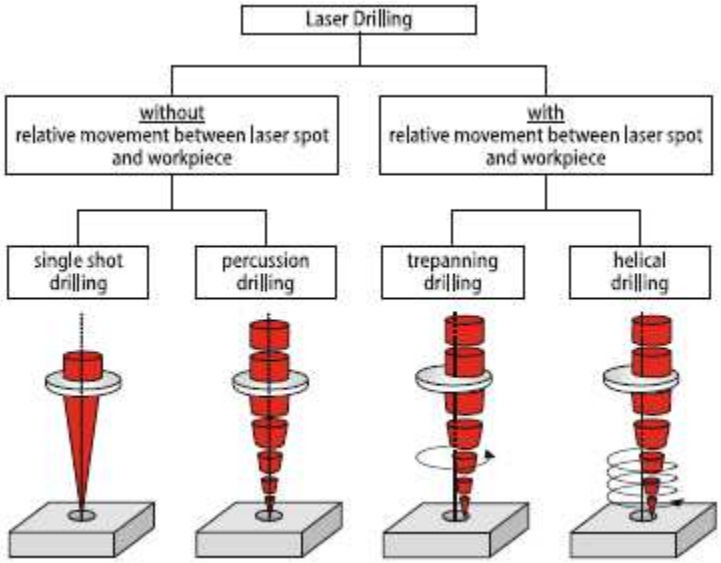

Figure 8: Drilling approaches [Sugioka et al., 2010].

2.5.1 Laser drilling without relative movement between laser spot and workpiece

These are characterized by the absence or neglectability of a relative movement between laser spot and workpiece during the drilling process. Therefore, the hole diameter strongly corresponds to the focal diameter and the applied pulse energy. This simplifies the process but also decreases the flexibility when changing the diameter of the drilled hole.

2.5.1.1 Single pulse drilling

Only one laser pulse hits the target and generates the complete drilling. Therefore, very high pulse energies are required. The pulse duration is usually in the range of several hundred us. This approach presents the limitation of the material thickness. A typical material thickness for single pulse drilling is about one mm in steel materials. The achievable aspect ratio is

approximately 1:10. Holes drilled with single pulse drilling often show a decrease in diameter on the backside of the workpiece.

2.5.1.2 Percussion drilling

Multiple laser pulses are directed on the same spot to form a through hole. It can be used to increase accuracy by ablating smaller volumes with each pulse and to increase the depth of the drilled hole up to several mm depth.

Percussion drilling is the most common approach for laser drilling without relative movement between laser spot and workpiece, since is clearly brought out the fact that more efficient hole drilling and better quality holes are obtained through the use of multiple low-energy laser pulses than with a single high-energy laser pulse [Bandyopadhyay et al., 2002].

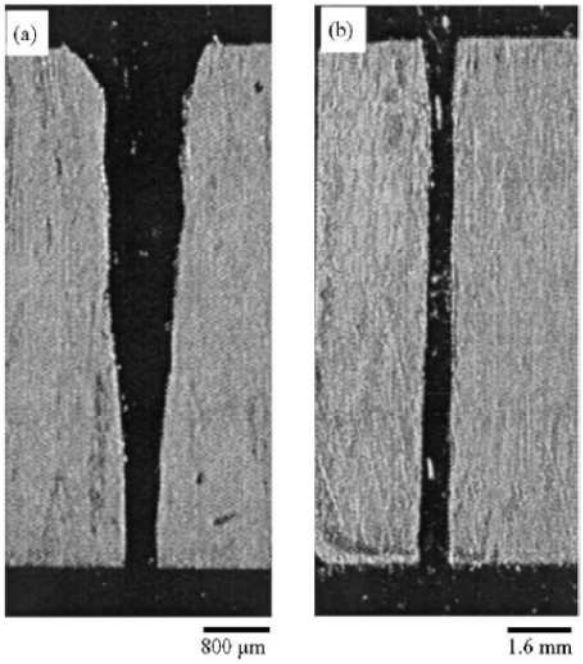

Figure 9: Longitudinal cross-sections of laser drilled hole in: (a) 4 mm, (b) 8 mm thick Ti-6Al-4V (pulse width: 0.7 ms, pulse energy: 7 mJ, pulse frequency: 4 kHz) [Bandyopadhyay et al., 2002].

Many authors investigated this drilling approach for different materials. Wang et al. [2012] investigated the number of pulses for drilling through the sample and the average drilling rates with different laser fluences, sample's thickness, repetition rates and ambient gas pressures in the nanosecond drilling of stainless steel. Bandyopadhyay et al. [2002] found the focal position, the pulse energy and the pulse duration the most significant process parameters influencing the hole quality in the laser drilling of thick sections of inconel 718 and titanium alloy (Figure 9). Biswas et al. [2010] studied the influence of lamp current, pulse frequency, air pressure and thickness of the job on the hole circularity at exit and the hole taper of the drilled hole for laser drilling of gamma-titanium-aluminide. Mishra et al. [2013a and 2013b] modeled and optimized laser beam percussion drilling of aluminium sheet and inconel 718.

2.5.2 Laser drilling with relative movement between laser spot and workpiece

These are characterized by relative movement between the laser spot and the workipece. Although these approaches are presented as a drilling process they may be considered as laser cutting and laser milling processes. They allow obtaining holes with different diameters independent of the laser spot size.

2.5.2.1 Trepanning drilling

The holes are produced by drilling a series of overlapping holes around a circumference of a circle so as to cut contour out of the plate. It is usually performed with long pulsed lasers. This approach consists in a laser cutting of holes, so the process itself is described in the next section.

Few authors studied these drilling approach; Choudhury et al. [2012] studied the effect of laser power, assist gas pressure, cutting speed and stand-off distance on the hole taper and hole circularity in laser trepanning of polymeric materials. Yilbas et al. [2011] investigated laser trepanning of small diameter hole into Ti–6Al–4V alloy. Ashkenasi et al. [2011] presented laser trepanning of different tapered through holes with an entrance diameter of 90 to 150 μm in different 1 mm thick metal and ceramic.

2.5.2.2 Helical drilling

The hole is drilled with more than one revolution of the laser spot and can be understood as multi pass trepanning. With each pass, the ablation front moves downward on a helical path. The amount of material ablated with each pulse is smaller compared to trepanning. This leads to an increase in contour accuracy and a decrease in thermal load of the workpiece. It is generally performed with short and ultrashort pulsed laser sources. In this case, this approach can be understood as a laser milling process which is described in following sections.

2.6 Laser cutting

Laser cutting is a two-dimensional machining process in which material removal is obtained by focusing a highly intense laser beam on the workpiece. It is a high-speed, repeatable, and reliable method for a wide variety of material types and thicknesses producing very narrow and clean-cut width. The conditions and the advantages of the laser machining, makes the laser cutting a high speed process with fine and precise cut dimensions (very narrow kerf width such that process can be used for fine and profile cutting) [Dahorte et al., 2008].

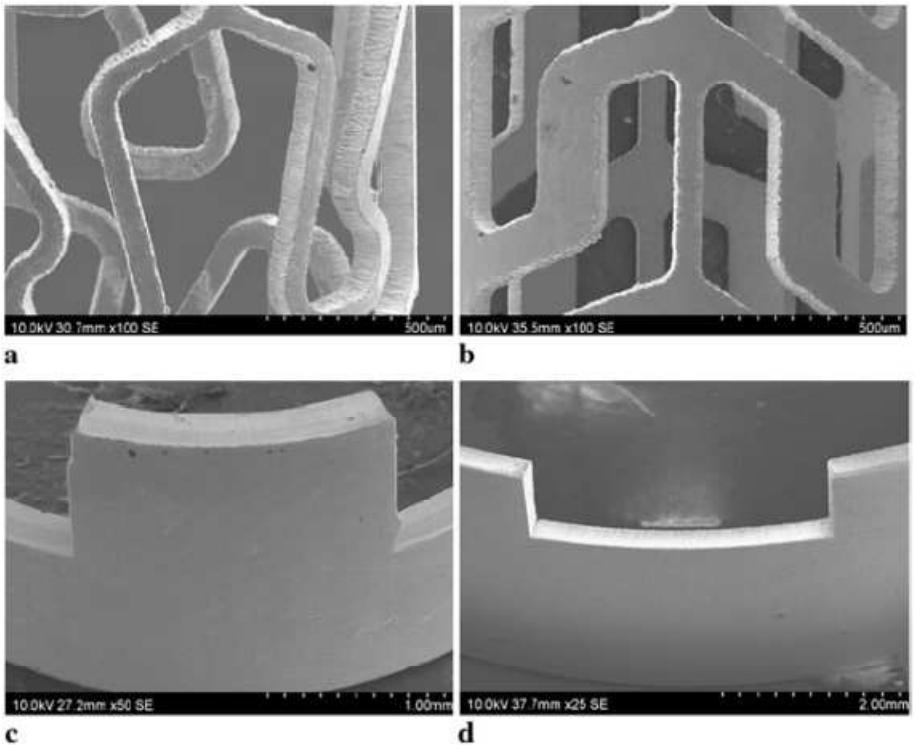

Figure 10: SEM images of picoseconds laser cutting of stents (a) nitinol, (b) cobalt chromium, (c) silver, and (d) titanium [Muhammad et al., 2011].

As explained in previous section, lasers are now used for cutting a variety of materials ranging from metals, plastics, ceramics, to composites. Due to the high machining precision and processing speed, laser cutting offers tremendous economical benefits in the production lines. One of the top applications is the micro-machining of coronary stents which requires of high quality cuts with very small kerf widths. Many authors investigated the cutting of stents in stainless steel [Muhammad et al., 2010; Meng et al., 2009 and Kathurya, 2005] and nitinol among other materials [Muhammad et al., 2011] (Figure 10) with different laser types.

Laser cutting techniques can be subdivided into two groups considering the mechanisms responsible for material ejection at the cutting front.

2.6.1 Melt cutting

Contains processes where the laser provides the energy to heat and melt the material but does not deliver the energy to remove the material from the processing zone. In melt cutting, the laser induced melt is removed by a coaxial cutting gas jet that is applied by a gas nozzle close to the laser material interaction zone.

Therefore, the laser optics and the gas nozzle usually form a unit, which is moved over the workpiece surface, along the cutting path. In the steady state cutting process, a part of the laser radiation is absorbed at the solid workpiece surface resulting in pre-heating. Another

part of the laser radiation is absorbed at the liquid cutting front, where heat diffusion and advection transport the heat to the solid liquid interface, i.e., the melting front.

This group of laser cutting is the most common. Choudhury et al. [2010] evaluated the effect of laser power, cutting speed and compressed air pressure on the laser HAZ, surface roughness and dimensional accuracy. They used a CW CO_2 laser for cutting of PP, PC and PMMA polymers with an air compressed gas. Pfeifer et al. [2010] used a nanosecond Nd:YAG laser to cut Nitinol sheets to investigate the influence of different cutting parameters on the cut quality and the material properties. Yan et al. [2012] studied the effects of different parameters on striation characteristics of laser cutting of alumina sheets with 1mm thickness using a nanosecond Nd:YAG laser. Yilbas et al. [2009] analyzed the effect of cutting parameters on the kerf size variations of the CO_2 laser cutting of thick steel sheets with nitrogen as an assisted gas.

2.6.2 Laser ablation cutting

Using pulsed laser radiation or high brilliance CW lasers leads to vaporization and eventually plasma formation at the laser material interaction zone. The resulting pressure gradient at the gas melt interface is responsible for melt ejection. Hence these processes do not require an external gas jet to remove the material which is molten or vaporized. Pulsed laser with peak intensities are used for laser ablation cutting, resulting in melting, vaporization, and plasma ignition. While the plasma plume expands, pressure gradients at the gas liquid interface lead to the ejection of molten and vaporized material out the cutting zone. Laser ablation cutting is mostly performed with high pulses energies (>10 uJ) and repetition rates in the kHz regime. Laser ablation cutting can be classified with respect to the pulse duration into short pulsed and ultrashort pulsed laser cutting, however the most common is the ultra-short pulse laser cutting.

Due to the very high peak intensities of ultra-short pulses, nonlinear effects dominate the absorption of the laser radiation. Therefore, almost every material can be cut regardless of the used wavelength. Ultrashort pulse laser cutting is considered to be without thermal impact on the workpiece. Although cutting without thermal impact is possible, the use of gas jet is often used even when an ultrashort pulse laser is used [Muhammad et al., 2011]. Few authors researched the laser cutting ablation without the use of assisted gas. Yung et al. [2005] investigated the micro-machining of NiTi using a 355nm nanosecond Nd:YAG laser and the influence of the process parameters on the kerf geometry and cutting quality. Wang et al. [2010] studied the effects of various conditions on the cutting quality of alumina substrates with a Ti:sapphire femtosecond laser cutting process. Li et al [2006] also investigated femtosecond laser processing of NiTi SMA with any gas assistant.

2.7 Laser milling

The laser milling is based on the generation of overlapping shallow multiple grooves by scanning a single laser beam to systematically remove the surface layer of the workpiece material. Vaporization of the material during laser scanning is a primary material removal mechanism for the formation of each groove. Overlapping of the grooves is realized by applying a continuous feed motion to the workpiece perpendicular to the laser scanning direction. The process is repeated to remove the additional layers of material by applying intermittent feed motion perpendicular to the previously machined surface to either the workpiece or the focusing lens.

The laser beam is directed along the z-axis, while, the workpiece is moved in x- and y-directions by linear translational stages. During machining, the workpiece is translated relative to the focal spot of the beam in +x- direction. The formation of continuous groove is facilitated by adjusting the workpiece translation speed and repetition rate of the laser. Figure 11 shows a schema of the laser milling process.

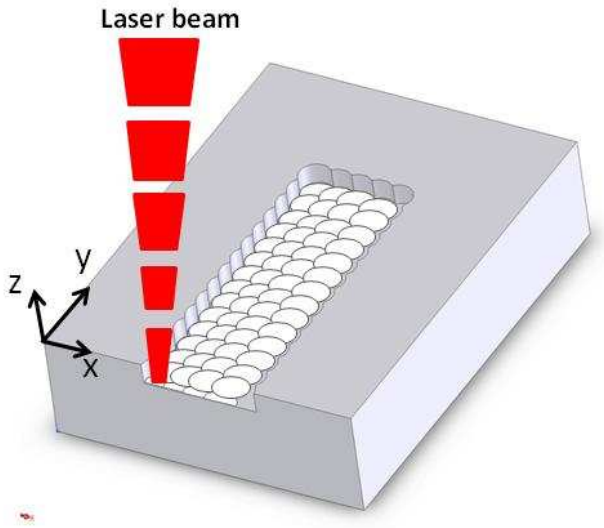

Figure 11: Schematic illustration of the laser milling process.

Laser milling is a very complex process because it is affected by the characteristics of the laser beam and the workpiece but is mainly determined by the way that both interact. Moreover, the structure and the characteristic of the material changes after each pass of the laser. Therefore, the material removal will not be the same for each laser pass. Trying to understand this complex process the authors focused the research in three levels of the process.

2.7.1 Single shot

The first level is the study of the grooves machined with a single-shot of the laser. The characteristics of a crater produced with a single-shot can be used as a good approximation to predict the machining process of a superposition of several grooves in the different directions of the laser movement.

Dobrev et al. [2006] developed a model of the crater formation to investigate the factors affecting the resulting surface finish in laser milling. Kumar et al. [2010] investigated the dependence of groove depth on laser power, repetition rate, number of scans and gas pressure in the generation of micro-notches with a nanosecond pulsed fiber laser in stainless steel and aluminum. Bordatchev et al. [2003] investigated experimentally the effect of pulse energy on the accuracy, precision and surface quality of cooper machined parts. The results showed that the crater diameter and depth increase in accordance with increase in the pulse energy. Yousef et al. [2003] used a nanosecond Nd:YAG laser in order to machine craters on brass, copper and stainless steel as bulk material. They investigated, analyzed and modeled the effect of the pulse energy on the geometry of the crater (diameter, depth and volume of material removed) and final surface profile.

2.7.2 Single pass (Laser scribing)

Laser scribing creates only superficial grooves and does not generate a complete through cut. The process is realized in one single pass of the laser which moves within the x and y axes. Thus, the machining is realized in just one layer. One of the most common applications of laser scribing is selective ablation of layer systems such as in thin-film solar cells [Gecys et al., 2011; Lauzurica et al., 2011 and García-Ballesteros, 2011]. The film-solar cells consist of several layers of materials. Some of these layers have to be patterned without delamination or damage of other layers. The other application consists in the microfluidic devices which are used to manipulate liquids and gases in diagnostics and biomedical research. Microfluidics are channels in transparent materials (polymer or glass) having cross-sectional dimensions on order of 10-500 μm. [Gomez et al., 2005; Teixidor et al., 2012 and Romoli et al., 2011]

2.7.3 Multi passes (3D milling)

The multi pass approach is the complete laser milling process. The authors study the effects of the process parameters on the final geometry. There are many investigation of the laser milling, from simple geometries like channels in a macro level [Bartolo et al., 2006 and Samant et al., 2010] to the machining of final parts [Pham et al., 2007 and Kaldos et al., 2004]. Other authors studied the process machining complex shapes with round shapes, angles or taper walls [Ciurana et al., 2009 and Dhupal et al., 2007].

Chapter 3. Modeling laser micromachining of micro-channels using machine learning techniques

Chapter 3 presents an experimental study of the process parameters (scanning speed, pulse intensity and pulse frequency on the dimensional accuracy, surface roughness and material removal rate on the machining of micro-channels on hardened steel. Different machine learning techniques ((k-Nearest Neighbours, neural networks, decision trees and linear regression models) are tested on the datasets to try to build high accuracy models for each output variable.

This study was presented in an article entitled "*Modeling pulsed laser micromachining of micro geometries using machine learning techniques*", submitted to the Journal of Intelligence Manufacturing in June 2013.

Modeling pulsed laser micromachining of micro geometries using machine-learning techniques

Teixidor, D., Grzenda M., Bustillo, A., Ciurana, J.

Department of Mechanical Engineering and Industrial Construction
Universitat de Girona, Girona, Spain

Faculty of Mathematics and Information Science, Warsaw University of Technology,

Warsaw, Poland

Department of Civil Engineering, University of Burgos, Burgos, Spain

Abstract

A wide range of opportunities are emerging in the micro-system technology sector for laser micro-machining systems, because they are capable of processing a various types of materials with micro-scale precision. However, few process datasets and machine learning techniques are optimized for this industrial task. This article aims to show how the process parameters of micro-laser milling influence the final features of the microshapes that are produced and aims to identify, at the same time, the most accurate machine learning technique for the modelization of this multivariable process. We studied the capabilities of laser micro-machining by performing experiments on hardened steel with a pulsed Nd:YAG laser. Arrays of micro-channels were manufactured using various scanning speeds, pulse intensities and pulse frequencies. The results are presented in terms of the main industrial requirements for any manufactured good: dimensional accuracy (in our case, depth and width of the channels), surface roughness and material removal rate (which is a measure of the productivity of the process). Different machine learning techniques were then tested on the datasets to try to build high accuracy models for each output variable. The selected techniques were: k-Nearest Neighbours, neural networks, decision trees and linear regression models. Our analysis of the correlation coefficients and the mean absolute error of all the generated models show that neural networks are better at modelling channel width and that decision trees are better at modelling surface roughness; both techniques are similar for depth and material removal rate. In all cases these two techniques are more accurate than the other two. It can be concluded that decision trees can be used for modelling laser micro-machining of micro geometries, if the dimensional accuracy of the workpiece is the main industrial requirement, while neural networks are better in the other cases.

1. Introduction

Laser systems are increasingly employed in many diverse micro-system technology sectors such as biomedicine, automotive manufacture, telecommunications, display devices, printing technologies and semiconductors (Rizvi, 2002). Material removal during the laser machining process depends, to a certain degree, on the characteristics of the laser and the properties of the workpiece; however, it is primarily affected by the interaction between the laser and the workpiece (Pham, 2007). In real factory conditions, this interaction is influenced by other types of machine-tool parameters that are easily controlled, such as pulse frequency, peak power, scanning speed and overlapping. Although many of these process parameters can be adjusted, in order to obtain the desired quality and to optimize the efficiency of the features being produced, there is a lack of knowledge about how they affect the laser machining process, especially in new sensitive applications like micro-machining of the shape of micro geometries (Brousseau, 2011).

Various studies have investigated how laser process parameters affect the quality of the resultant machined features. Campanelli et al. (Campanelli, 2007) analyzed the influence of frequency, scanning strategy and overlap on depth and surface roughness, during laser machining of an aluminum-magnesium alloy. The experiments and the analysis of variance showed that, in general, optimizing surface roughness was conversely related to maximizing depth. Cicala et al. (Cicala, 2008) studied the effects of pulse frequency, power, scanning speed and overlap on the MRR and surface roughness. The results showed that pulse frequency and scanning speed were the main parameters affecting surface roughness, which was reduced with lower scanning speeds and higher frequencies. The Material Removal Rate (MRR) mainly depends on pulse frequency alone. Bartolo et al. (Bartolo, 2006) analyzed the incidence of the same parameters while looking at the scanning strategy, in the process of machining channels in tempered steel and aluminum. Their results suggested that, with lower frequencies and reduced laser power, the surface quality is better. However, both parameters need to be increased, in order to achieve an optimum value for a higher MRR. Kaldos et al. (Kaldos, 2004) used a CNC milling machine with a Nd:YAG laser source, on die steel, to study the impact of lamp current, pulse frequency, overlapping and scanning speed on surface roughness and the MRR. They concluded that an increase in current intensity or an insufficient overlap of laser passes results in a less well finished surface. Semaltianos et al. (Semaltianos, 2010) studied the effects of fluence and pulse frequency on surface roughness and MRR in nickel-based alloys with a Nd:YVO4 picosecond laser. They also analyzed the surface morphology of these alloys with AFM and SEM techniques.

Ciurana et al. (Ciurana, 2009) used a pulsed Nd:YAG laser to study the effect of the process parameters on minimum volume error and surface roughness in laser machined tool steel for macro scale geometry, although micro scale geometry was not evaluated. The experimental results were inconsistent for large shapes. Dhara et al. (Dhara, 2008) micro-machined die steel while modifying pulse intensity, pulse frequency, pulse duration and air pressure, in order to predict the optimum process parameter settings for maximum depth with a minimum recast

layer. Kumar et al. (Kumar, 2010) investigated the influence of laser power, pulse frequency, number of scans and air pressure, on the groove depth in the generation of micro-notches with a nanosecond pulsed fiber laser on stainless steel and aluminum. Karazi et al. (Karazi, 2009) machined and characterized micro-channel formation by laser machining. They studied the effects of laser power, pulse frequency and scanning speed on the width and depth of the channels. They also modeled the process using Artificial Neural Networks (ANN).

The application of Artificial Intelligence (AI) techniques to model micro machining of metal components is an open issue. Most of the very few works on this topic focus on the application of ANNs to this task: the work of Desai et al. (Desai, 2012) predicted the depth of cut for single-pass laser micro-milling process using ANN and genetic programming approaches and the work of Karazi et al. (Karazi, 2009) compared ANN and DoE models for the prediction of laser-machined micro-channel dimensions. If we open the state of the art to the application of AI techniques to machining processes similar to laser milling, we can conclude that ANNs are the most common technique used for most of these processes such as milling, drilling or laser finishing (Chandrasekaran, 2010), although many other AI techniques have also been applied for such purposes. Bustillo et al. proposed the use of Bayesian Networks and ensembles to predict surface roughness in drilling (Bustillo, 2012), laser finishing (Bustillo 2011a) and roughing (Bustillo 2011b) operations, Grzenda et al. proposed different evolutionary algorithms to improve ANNs accuracy (Grzenda 2012a) and 2012b) in drilling and milling operations and Mahdavinejad et al. proposed the use of artificial immune systems to model milling processes (Mahdavinejad, 2012). In any case, most of the most recent works use ANNs as a standard technique to be improved by new approaches, such as those proposed by Bustillo et al. (Bustillo, 2011b), Correa et al. (Correa, 2009), Desai et al. (Desai, 2012), Mahdavinejad et al. (Mahdavinejadm 2012) and Diez-Pastor et al. (Diez-Pastor, 2012).

The aim of this work is to describe the information needed to improve the laser micro-machining process in the production of microshapes and to develop a suitable AI model for the modelization of this industrial task. The process parameter settings are optimized with regression models developed from experimental work, to achieve the required dimensional precision, surface quality and productivity. Arrays of micro-channels are fabricated on hardened tool steel using laser machining processes, while measuring feature size, geometric accuracy, surface roughness and the MRR. This work will contribute to the selection of appropriate process parameters through an analysis of the influence of scanning speed, pulse frequency and pulse intensity on the final quality of the machined micro-feature. Moreover, machine learning methods are used to evaluate the complexity of prediction tasks. Representatives of rule-based, instance-based and linear and nonlinear models are applied. Prediction accuracy remains at different levels depending on the parameter to be modeled rather than the technique used to model it. Hence, the complexity of modeling individual features of interest has been determined.

2. Experimental set up

The experiments, set up to study the influence of the process parameters, were carried out with a pulsed Nd:YAG, Deckel Maho Lasertec 40 machine, with 100W average laser power and a wavelength of 1,064nm.

Although the pulse intensity level on the surface was not measured during our experiments, based on the technical data of the laser system, we can provide an ideal pulse intensity level, which is given by:

$$\mathrm{PI} = \frac{\mathrm{P}}{\pi\left(\frac{\mathrm{d}}{2}\right)^2} \tag{1}$$

where, P is the laser power (100 W), and d is the beam spot diameter (0.003 cm). Therefore the ideal pulse intensity was estimated to be 1.4 W/cm2. Furthermore, we can determine the ideal Peak Pulse Power (PPP), which is given by:

$$\mathrm{PPP} = \frac{\mathrm{P}}{\tau} \tag{2}$$

where, P is the laser power (100 W) and τ is the laser pulse duration (10 ns). For the laser characteristics used in this study, the PPP is estimated to be 10 MW/s. The specifications of the micro channels are: 200µm in width (W) and 50µm in depth (D), machined by the motion of the laser beam in the x and y directions removing material in all three directions (x, y and z). As shown in Figure 1, in order to machine the entire cavity, there is overlap between adjacent pulses (Oy) within a pass of length (L) and overlap between successive passes (Ox). All the experiments were performed with a laser spot size (Ø) of 0.03mm and a track displacement (distance between passes, a) of 10µm. The overlap Ox between successive passes is given by (Samant, 2010):

$$\mathrm{O_x} = \left(1 - \frac{\mathrm{a}}{\emptyset}\right) \cdot 100 \tag{3}$$

In this study, Ox was 66.6%. The overlap between adjacent pulses (Oy) depends on the scanning speed, the pulse frequency and the spot diameter. It is therefore different for each experiment. Oy is given by:

$$\mathrm{O_y} = \left(1 - \frac{\mathrm{SS}}{\mathrm{PF}\cdot\emptyset}\right) \cdot 100 \tag{3}$$

where, SS is the scanning speed and PF is the pulse frequency, which are different for each experiment.

The workpiece material was hardened AISI H13 tool steel, selected because it is a widely used material in the moulds and dies industry.

Dimensional measurements were performed with a ZEISS SteREO Discovery.V12 stereomicroscope. Quartz PCI© software was used to measure the feature dimensions and Mitutoyo SV2000 Surftest equipment was used to measure surface roughness.

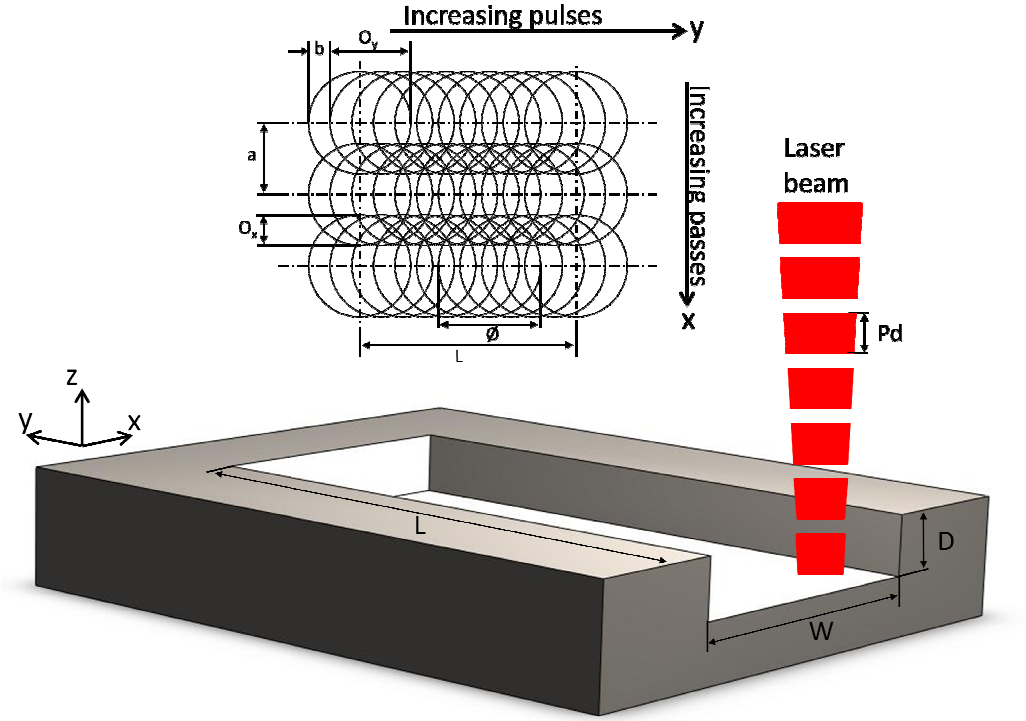

Figure 1. A schematic illustration of the 3D-laser milling and the overlapping of the laser pulses.

Some screening experiments were performed to select the appropriate factor levels of the process parameters. Several micro-channels were machined, in each case changing one single parameter while the others remained fixed. In this way, we could observe the impact of each single control variable, in order to determine the control parameter range. This pre-evaluation provides a full factorial design with the variable factors and factor levels presented in Table 1, which is then used to study the influence of the input parameters on the finished workpiece, for which the response parameters are surface roughness [µm], the MRR[mm3/min] and the width and depth dimensions [µm].

Table 1. Variable factors and factor levels.

Variable Factors	***Factor Levels***		
Scanning Speed (SS) [mm/s]	200	225	250
	275	300	325
	350	375	400
Pulse Intensity (PI) [%]	35	40	45
Pulse Frequency (PF)[kHz]	35	40	-

3. Experimental results and discussion

Following the design of the experiments summarized in Table 1, 54 micro channels were machined with the laser machining process. Surface roughness was measured in five different sections of each micro-channel to get the mean value of the entire channel. Then, each channel was cut into three parts to get the cross-section profiles, from which the measurements of depth and width were taken by processed digital images. Once again, five different measurements, proportionally distributed along the depth and the width, were measured. The removed area was also measured for each channel profile, in order to calculate the material removal rate. The mean values of the experimental results obtained from the machined features for all the combinations of the variable factors are shown in Table 2. The micro-channels presented variations in dimensions and shape. These variations are clearly represented in Figure 2, which presents the images of six micro-channels. Analysis of Variance was performed for each response factor to study the influence of the process parameters.

Table 2. DoE with the experimental results.

#	PI (%)	PF (kHz)	SS (mm/s)	depth (µm)	width (µm)	Ra (µm)	MRR (mm^3/min)	#	PI (%)	PF (kHz)	SS (mm/s)	depth (µm)	width (µm)	Ra (µm)	MRR (mm^3/min)
1	35	35	200	18.3	189	0.505	0.034	**28**	35	40	200	13.9	192.9	0.560	0.025
2	35	35	225	17.4	190	0.477	0.036	**29**	35	40	225	12.6	175.5	0.479	0.017
3	35	35	250	14.9	191	0.533	0.034	**30**	35	40	250	11.6	188.1	0.531	0.026
4	35	35	275	15.7	195.8	0.455	0.041	**31**	35	40	275	15.7	191.6	0.465	0.034
5	35	35	300	12.9	197.7	0.456	0.033	**32**	35	40	300	8.1	193.2	0.506	0.026
6	35	35	325	11.6	193.2	0.463	0.027	**33**	35	40	325	8.1	189.8	0.520	0.020
7	35	35	350	8.1	191.7	0.470	0.019	**34**	35	40	350	11.6	189.2	0.471	0.034
8	35	35	375	10.9	192.5	0.504	0.021	**35**	35	40	375	10.8	189.9	0.525	0.027
9	35	35	400	10.2	192.8	0.457	0.027	**36**	35	40	400	11.7	190.1	0.463	0.027
10	40	35	200	29.9	183.9	0.549	0.055	**37**	40	40	200	31.2	186.1	0.531	0.065
11	40	35	225	30.0	184.9	0.481	0.059	**38**	40	40	225	26.2	186.6	0.571	0.061
12	40	35	250	25.4	184.4	0.513	0.061	**39**	40	40	250	23.7	187.3	0.462	0.056
13	40	35	275	21.9	187.2	0.664	0.048	**40**	40	40	275	17.1	190.4	0.510	0.026
14	40	35	300	16.8	189.9	0.478	0.036	**41**	40	40	300	17.7	195.7	0.459	0.041
15	40	35	325	14.4	188.4	0.473	0.032	**42**	40	40	325	19.2	192.3	0.461	0.061
16	40	35	350	18.5	188.5	0.485	0.041	**43**	40	40	350	17.3	190.3	0.435	0.039
17	40	35	375	18.2	190.5	0.457	0.048	**44**	40	40	375	16.5	190.5	0.490	0.044
18	40	35	400	18.4	190.0	0.382	0.043	**45**	40	40	400	14.2	192.3	0.423	0.040
19	45	35	200	39.6	184.4	0.519	0.065	**46**	45	40	200	38.6	184.4	0.519	0.074
20	45	35	225	35.8	184.1	0.513	0.073	**47**	45	40	225	35.0	184.2	0.531	0.067
21	45	35	250	33.7	181.0	0.493	0.072	**48**	45	40	250	29.5	180.7	0.526	0.071
22	45	35	275	22.1	184.3	0.443	0.063	**49**	45	40	275	26.8	185.3	0.523	0.056
23	45	35	300	25.4	186.2	0.451	0.057	**50**	45	40	300	25.1	187	0.514	0.067
24	45	35	325	26.5	189.2	0.451	0.061	**51**	45	40	325	22.8	186.8	0.446	0.062
25	45	35	350	20.8	191.1	0.447	0.047	**52**	45	40	350	19.3	187.3	0.509	0.039
26	45	35	375	19.8	189.9	0.397	0.054	**53**	45	40	375	17.5	187.6	0.408	0.040

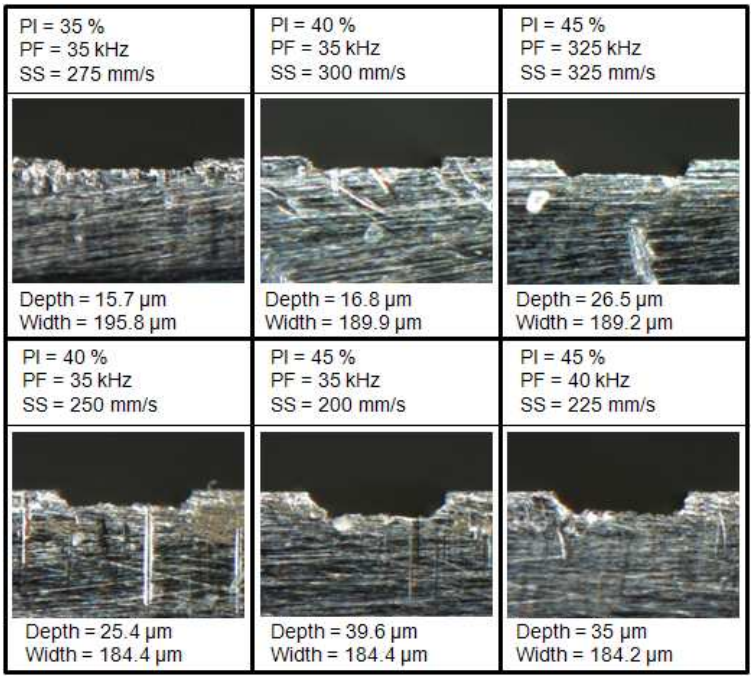

Figure 2. Images of micro-channels

3.1 Micro-channel depth

As can be seen in Table 2, which shows the results obtained for the micro-channel depths, the target depth of 50µm was never reached. This is clear in Figure 3, where the influence of the scanning speed and the pulse intensity on the depth dimension is summarized. It shows that almost all of the machined depths are within the 10 to 25 µm range and only few experiments achieved depth values above this range.

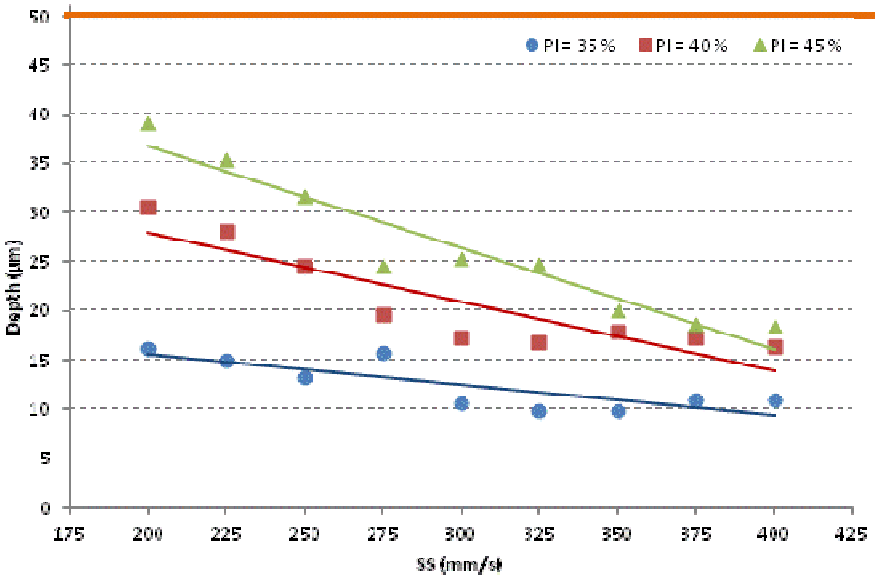

Figure 3. Influence of scanning speed and pulse intensity on depth dimension.

The trend lines presented in Figure 3 clearly show that higher scanning speeds result in smaller depths and higher pulse intensities result in deeper micro-channels. Thus, the greatest depth was reached with the lowest scanning speed (200mm/s) and the highest pulse intensity (45%). In a laser milling process (with 3D movements), slower displacements of the laser beam means that the surface is machined with high energy for a longer time, which allows a larger amount of energy to be absorbed by the material resulting in channels of greater depths. This demonstrates that higher pulse intensity values would be necessary to obtain depth values closer to the target.

Table 3 summarizes the results of the ANOVA revealing that the most significant factors for the average depth of micro-channels are scanning speed and pulse intensity, as previously pointed out ($p<0.005$). The F-values indicate that pulse intensity is the most significant factor, which is made clearer by the contribution values.

Table 3. ANOVA analysis for depth.

Factor	***Degrees of freedom (DOF)***	***Sum of squares (SS)***	***Mean squares (MS)***	***F-value***	***P-value***	***Contribution (%)***
PI	2	1775.26	887.63	94.72	0.000	83.9
PF	1	25.43	25.43	2.71	0.107	2.4
SS	8	1163.59	145.45	15.52	0.000	13.7
Residual	42	393.61	9.37	-	-	-

Compared with other authors, the experimental results shows that higher pulse intensity and lower scanning speeds tend to give deeper channels, which is in line with the idea that the number of pulses per mm increases, as the laser beam moves more slowly across the workpiece, thus removing more material. Furthermore, when the intensity is higher, the pulse energy increases, which in turn results in greater depth values (Bordatchev, 2003 and Youseff, 2003).

3.2 Micro-channel width

Table 2 presents width dimensions that range from 175.5 to 197.7 µm. Once again, no experiment achieves the target value (200 µm). Figure 4 shows how the scanning speed and the pulse intensity affect the average width. In this case, in contrast to the results on depth, the experimental values are closer to the target width when the scanning speed is high and the pulse intensity is low. These converse effects on width and depth are due to the fact that straight walls are really difficult to achieve. Thus, as the channel becomes deeper, the width becomes narrower, producing a smaller mean width value.

Table 4 summarizes the results of the ANOVA analysis on the average width. It can be seen that the pulse frequency has no statistically significant effect on width dimension. The parameters that do have a significant effect on the width are pulse intensity and scanning speed, with pulse intensity being the most significant, as is clearly indicated by the results of the F-value, with a contribution of 69.5 %

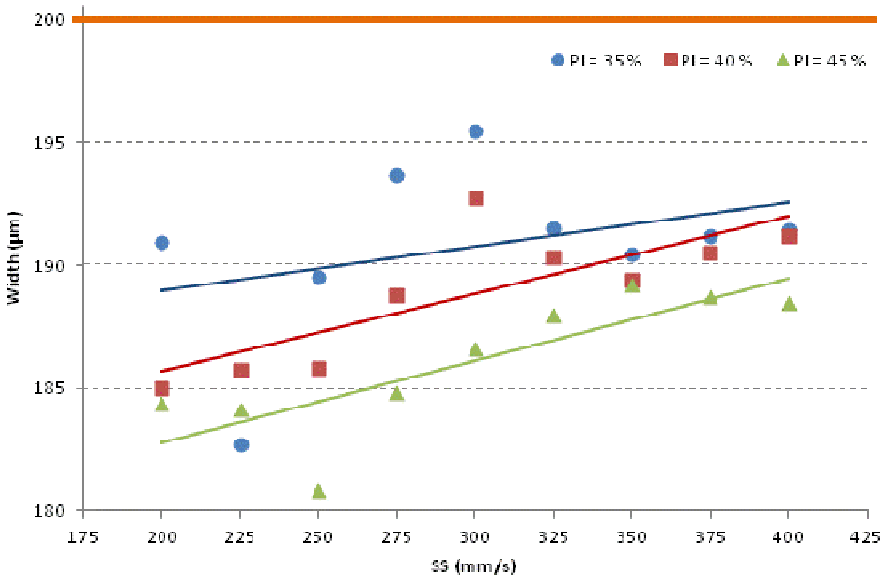

Figure 4. Influence of scanning speed and pulse intensity on width dimension.

Table 4. ANOVA analysis for width.

Factor	***Degrees of freedom (DF)***	***Sum of squares (SS)***	***Mean squares (MS)***	***F***	***P***	***Contribution (%)***
PI	2	195.88	97.94	12.15	0.000	69.5
PF	1	5.01	5.01	0.62	0.435	3.5
SS	8	304.22	38.03	4.72	0.000	27
Residual	42	338.43	8.06	-	-	-

Although other studies using single laser shots (Bordatchev, 2003 and Youseff, 2003) have concluded that crater depth and diameter increase with pulse energy, in our case, the width decreases. This effect can be explained because in the laser milling process several passes are necessary along all axes to obtain the final shape. Thus, because of the difficulty in achieving straight walls due the Gaussian shape of the laser beam, as the channel gets deeper, the width narrows. Therefore, the mean width of the channel decreases.

3.3 Micro-channel surface roughness

The influence of the variable factors on surface roughness was also evaluated. Figure 5 shows the effect of the scanning speed and the pulse intensity on surface roughness. The trend lines indicate that surface roughness decreases at high scanning speeds. The influence of pulse intensity is less clear, although it does seem to indicate that higher intensity results in lower surface roughness. Slow scanning speeds do not improve surface roughness and fast movements hardly affect it. Furthermore, the experimental results show no large differences, with a range between 0.4 and 0.55µm. The best surface roughness values were obtained with a combination of the highest pulse intensity and highest scanning speed.

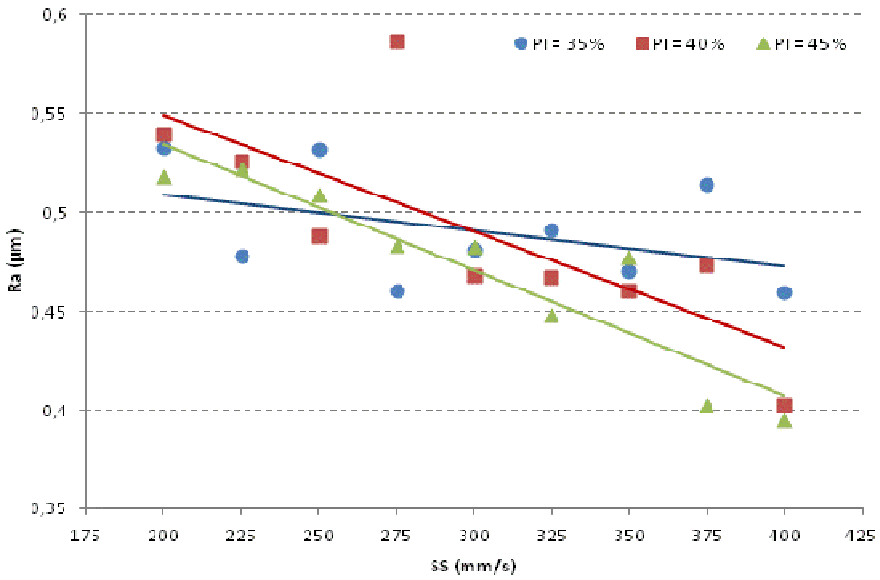

Figure 5. Influence of scanning speed and pulse intensity on surface roughness.

Table 5 summarizes the results of the ANOVA, which reveal that scanning speed is the most significant factor in surface roughness, while neither pulse intensity nor pulse frequency has a statistically significant effect on surface roughness. However, the contribution of the scanning speed is relatively small at 46.1 %.

Table 5. ANOVA analysis for surface roughness.

Factor	***Degrees of freedom (DF)***	***Sum of squares (SS)***	***Mean squares (MS)***	***F***	***P***	***Contribution (%)***
PI	2	0.004	0.002	1.92	0.160	13.4
PF	1	0.005	0.005	5.79	0.021	40.5
SS	8	0.051	0.006	6.58	0.000	46.1
Residual	42	0.039	0.001	-	-	-

The experimental results shows that high pulse intensities and slower scanning speeds mean that more energy is applied to the workpiece, increasing the damage caused to the surface. Therefore, lower pulse intensities and higher scanning speeds will improve the final quality of the machined parts, because surface roughness will be reduced (Bordatchev, 2003).

3.4 Micro-channel material removal rate

The effect of the process parameters on the MRR was also studied. Figure 6 presents the effects of pulse intensity and scanning speed on the MRR. The trend lines clearly indicate that MRR increases with lower scanning speeds and higher pulse intensities. Although higher scanning speeds result in faster processes, the area of material removal is smaller, thus the MRR decreases. On the other hand, higher pulse intensity results in deeper channels and, in consequence, higher MRRs.

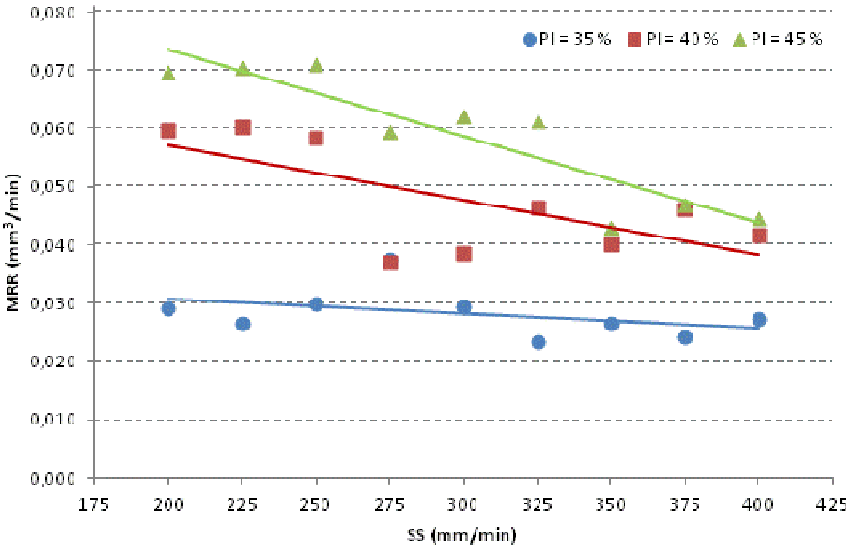

Figure 6. Influence of scanning speed and pulse intensity on MRR.

The ANOVA results for MRR are shown in Table 6. It can be seen that pulse frequency has no statistically significant effect on MRR. Pulse intensity is found to have the most significant effect on MMR with a contribution of 93.1 %, while scanning speed has a somewhat lesser impact, with a contribution of 5.9 %.

Table 6. ANOVA analysis for MRR.

Factor	*Degrees of freedom (DF)*	*Sum of squares (SS)*	*Mean squares (MS)*	*F*	*P*	*Contribution (%)*
PI	2	0.0086	0.0043	57.92	0.000	93.1
PF	1	$4.82 \cdot 10^{-5}$	$4.82 \cdot 10^{-5}$	0.65	0.424	1
SS	8	0.0021	0.0002	3.65	0.003	5.9
Residual	42	0.0031	$7.4 \cdot 10^{-5}$	-	-	-

Since MRR is directly proportional to the width and depth of the channel, the MRR plot has a shape that is similar to the depth plot, due to the fact that the influence of the depth is greater than that of the width.

4 Modeling

Following the experimental tests and the study and ANOVA analysis of the relationship between the parameters, various machine learning techniques were then selected and tested for the depth and width dimension, surface roughness and MRR, in order to determine their correlation with the process parameters. The objective was to obtain the most appropriate process parameters for producing minimal surface roughness with the highest material removal rate. This selection included the k-Nearest Neighbors (kNN) technique with k set to 1,...,5, linear regression, decision trees, and multilayer perceptrons. Hence, these methods were considered, which have clear decision rules and the capability to perform both linear and nonlinear transformations on the input data. A 10 fold cross-validation was applied, which takes account of the capability of the models to predict output parameter values from new input data. A naïve approach was adopted as a baseline, to ensure that the new models are extracting useful information from the dataset. The correlation coefficient (R2) and Mean Absolute Error (MAE) for individual input parameters modeled with the naïve approach were analyzed. The results are shown in Table 7, in which it may be seen that the correlation coefficient for the four models with the naïve approach is very low.

Table 7. Naïve prediction for individual parameters.

Parameter	***Correlation coefficient (R^2)***	***Mean absolute error (MAE)***
Depth	0.178	6.49
Width	0.133	3.078
Surface Roughness (R_α)	0.239	0.0397
MRR	0.178	0.0141

Starting with the low accuracy provided by a naïve approach, different machine learning models were built for each output parameter. First, the accuracy, in terms of R2 and MAE, of the depth modelling are shown in Table 8. The best results are observed for decision trees (in bold in Table 8), which yield the highest correlation coefficient and lowest MAE out of all analyzed models. It can be observed that 1NN is the best technique out of all the analyzed kNN simulations. This suggests limited noisiness of depth, i.e. the most similar input features provide the best estimation of the output parameter. It is interesting to investigate the definition of the tree shown in Fig. 7. As is clear from the ANOVA analysis, pulse intensity is the main parameter (83.9%) for this process, therefore the first node refers to this parameter; scanning speed is the second parameter from the ANOVA analysis (13.7%) and forms the

second level nodes of the tree; leaving the last level for the lower influence: the pulse frequency. It is also interesting how the tree generates the final leaves at different scanning speeds depending on the pulse intensity, a conclusion that was expected considering the relation between both parameters shown in Figure 3: this capability of decision trees, which produce clear graphical conclusions on the influence of each parameter, makes them the most accurate technique. Linear regression models do not also achieve the required accuracy; this result fits well with the conclusion presented in Section 3 that channel depth depends mainly on scanning speed and pulse intensity and that this dependency is not linear.

Table 8. Accuracy of different models of laser milling depth

	1NN	***2NN***	***3NN***	***4NN***	***5NN***	***Linear regression***	***Decision tree***	***Multilayer perceptron***
R^2	0.870	0.870	0.819	0.799	0.807	0.82	**0.955**	0.940
MAE	2.04	2.04	2.60	2.81	2.80	2.90	**1.31**	1.44

Figure 7. Decision tree for the estimation of depth

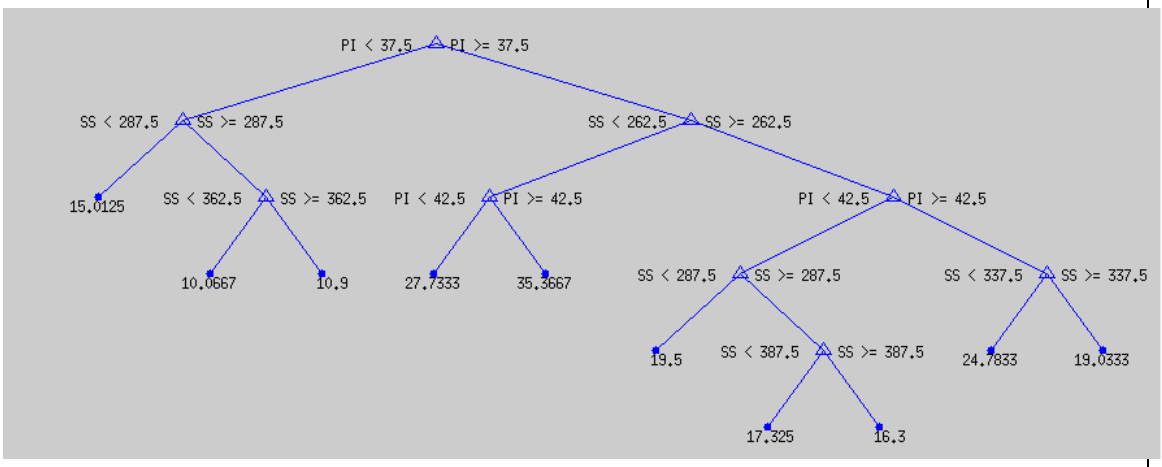

Next, the results for width were analyzed. These are shown in Table 9. The best method turns out to be a multilayer perceptron (in bold in Table 9), which suggests that a nonlinear method is needed this time. It can be observed than the 3NN method provides the best correlation of all the kNN simulations that were analyzed. However, the lowest MAE rate for kNN methods is observed for k=1. As already observed for width modelling, linear regression models do not achieve the expected accuracy; this result fits well with the conclusion presented in Section 3, that channel width depends mainly on scanning speed and pulse intensity and that this dependency is clearly not linear.

Table 9. Accuracy of different models of laser milling width

	1NN	*2NN*	*3NN*	*4NN*	*5NN*	*Linear regression*	*Decision tree*	*Multilayer perceptron*
R^2	0.325	0.325	0.393	0.364	0.348	0.367	0.371	**0.606**
MAE	1.82	1.82	1.95	2.07	2.14	2.09	2.18	**1.80**

In the case of surface roughness modeling, an interesting phenomenon is observed (Tables 10 and 11). The correlation coefficient values appear to grow with higher values of k. Hence, extended analysis for the values of k exceeding 5 was conducted, as shown in Table 11.

Table 10. Accuracy of different models of laser milling surface roughness

	1NN	*2NN*	*3NN*	*4NN*	*5NN*	*Linear regression*	*Decision tree*	*Multilayer perceptron*
R^2	0.0903	0.0903	0.2053	0.2361	0.3053	0.323	**0.5952**	0.4809
MAE	0.043	0.043	0.035	0.034	0.033	0.030	**0.023**	0.029

As expected, the value of correlation coefficient deteriorates for k>5. Obviously, it will converge to naïve results that are guessed. The main conclusion here is that the impact of process settings on surface roughness is quite sophisticated and possibly noisy, as averaging roughness from the most similar experiments to K=5 yields the best roughness prediction out of all kNN experiments. At the same time, the best overall correlation coefficient value and MAE rate is attained for decision trees (in bold in Table 10) and is largely superior to kNN. As already observed for width and depth modelling, linear regression models do not achieve the expected accuracy. This result fits well with the conclusion in Section 3, which states that channel roughness depends mainly on scanning speed with a very noisy dependency, which in no case is ever linear.

Table 11. Accuracy of different models of laser milling surface roughness – part II

	6NN	*7NN*	*8NN*	*9NN*	*10NN*	*11NN*	*12NN*	*13NN*	*14NN*	*15NN*
R^2	0.242	0.231	0.263	0.264	0.240	0.152	0.116	0.100	0.096	0.090
MAE	0.034	0.033	0.032	0.033	0.034	0.036	0.037	0.037	0.037	0.038

In the case of MRR modelling, Table 12, multilayer perceptrons and decision trees yield the best and virtually identical results (in bold in Table 12). In this case, 1NN proves to be the best method out of kNN methods for k ranging from 1 to 5. This is in line with previous findings for depth i.e. the closest input settings produce the most similar output parameter value: this

time, the MRR rates. Linear regression models do not achieve the required accuracy; this result fits well with the conclusion presented in Section 3, that MRR depends mainly on pulse intensity (more than 93% in the ANOVA test) and that this dependency is not linear.

Table 12. Accuracy of different models of laser milling MRR

	1NN	***2NN***	***3NN***	***4NN***	***5NN***	***Linear regression***	***Decision tree***	***Multilayer perceptron***
R^2	0.769	0.769	0.680	0.650	0.657	0.702	**0.825**	**0.828**
MAE	0.006	0.006	0.007	0.007	0.008	0.007	**0.005**	**0.005**

To sum up, prediction accuracy evaluation, depth and MRR can be modeled with high accuracy. Lower, but still significant accuracy is observed for surface roughness and width modelling. In the case of surface roughness, a higher value of k, meaning the averaging of roughness based on many similar experiments gives better results than using the roughness from the most similar experiment in terms of input settings. This fact suggests noisiness of the data, dependencies between inputs and outputs that are difficult to capture and even the need to collect other parameter values that contribute to the problem. In accordance with the bibliography (Bernardos 2003), it can be concluded that surface roughness depends on too many variables to assure a complete determination of the milling process and therefore models are expected to be, in any case, less accurate than the other performance parameters under study. In no case did the linear regressions show high accuracy, a result that was expected, considering the non-linear dependencies between input and output parameters in all cases.

4. Conclusions

Micro-laser milling is a machining process suitable for fabricating micro-moulds. However, it requires the most appropriate process parameters settings. In this study, the surface quality, dimensional features and productivity of micro-channels have been studied in a micro laser milling process. Although the results obtained for the micro-channels present variations, they do suggest that laser machining is capable of producing micro-geometries. Several specific conclusions should be pointed out:

1. Low scanning speeds and high pulse intensities increase the depth and decrease the width of the micro-channels.
2. The surface quality of the channels improves with a rise in scanning speed, which in turn decreases surface roughness.
3. Laser micromachining productivity increases with high pulse intensities and low scanning speeds.
4. ANOVA results show that pulse frequency is not statistically significant for the responses under study.

5. Machine learning techniques are suitable techniques with which to model laser-milling manufacture of micro shapes. Higher accuracy is observed for surface roughness and width modelling, than for depth and material removal rate modelling. Neural networks were better at modelling width dimensions and decision trees were better at modelling surface roughness; both techniques were similar for depth and material removal rate. In all cases these two techniques showed better accuracy than the other two models: k-nearest neighbors and linear regression. The use of decision trees is therefore feasible, if the dimensional accuracy of the workpiece is the main industrial requirement, while neural networks are better in the other cases.
6. The Nearest Neighbor models with higher k values show greater accuracy for roughness prediction, allowing us conclude that the noisiness of this output is higher or that it depends on more parameters than the other variables, as suggested in the previous literature.

Future work will consider other AI techniques, such as ensembles of classifiers or regressors. These ensembles are built by combining different basic classifiers that could improve final model accuracy. This experimental methodology, in which the best process parameter combination is selected, will also be applied to other types of materials, such as transparent polymers typically used for disposable lab-on-chip devices and ceramics used for various industrial applications in aeronautics, automobile manufacturing, electronics, medicine and semiconductors.

Acknowledgments

This work was partially carried out with the grant supports from the European Commission project IREBID (FP7-PEOPLE-2009-IRSES-247476) and the Spanish Science and Innovation Minister project TECNIPLAD (DPI2009- 09852).

References

Bartolo P, Vasco J, Silva B, Galo C. Laser micromachining for mould manufacturing: I. The influence of operating parameters. Assem Autom 2006;26(3):227-234.

Benardos P.G., Vosniakos G.C., "Predicting surface roughness in machining: a review", Int J Mach Tools Manuf 43(8), 2003, 833–844.

Bordatchev EV, Nikumb SK. An experimental study and statistical analysis of the effect of laser pulse energy on the geometric quality during laser precision machining. Mach Sci Technol 2003;7(1):83-104.

Brousseau E., Eldukhri E., "Recent advances on key technologies for innovative manufacturing", Journal of Intelligent Manufacturing, 22(5), 2011, 675-691.

Bustillo A., Díez-Pastor J.F., Quintana G. and García-Osorio C., "Avoiding neural network fine tuning by using ensemble learning: application to ball-end milling operations", The International Journal of Advanced Manufacturing Technology, 57(5), 2011, 521-532.

Bustillo A., Ukar E., Rodriguez J. J., Lamikiz A. "Modelling of process parameters in laser polishing of steel components using ensembles of regression trees", International Journal of Computer Integrated Manufacturing, 24(8), 2011, 735-747.

Bustillo A., Correa M., "Using artificial intelligence to predict surface roughness in deep drilling of Steel Components", Journal of Intelligent Manufacturing, 23(5), 2012, 1893-1902.

Campanelli SL, Ludovico AD, Bonserio C, Cavalluzzi P, Cinquepalmi M. Experimental analysis of the laser milling process parameters. J Mater Process Technol 2007 8/1;191(1-3):220-223.

Chandrasekaran M, Muralidhar M, Krishna C, Dixit U "Application of soft computing techniques in machining performance prediction and optimization: a literature review". Int J Adv Manuf Technol 46(5), 2010, 445–464.

Cicală E, Soveja A, Sallamand P, Grevey D, Jouvard JM. The application of the random balance method in laser machining of metals. J Mater Process Technol 2008 1/21;196(1-3):393-401.

Ciurana J, Arias G, Ozel T. Neural network modeling and particle swarm optimization (PSO) of process parameters in pulsed laser micromachining of hardened AISI H13 steel. Mater Manuf Process 2009;24(3):358-368.

Correa, M., Bielza, C., & Pamies-Teixeira, J. "Comparison of Bayesian networks and artificial neural networks for quality detection in a machining process", Expert Systems with Applications, 36, 2009, 7270–7279.

Desai C. K., Shaikh A., "Prediction of depth of cut for single-pass laser micro-milling process using semi-analytical, ANN and GP approaches" International Journal Of Advanced Manufacturing Technology, 60(9-12), 2012, 865-882.

Dhara SK, Kuar AS, Mitra S. An artificial neural network approach on parametric optimization of laser micro-machining of die-steel. Int J Adv Manuf Technol 2008;39(1-2):39-46.

Díez-Pastor J. F., Bustillo A., Quintana G. and García-Osorio C., "Boosting Projections to improve surface roughness prediction in high-torque milling operations", Soft Computing, 16(8), 2012, 1427-1437.

Grzenda M., Bustillo A., Zawistowski P., "A soft computing system using intelligent imputation strategies for roughness prediction in deep drilling", Journal of Intelligent Manufacturing, 23(5), 2012, 1733-1743.

Grzenda M., Bustillo A., Quintana G.and Ciurana J., "Improvement of surface roughness models for face milling operations through dimensionality reduction", Integrated Computer-Aided Engineering, 19(2), 2012, 179-197.

Kaldos A, Pieper HJ, Wolf E, Krause M. Laser machining in die making—a modern rapid tooling process. J Mater Process Technol 2004 11/30;155-156:1815-1820.

Karazi SM, Issa A, Brabazon D. Comparision of ANN and DoE for the prediction of laser – machined micro-channel dimensions. Optics and Lasers in Engineering 2009;47:956-964.

Kumar A, Gupta MC. Laser machining of micro-notches for fatigue life. Optics and Lasers in Engineering 2010; 48(6):690-697.

Mahdavinejad, R.A., Khani, N., Fakhrabadi, M.M.S. “Optimization of milling parameters using artificial neural network and artificial immune system”, Journal of Mechanical Science and Technology, 26 (12), 2012, 4097-4104 .

Pham DT, Dimov SS, Petkov PV. Laser milling of ceramic components. Int J Mach Tools Manuf 2007 3;47(3-4):618-626.

Quintana G., Bustillo A., Ciurana J., "Prediction, monitoring and control of surface roughness in high-torque milling machine operations, International Journal of Computer Integrated Manufacturing, 25(12), 2012, 1129-1138.

Rizvi NH, Apte P. Developments in laser micro-machining techniques. J Mater Process Technol 2002;127(2):206-210.

Samant AN, Dahotre NB. Three-dimensional laser machining of structural ceramics. Journal of Manufacturing Processes 2010;12(1):1-7.

Semaltianos NG, Perrie W, Cheng J, French P, Sharp M, Dearden G, et al. Picosecond laser ablation of nickel-based superalloy C263. Applied Physics A: Materials Science and Processing 2010;98(2):345-355.

Yousef BF, Knopf GK, Bordatchev EV, Nikumb SK. Neural network modeling and analysis of the material removal process during laser machining. Int J Adv Manuf Technol 2003;22(1-2):41-53.

Chapter 4. Optimization of process parameters for laser milling of micro-channels on tool steel

Chapter 4 presents experimental models to study the relation between process parameters and quality characteristics. Multi-criteria decision making for material and process parameter selection for desired surface quality and dimensional accuracy is investigated using an evolutionary computation method based on particle swarm optimization (PSO).

This study was presented in an article entitled "*Optimization of process parameters for pulsed laser milling of micro-channels on AISI H13 tool steel*", published by Robotics and Computer-Integrated Manufacturing in June of 2012 (Teixidor, 2013).

D. Teixidor, I. Ferrer, J. Ciurana, T. Özel. “Optimization of process parameters for pulsed laser milling of micro-channels on AISI H13 tool steel”. *Robotics and Computer-Integrated Manufacturing*. Vol. 29, Issue 1 (February 2013) : 209-218. DOI 10.1016/j.rcim.2012.05.005

http://dx.doi.org/10.1016/j.rcim.2012.05.005

http://www.sciencedirect.com/science/article/pii/S0736584512000774

Received 15 July 2011

Received in revised form 15 May 2012

Accepted 25 May 2012

Available online 27 June 2012

Abstract

This paper focuses on understanding the influence of laser milling process parameters on the final geometrical and surface quality of micro-channel features fabricated on AISI H13 steel. Optimal selection of process parameters is highly critical for successful material removal and high dimensional and surface quality for micro-sized die/mold applications. A set of designed experiments is carried out in a pulsed Nd:YAG laser milling system using AISI H13 hardened tool steel as work material. Arrays of micro-channels have been fabricated using a range of process parameters such as scanning speed (SS), pulse intensity (PI), and pulse frequency (PF). The relation between process parameters and quality characteristics has been studied with experimental modeling. Multi-criteria decision making for material and process parameter selection for desired surface quality and dimensional accuracy is investigated using an evolutionary computation method based on particle swarm optimization (PSO).

Keywords

Process parameters optimization

Process parameters selection

Laser milling process

Chapter 5. Effect of process parameters in laser micromachining of PMMA micro-channels

Chapter 5 presents investigations on the effects of nanosecond laser processing parameters on depth and width of microchannels fabricated from PMMA polymer. Hence, experiments are conducted at NIR and UV wavelengths. The laser processing parameters of pulse energy pulse frequency, focal spot size and scanning rate are varied to obtain a wide range of fluence and processing rate. The effects of these process parameters on channel geometry (width and depth) and MRR are studied. The relationship between process variables (width and depth of laser-ablated microchannels) and process parameters is investigated. Mathematical modeling for predicting microchannel profile was developed and validated with experimental results.

This study was presented in an article entitled "*Effect of process parameters in nanosecond pulsed laser micromachining of PMMA-based micro-channels at near-infrared and ultraviolet wavelengths*", published by the International Journal of Advanced Manufacturing Technology in October of 2012 (Teixidor, 2012).

D. Teixidor, F. Orozco, T. Thepsonthi, J. Ciurana, C.A. Rodríguez, T. Özel. “Effect of process parameters in nanosecond pulsed laser micromachining of PMMA-based microchannels at near-infrared and ultraviolet wavelengths”. *The International Journal of Advanced Manufacturing Technology*. Vol. 67, Issue 5-8 (July 2013) : 1651-1664. DOI 10.1007/s00170-012-4598-x

http://dx.doi.org/10.1007/s00170-012-4598-x

http://link.springer.com/article/10.1007/s00170-012-4598-x

Received: 21 June 2012

Accepted: 30 October 2012

Published online: 14 November 2012

Abstract

This paper presents investigations on the effects of nanosecond laser processing parameters on depth and width of microchannels fabricated from polymethylmethacrylate (PMMA) polymer. A neodymium-doped yttrium aluminium garnet pulsed laser with a fundamental wavelength of 1,064 nm and a third harmonic wavelength of 355 nm with pulse duration of 5 ns is utilized. Hence, experiments are conducted at near-infrared (NIR) and ultraviolet (UV) wavelengths. The laser processing parameters of pulse energy (402–415 mJ at NIR and 35–73 mJ at UV wavelengths), pulse frequency (8–11 Hz), focal spot size (140–190 μm at NIR and 75 μm at UV wavelengths) and scanning rate (400–800 pulse/mm at NIR and 101–263 pulse/mm at UV wavelengths) are varied to obtain a wide range of fluence and processing rate. Microchannel width and depth profile are measured, and main effects plots are obtained to identify the effects of process parameters on channel geometry (width and depth) and material removal rate. The relationship between process variables (width and depth of laser-ablated microchannels) and process parameters is investigated. It is observed that channel width (140–430 μm at NIR and 100–150 μm at UV wavelengths) and depth (30–120 μm at NIR and 35–75 μm at UV wavelengths) decreased linearly with increasing fluence and increased non-linearly with increasing scanning rate. It is also observed that laser processing at UV wavelength provided more consistent channel profiles at lower fluences due to higher laser absorption of PMMA at this wavelength. Mathematical modeling for predicting microchannel profile was developed and validated with experimental results obtained with pulsed laser micromachining at NIR and UV wavelengths.

Keywords

Laser micromachining; Ablation; Polymethylmethacrylate; Process modeling; Microfluidics

Chapter 6. Multi-objective optimization of laser milling parameters of micro-cavities

Chapter 6 presents a multi-objective optimization (NSGA-II) of the laser milling process of micro-cavities for the manufacturing of DES. The diameter, depth and volume error are optimized in function of the key process parameters and the initial feature geometry. A set of designed experiments is carried out in a pulsed Nd:YAG laser system using 316L SS as a work material. The capability of the process to manufacture within a level of error is also investigated.

This study was presented in an article entitled "*Multi-objective optimization of laser milling parameters of micro-cavities for the manufacturing of DES*", accepted by the International Journal of Materials and Manufacturing Processes in June 2013.

Multi-objective optimization of laser milling parameters of micro-cavities for the manufacturing of DES

Daniel TEIXIDOR[1] , Joaquim CIURANA*[1], and Ciro RODRÍGUEZ[2]

[1]Department of Mechanical Engineering and Industrial Construction, Universitat de Girona, Spain

[2]Center for Innovation in Design and Technology, Tecnológico de Monterrey, Monterrey, Mexico

***Corresponding Author**: quim.ciurana@udg.edu

Abstract

This paper presents a multi-objective optimization of the laser milling process of micro-cavities for the manufacturing of drug eluting stents (DES). The diameter, depth and volume error are considered to be optimized in function of the process parameters including laser intensity, pulse frequency and scanning speed. A set of designed experiments is carried out in a pulsed Nd:YAG laser system using 316L Stainless Steel as a work material. Two different geometries are studied, and they are considered as another variable for the model. The multi-objective optimization problem is solved by NSGA-II algorithm, and the non-dominated Pareto-optimal fronts are obtained. The capability of the process to manufacture within a level of error is also investigated. Relative error capability maps for different scale of features are presented.

Introduction

Micro-manufacturing processes in the fields of electronics, optoelectronics, micro- and nanomachining, new materials synthesis, and medical and biological applications have become a growing area. This creates the need to find processes to manufacture these components with better precision, higher resolution, smaller feature size, true 3D fabrication, and higher piece part fabrication throughput.

Coronary artery stents revolutionized the practice of interventional cardiology after they were first introduced in the mid-1980s. Since then, there have been significant developments in their design, the most notable of which has been the introduction of drug-eluting stents (DES). During the last years many type of DES have been developed. One of these types is the DES with biodegradable polymer. Interest has focused on these stents because initially after implantation, they theoretically may offer the antirestenotic benefits of a standard DES, whereas once the polymer has biodegraded, they speculatively may offer the safety benefits of a metallic stent [1]. Some of these DES are metallic stents that include reservoirs where the

polymer and the drug are contained. Like the Janus stent [2] which incorporates micro-reservoirs cut into its abluminal side that are loaded with drug.

Laser systems can provide unique solutions in materials processing, offer the ability to manufacture otherwise unattainable devices, and yield cost-effective solutions to complex manufacturing processes [3]. Thus, the use of lasers in materials processing, machining, diagnostics, and medical applications is a rapidly growing area of research.

In laser milling technology the material is removed by a laser beam through the layer by layer ablation mechanism. The removal of material during laser milling is affected by the characteristics of the laser beam and the workpiece but is mainly determined by the way that both interact [4]. The key process parameters which can be controlled and modified in order to obtain optimal machining results are the pulse frequency, the pulse intensity, and the scanning speed. The selection of the laser and its parameters significantly affects the quality of the micro-feature created and also the material removal rate.

There are several experimental research works which deal with the effect of the laser process parameters on the quality of the final parts of laser machining in macro scale. Many authors analyzed the influence of the pulse frequency, scanning speed and pulse intensity on the surface roughness and material removal rate. Bartolo et al. [5] experimented with tempered steel and aluminum pointing out that better surface quality is achieved with low pulse frequencies and laser power are used. However, the higher material removal rate is achieved increasing both parameters. Cicala et al. [6] used an Nd:YAG pulsed laser for machining of aluminum alloy, stainless steel and titanium materials. Their results showed that the material removal rate depends mainly on the frequency of the laser pulses. They obtained the lowest levels of surface roughness with low scanning speeds and the highest frequency. Cheng et al. [7] used a femtosecond and picoseconds lasers on cooper, aluminum and titanium alloys to study the effects of pulse overlap, repetition rate and number of overscan. Saklakoglou and Kasman [8] machined 10x10mm square geometries into tool steel to study the effect of different process parameters on surface roughness and maximum milling depth using 30W fiber laser machine.

In the micro scale there are many works investigating the laser machining process in laser microdrilling (Biswas / Kumar) and laser micro-cutting (Muhammad / Meng), there are few researches about laser 3D micromilling. Biswas et al. [9] studied the influence of lamp current, pulse frequency, air pressure and thickness of the job on the hole circulatity at exit and the hole taper of the drilled hole for laser drilling of gamma-titanium-aluminide. Kumar et al.[10] investigated the dependence of groove depth on laser power, repetition rate, number of scans and gas pressure in the generation of micro-notches in stainless steel and aluminium. Muhammad et al. [11] investigate the basic characteristics of fiber laser cutting of stainless steel 316L tube and understand the effect of introducing water flow in the tubes on minimizing back wall damages and thermal effect. The influence of laser parameters upon cutting quality for fixed gas type and gas pressure was investigated. Meng et al. [12] designed a cardiovascular stent cutting system based on fiber laser where the kerf width size was studied

for different cutting parameters including laser output power, pulse length, repeat frequency, cutting speed and assisting gas pressure. Karanakis et al. [13] discussed the merits of laser micromilling using lasers with different pulse durations and wavelengths. They generated 2.5D structures in different industrial materials. Volume removal rates and surface roughness were analyzed presenting good results. Teixidor et al. [14] studied the effect of the key laser parameters on target dimensions and surface roughness for laser milling of micro-channels on tool steel. They adopted a multi-objective process optimization to predict the best combination of process parameters.

Many other research works developed models and methods to simulate the process and predict the best set of parameters for the final result. Campanelli et al. [15, 16] implemented an Artificial Neural Network and a multi objective statistical optimization on the laser milling of aluminium 5754 using a Nd:YAG laser. In the first model they determined the values of the scan speed and the repetition rate for the preset ablation depth. In the second algorithm they evaluated the influence of the main parameters on the depth, MRR and surface roughness. Dhara et al. [17] developed a strategy for predicting the optimum machining parameter setting for the generation of the maximum depth of groove with minimum height of recast layer. Finally, Ciurana et al. [18] developed neural network models and multi-objective particle swarm optimization (PSO) of process parameters for laser ablation of t-shaped features.

There is a lack of research in the literature for the laser milling of 3D micro-geometries. Therefore, the objective of this work is to study the capability of a nanosecond Nd:YAG laser to produce micro-cavities with preset dimensions. These cavities have the dimensions and shape to be manufactured into stent struts in order to produce DES. It is necessary to capture the influence of laser milling process parameters on the desired dimensional quality. Thus, multi-objective optimization (NSGA-II) method is adopted to find the optimal set of parameters to improve the dimensional accuracy reducing the error of the dimensions of the cavities manufactured. Finally, a deeper analysis has been carried out with respect to the errors of the dimensions at different scales in order to understand the capabilities of the process at error level.

2. Multi-Objective Optimization using NSGA-II

Multi-objective optimization problems can be solved by using evolutionary computational algorithms such as genetic algorithms [19]. NSGA-II (Non-dominated Sorting Genetic Algorithm, modified version of NSGA [20, 21]), is one of the most popular multi objective optimization algorithms with three special characteristics; fast non-dominated sorting approach, fast crowded distance estimation procedure and simple crowded comparison operator [20]. It has been most widely applied for optimizing machining process parameters and recognized as one of the best evolutionary algorithms for multi-objective optimization [22].

Generally, NSGA-II can be roughly detailed as follows: Once the population is initialized the population is sorted based on non-domination into each front. Once the sorting is complete, the crowding distance value is assign front wise. The individuals in population are selected based on rank and crowding distance. The crowding distance is a measure of how close an individual is to its neighbours. Large average crowding distance will result in better diversity in the population. Parents are selected from the population by using binary crossover and polynomial mutation based on the rank and crowding distance. Offspring population and current generation population are combined and the individuals of the next generation are set by selection. The new generation is filled by each front subsequently until the population size exceeds the current population size. The selection is based on rank and the on crowding distance on the last front.

This work conducted multi-criteria optimization to investigate the dimensional accuracy in laser milling of 316L stainless steel for micro-cavities fabrication. Optimal selection of process parameters of laser milling can be formulated and solved as an optimization problem. A simultaneous consideration of multiple objectives is required. Usually, process parameters selected for one objective function may not be suitable for the other objective function presenting conflicting objectives. This presents a challenge for the optimization problem, since selection of the parameter settings (decision variables) for given multiple choices which may be in conflict to each other.

To set up the optimization model of machining parameters, the mathematical relationships between machining parameters and optimization objectives should be determined firstly. Since there is no equation that relates them, a second order model is used to establish input-output relationship between response and process parameters efficiently. These models take the following generic form:

$$y = \beta_0 + \sum_{i=1}^{k} \beta_i x_i + \sum_{i=1}^{k} \beta_{ij} x_i x_j + \sum_{i=1}^{k} \beta_{ii} {x_i}^2 + \varepsilon \quad (1)$$

where ε is the residual error.

Second order models are used to find the optimum values for a response. It includes the interaction terms and second order terms making it more suitable than linear regressions.

The generic regression form in Eq. (1) is used to develop experimental models for the responses by using the experimental test data and establish the effect of variables on the outputs. The following section describes the experiments used to provide data for the optimization process with the different levels of the process variables.

3. Experimental background

3.1 Laser system

The laser system used for the performance of the experiments was a nanosecond Nd:YAG laser Lasertec 40 machine from Deckel Maho. This system is a lamp pumped solid-state laser with 1,064nm wave length. The laser has 100W average laser power and with a laser beam spot diameter of 30 µm, which results in an ideal maximum pulse intensity of 1.4 W/cm2 (theoretically estimated as [14]). The x and y movements are guided by highly dynamic scanner as optical-axis-system with a scanning field of 60x60 mm. The machine program itself is generated automatically by the 3D-CAD data by the Lasersoft shape software

3.2 Material

In this work 316L Stainless steel was used as a workpiece material test. This material was selected because it is commonly used for coronary stents fabrication.

3.3 Milling experiments

The experiments were carried out machining micro cavities in two different geometries. The first geometry has a half spherical shape defined by depth and diameter dimensions. The second geometry has a half cylindrical shape with a quarter sphere at both sides, defined by depth, diameter and length dimensions. The geometries were fabricated with three different combinations of dimensions where the volume is the same. Thus, the experiments are performed in six different geometries. Figure 1 and Table 1 and 2 present the geometries and the dimensions for the spheres and the cylinders, used in the experiments, respectively. The geometries and dimensions used would allow machining the cavities in cardiovascular stent struts in order to manufacture drug eluting stents.

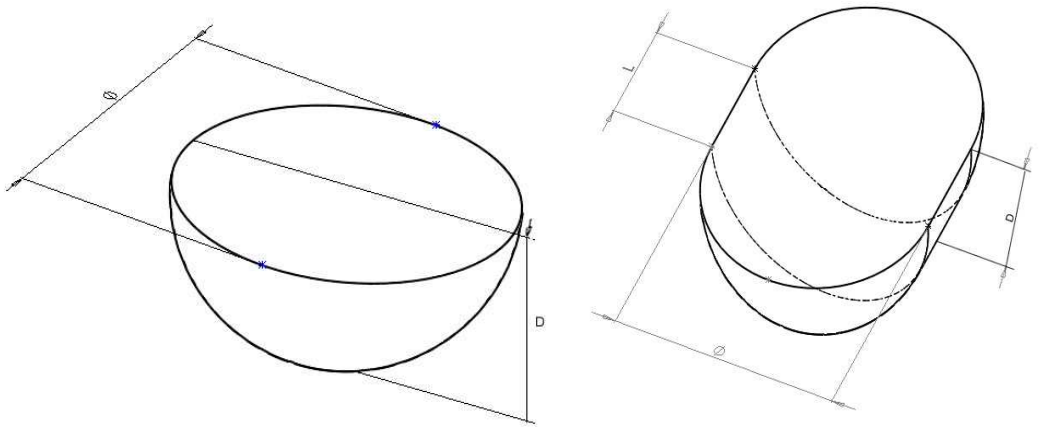

Figure 1. Cavity geometries used in the experiments.

Table 1. Sphere geometry dimensions.

Geometry	Depth (µm)	Ø (µm)	Volume (μm^3)
Sphere 1 (e1)	50	166	721414
Sphere 2 (e2)	70	140	718377
Sphere 3 (e3)	90	124	724576

Table 2. Cylinder geometry dimensions.

Geometry	Depth (µm)	Ø (µm)	Length (µm)	Volume (μm^3)
Cylinder 1 (c1)	50	130	55	723220
Cylinder 2 (c2)	70	110	46	721676
Cylinder 3 (c3)	90	100	36	725707

In the experiments, the scanning speed (SS), the pulse frequency (PF) and pulse intensity levels (PI) were considered as input parameters. A full factorial design was used. A preliminary test was carried out to determine the proper process parameters to be used. From the result, three different levels were selected for each factor, as is presented in Table 3. These design of experiments results in a total of 27 unique factor level combination for each geometry studied. Thus, a total of 162 experiments were carried out. All the experiments were machined in the same 316L SS blank under the same ambient conditions with a track displacement (distance between passes, a) of 10µm. The response variables investigated were the cavity dimensions depth (D) and diameter (Ø) and the volume of removed material. Although the cylinder shape has three target dimensions just two have been modeled, understanding that the results will be similar.

Dimensional measurements and characterization of the laser cut samples was conducted by confocal microscope Axio CSM 700 from Carl Zeiss. Surface replicant silicone for was used in order to obtain the negative of some of the samples. 3D SEM images of these negatives were obtained.

Table 3. Factors and factor levels.

Factors	Factor Levels		
Scanning Speed (SS) [mm/s]	200	400	600
Pulse Intensity (PI) [%]	60	78	100
Pulse Frequency (PF) [kHz]	30	45	60

4. Simulation

The experimental data measured is used to develop the second order models using the generic form in Eq (1) for responses of the relative error of depth, diameter and volume for the mean values (μ) and the standard deviation (σ) values. Six equations are obtained where the six responses are related with the four controllable process variables including the interaction terms and the second order terms. These constitute the six objective functions for the optimization model, which are considered separately.

$$\text{minimize } \{f(x), g(x), h(x), j(x), k(x), l(x)\}$$

$$\text{s.t.} \quad f(x) \leq b_1, g(x) \leq b_2, h(x) \leq b_3, j(x) \leq b_4, k(x) \leq b_5 \text{and } l(x) \leq b_6 \text{ where } x \in X. \qquad (7)$$

In the optimization problem formulation in Eq. (7) $f(x)$, $g(x)$, $h(x)$, $j(x)$, $k(x)$ and $l(x)$ represent the objective functions for depth error mean, depth error variance, diameter error mean, depth error variance, volume error and variance, respectively with a set of process parameters ($x = x_1 + \cdots + x_n$, $n = 1, 2, 3 \text{ or } 4$). X is the solution space with all feasible values for the process parameters.

The four controllable process variables are x1=Geo , x2=PI, x3=PF, x4=SS, where Geo is the type of geometry (spherical or cylindrical), PI is the Pulse Intensity (%), PF is the pulse frequency (kHz) and SS is the scanning speed (mm/s).

In the above given formulation, the objective is to simultaneously minimize the objective functions. In solving this optimization problem, a general approach based on Pareto-optimal set of non-dominated decision variables settings is considered. The selection of a Pareto-optimal set avoids the problem of a single combined objective function with weights which often leads to a unique solution but offers no other solution to the decision maker for optimum parameter selection.

In the case of laser machining process, the optimization problem is defined with multiple objectives. Decision variables such as geometry (Geo) scanning speed (SS), pulse intensity (PI), and pulse frequency (PF) are constrained within the ranges of the experiments (see Table 3).

The simulations were run by using a population of 200 individuals and a maximum number of 300 iterations. After obtaining the best individuals values in each iteration of the simulation, the individuals are plotted in a two-dimensional objective space for viewing. This procedure is repeated until a clear Pareto frontier forms. Matlab R2011b is used to simulate the optimization model. The Pareto frontiers of the non-dominated solution sets are obtained by using multi-objective NSGA-II method as shown in Figure 2 through Figure 5.

Figure 2 presents the multi-objective optimization for the relative error diameter for the mean and the variance value. The pareto frontier is almost a straight line. All the process presents a very good tolerance for the diameter dimension. However, reducing this to 2% increases the

relative error for the mean until the 33%. Therefore, better results can be achieved reducing the diameter error mean getting a little bit more of variance.

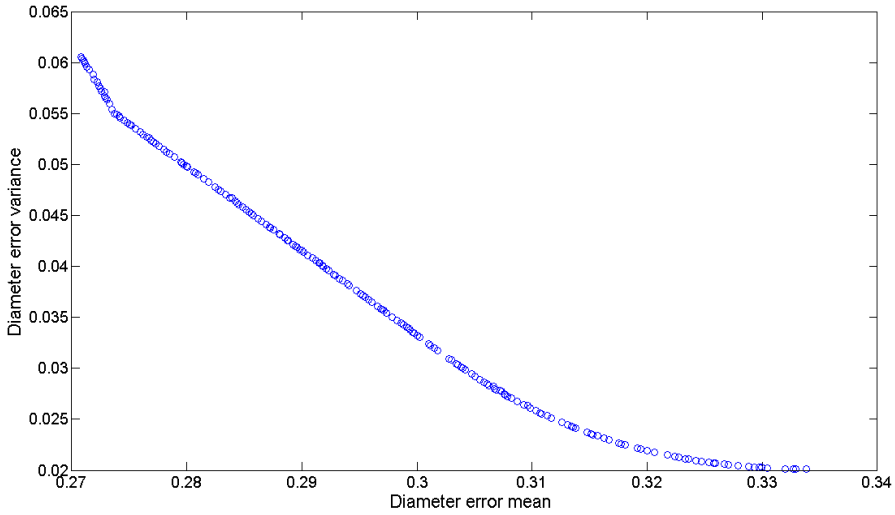

Figure 2. Pareto frontier of optimal diameter mean and diameter variance relative error laser parameters.

Figure 3 presents the multi-objective optimization for the depth and diameter relative errors. The convexity shape of the Pareto frontier shows a clear independence between both error objective parameters. A lower diameter error will result in a higher depth dimensional error. However, paying attention to the values at the axes, the range of the diameter is much lower than the one for the depth error. Diameter errors are between 0.27 and 0.274 while the error range for the depth is from 0.32 and 0.4. Therefore, in order to find the best combination of parameters, would be a good solution trying to reduce the depth error, since the diameter error won't increase much.

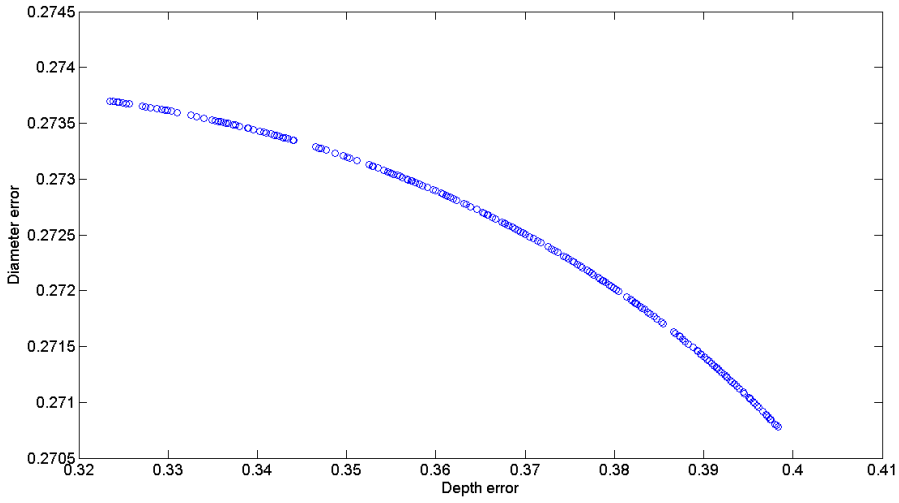

Figure 3. Pareto frontier of optimal diameter and depth relative error laser parameters.

Figure 4 and 5 show the pareto frontier for the volume with the diameter and the depth relative errors, respectively. The concavity shape of both lines shows that volume is related to both parameters. Therefore, as expected, reducing the error for depth and diameter dimensions, the volume will get closer to the target. In the Figure 4, the pareto frontier is formed by two straight lines, with different inclinations. Small improvements in the diameter increases further the volume.

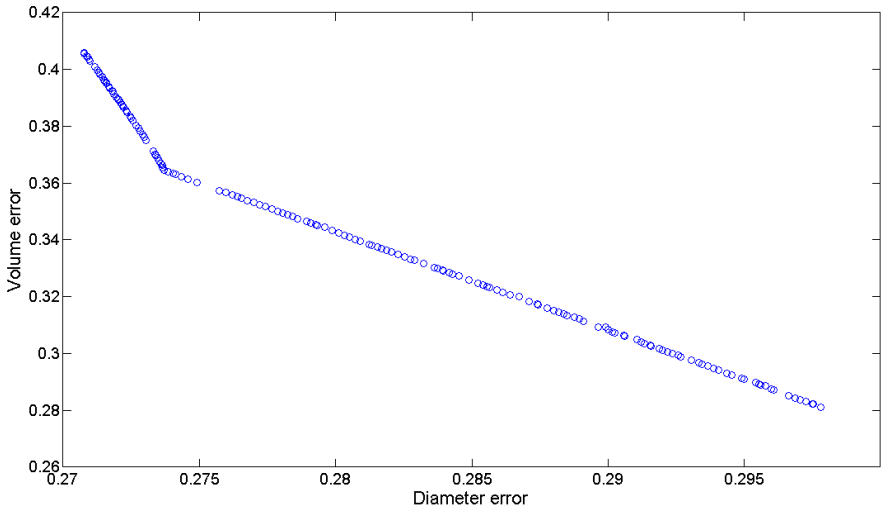

Figure 4. Pareto frontier of optimal volume and diameter relative error laser parameters

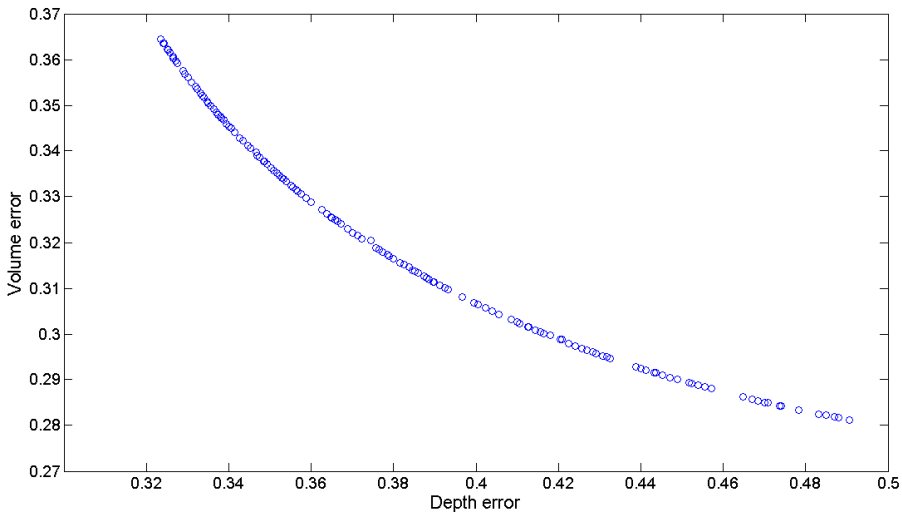

Figure 5. Pareto frontier of optimal volume and depth relative error laser parameters

Figure 6 shows the multi-objective optimization for the three main objective functions as volume, diameter and depth relative errors. As pointed out the previous figures, reducing depth relative error is the main objective of the process, concerning the dimension quality. If this error is reduced the volume error will decrease and the diameter error will not increase much because the range of all the optimum combinations is lower. Although, it can be claimed that there is not combination that reaches an optimal result, a good parameter selection could be a pulse intensity of the 60%, pulse frequency of 45 kHz and scanning speed of 600mm/s.

This result confirms what was pointed out in a previous study [14]. As pointed out, this combination reduces the depth relative error, keeping the other objective functions in low values.

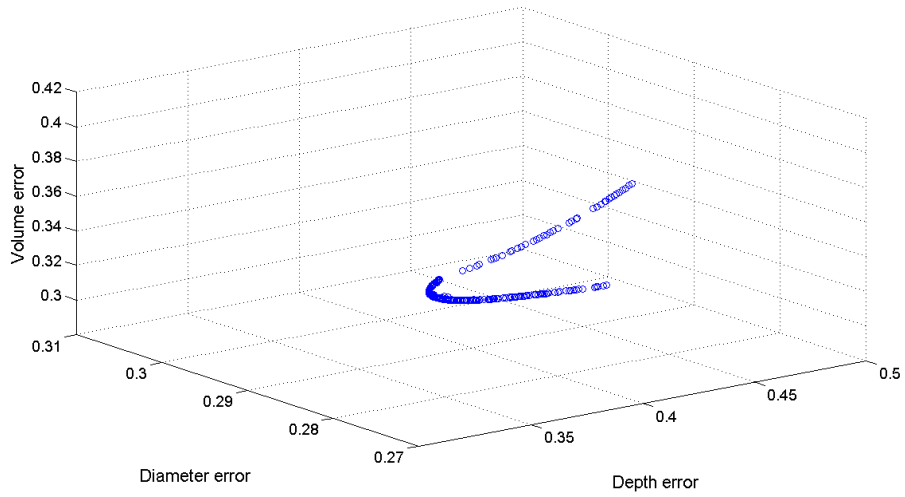

Figure 6. Multi-objective optimization for volume, diameter and depth relative error laser parameters

5. Error analysis

In order to deepen the study of dimensional error that occurs during laser milling, the experimentation was expanded to machining the same geometry but with a magnitude five times bigger. In this case, full factorial experimental design has not been carried out. Six experiments have been performed following the combinations of parameters presented in Table 4. This results in a total of 36 more experiments.

Table 4. Process parameter combinations for the second set of experiments.

Trial	PI (%)	PF (kHz)	CS (mm/s)
1	60	30	200
2	60	60	600
3	78	30	200
4	78	60	600
5	100	30	200
6	100	60	600

As in the previous experiments the depth and width dimensions were measured, as well as the relative error was calculated. In this way, capacity maps can be presented. In these maps, the 198 results of the experiments performed fill the space drawing a line which delimits the tolerance which the laser is capable to performance depending on the dimension.

Figure 7 and 8 present the capacity maps for the depth and diameter dimension respectively. The results on the map are plotted by the geometry. In both cases the precision of the laser gets better as the dimension increase. As expected, the depth dimension is clearly much more complicated to control than the diameter dimension. The dimensions in the x-y plane are mainly controlled by the movement of the laser, the laser spot size and the overlapping between the different pulses. Although the spot size varies depending on the process parameters, the other conditions are well controlled. Thus, this results in a good control of the diameter dimensions. On the other hand, for the depth control, the system establishes a constant removing depth for each pulse. This results in a bad approximation because the removed depth for each laser shot changes due to many aspects (thermodynamic equilibrium, process parameters), as is presented in many studies (10, 17)

Besides presenting much larger errors, the results are much more dispersed. Clearly, in dimensions around 50 microns depth, the process becomes poorly controlled. One would expect that in higher dimensions the results become better, as some results point out (about 0.5 relative error). However, in some conditions, the system moves away completely from the target set. This translates into a much lower tendency than expected, as it happens in the diameter map. Moreover, the results from the cylinder geometry are worst than the spherical ones. Is very evident in the smaller dimension where the sphere results are below 1 and many of the cylinder results are well above that value.

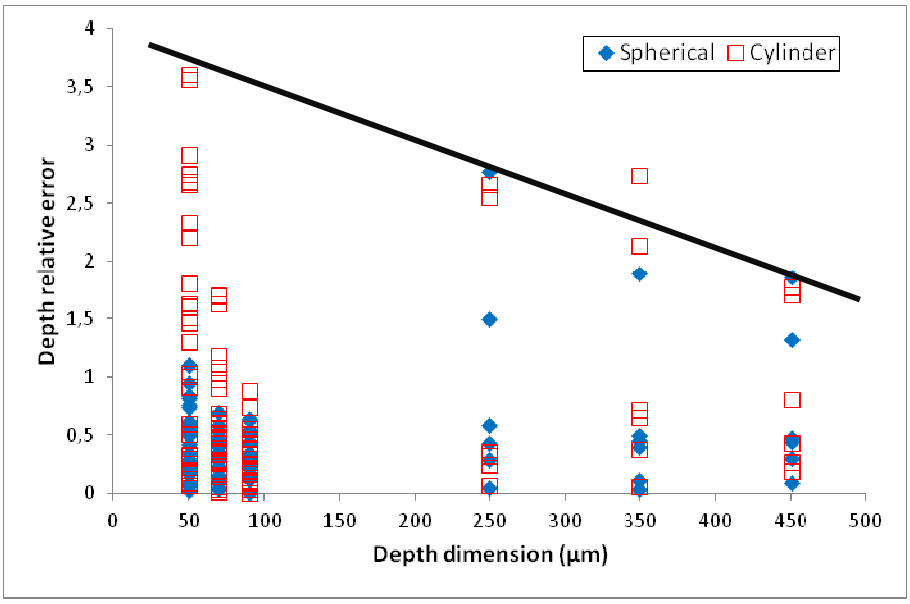

Figure 7. Capacity map for the depth dimension.

In the case of the diameter dimension, the tendency of the results follows a parabolic shape with very similar values for each dimension. Also, the results for both geometries present are very similar. Hence, as expected, this dimension is much more controlled. Being the spot size known, the error can be reduced. Nevertheless, for micrometric dimensions the errors are between 0.2 and 0.5 showing the difficulties in obtaining the preset dimensions.

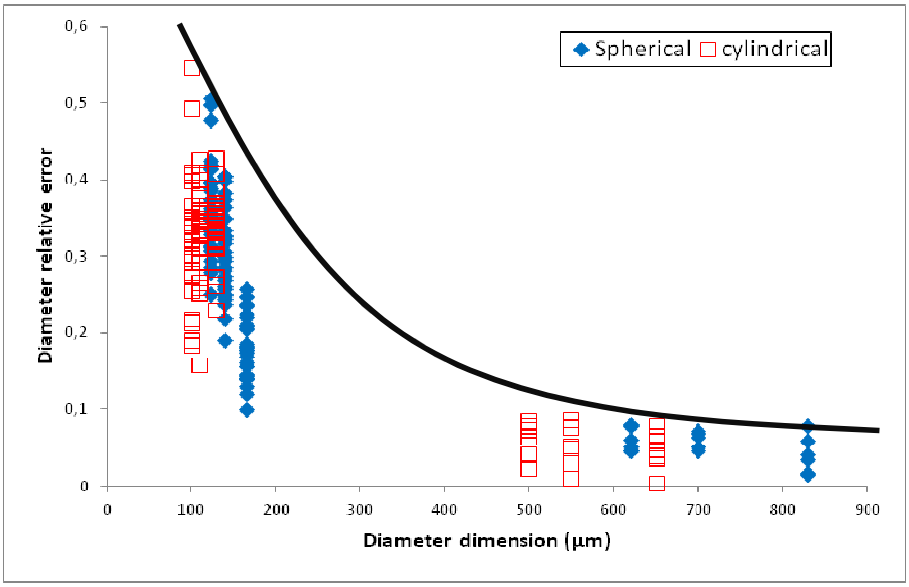

Figure 8. Capacity map for the diameter dimension.

Clearly, the results presented on a larger scale are better than those obtained in a smaller size. Although the depth is still difficult to control, the forms obtained are much better defined, as presented in Table 5. Although the process to obtain the negative of the cavities present more problems when the dimensions are much smaller, the cavities obtained in the second set of experiments present shape much similar to the target.

table 5. SEM images of cavities negative; a) geometry C1; PI = 60%, PF = 60 kHz and SS = 600mm/s, b) geometry c2; PI = 60%, PF = 30 kHz and SS = 200mm/s, c) geometry E1; PI = 60%, PF = 60 kHz and SS = 600mm/s, d) geometry e2; PI = 100%, PF = 60 kHz and SS = 600mm/s.

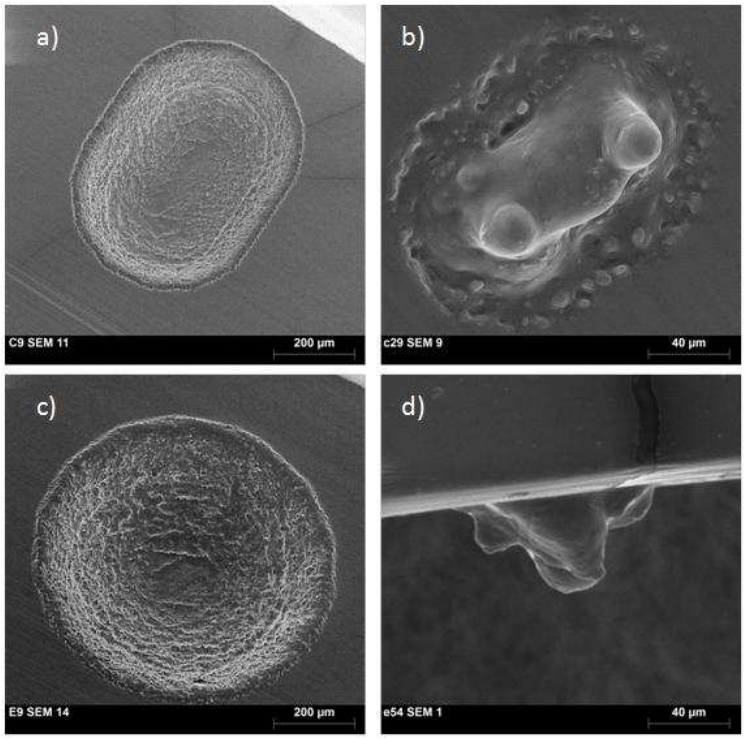

6. Conclusions

In this study a multi-objective optimization of the laser milling process of micro-cavities for the manufacture of drug eluting stents is presented. The optimization problem is solved by NSGA-II algorithm where the diameter, depth and volume errors are considered to be optimized function affected by four variables. These variables are the geometry of the cavity, the pulse intensity, the pulse repetition rate and the scanning speed. The objective is to minimize all three dimensional errors. Experiments in 316L Stainless Steel are carried out to provide data for the model. The capability of the process to manufacture within a level of error is also investigated. Relative error capability maps for different scale of features are presented. Clearly, the process presents more control on the diameter than on the depth dimension. This affects the volume error. Some trends and specific conclusions can be drawn as following:

1. Multi-objective NSGA-II provides Pareto frontiers of non-dominated solution sets for optimum laser milling process parameters, providing a resourceful and efficient means to the decision maker.
2. The nanosecond Nd:YAG laser is capable to produce micro-cavities with preset dimensions presenting relative error around 1,5 for the depth dimension and 0,3 for the diameter dimension.
3. The capability of the laser milling process to produce micro-geometries is limited by the scale of the feature. As bigger the dimensions of the cavity, smaller the dimensional error.
4. The diameter dimension error decreases more than the depth error when the scale of the cavity machined is increased.
5. The geometry of the feature to machine affects the process performance.
6. Although laser milling is a complex process and it is not easy to find the proper combination of process parameters to achieve the final part, a good parameter selection is presented for the laser milling of micro-cavities; pulse intensity of the 60%, pulse frequency of 45 kHz and scanning speed of 600mm/s.

7. Acknowledgements

The authors would like to express their gratitude to the GREP research group from the UdG, the Tecnologico de Monterrey for the facilities provided during the experiments. This work was partially carried out with the grant supports from the European Commission project IREBID (FP7-PEOPLE-2009-IRSES-247476) and the Spanish Science and Innovation Minister project TECNIPLAD (DPI2009- 09852).

8. References

[1] Garg S, Serruys PW. Coronary stents. Looking forward. Journal of American college of Cardiology 2010;56,10.

[2] Martin DM, Boyle Fj. Drug-eluting stents for coronary artery disease: A review. Medical Engineering & Physics 2011;33 148-163

[3] Sugioka K, Meunier M, Piqué A. Laser precision microfabrication. Springer 2010.

[4] Pham DT, Dimov SS, Petkov PV. Laser milling of ceramic components. Int J Mach Tools Manuf 2007;3;47(3-4):618-626.

[5] Bartolo P, Vasco J, Silva B, Galo C. Laser micromachining for mould manufacturing: I. The influence of operating parameters. Assem Autom 2006;26(3):227-234

[6] Cicală E, Soveja A, Sallamand P, Grevey D, Jouvard JM. The application of the random balance method in laser machining of metals. J Mater Process Technol 2008;1/21;196(1-3):393-401.

[7] Cheng J, Perrie W, Edwardson SP, Fearon E, Dearden G, Watkins KG. Effects of laser operating parameters on metals micromachining with ultrafast lasers. Appl Surf Sci 2009;12/15;256(5):1514-1520.

[8] Saklakoglou IE, Kasman S. Investigation of micro-milling process parameters for surface roughness and milling depth. Journal of Advanced Manufacturing Technology 2011;54:567–578

[9] Biswas R, Kuar AS, Sarkar S, Mitra S. A parametric study of pulsed Nd:YAG laser micro-drilling of gamma-titanium aluminide. Optics & Laser Technology 2010;42(1), 23–31.

[10] Kumar A, Gupta MC. Laser machining of micro-notches for fatigue life. Optics and Lasers in Engineering 2010;48(6):690-697.

[11] Muhammad N, Whitehead D, Boor A, Li L. Precision Machine Design. Comparison of dry and wet fibre laser profile cutting of thin 316L stainless steel tubes for medical device applications. Journal of Materials Processing Technology 2010;210 2261–2267.

[12] Meng H, Liao J, Zhou Y, Zhang Q. Laser micro-processing of cardiovascular stent with fiber laser cutting system. Optics & Laser Technology 2009;41 300– 302.

[13] Karnakis D, Rutterford G, Knowles M, Dobrev T, Petkov P, Dimov S. High quality laser milling of ceramics, dielectrics and metals using nanosecond and picosecond lasers. Proc. SPIE 6106, Photon Processing in Microelectronics and Photonics, 2006;610604–610604–11.

[14] Teixidor D, Ferrer I, Ciurana J, Özel T. Optimization of process parameters for pulsed laser milling of micro-channels on AISI H13 tool steel. Robotics and Computer-Integrated Manufacturing, 2013;29(1), 209–218.

[15] Campanelli SL, Casalino G, Ludovico AD, Bonserio C. An artificial neural network approach for the control of the laser milling process. Journal of Advanced Manufacturing Technology 2013;66:1777–1784.

[16] Campanelli SL, Casalino G, Contuzzi N. Multi-objective optimization of laser milling of 5754 aluminum alloy. Optics & Laser Technology 2013;52 48–56

[17] Dhara SK, Kuar AS, Mitra S. An artificial neural network approach on parametric optimization of laser micro-machining of die-steel. Int J Adv Manuf Technol 2008;39(1-2):39-46.

[18] Ciurana J, Arias G, Ozel T. Neural network modeling and particle swarm optimization (PSO) of process parameters in pulsed laser micromachining of hardened AISI H13 steel. Mater Manuf Process 2009;24(3):358-368.

[19] Coello Coello CA, Becerra RL. Evolutionary Multiobjective Optimization in Materials Science and Engineering, Materials and Manufacturing Processes, 2009;24 (2) 119 – 129.

[20] Deb K, Pratap A, Agarwal S, Meyarivan T. A Fast Elitist Multiobjective Genetic Algorithm: NSGA-II, IEEE Transactions on Evolutionary Computation 6 2002;2, 182 – 197.

[21] Srinivas N, Deb K. Multiobjective Optimization Using Nondominated Sorting in Genetic Algorithms, Evolutionary Computation 2 1994;3, 221 – 248.

[22] Gong MG. Research on Evolutionary Multi-Objective Optimization Algorithms. Journal of Software, 2009;20(2): p. 271-289.

Chapter 7. Dross formation and process parameters analysis of laser cutting

Chapter 7 presents an experimental study of fiber laser cutting of 316L stainless steel thin sheets. The effect of peak pulse power, pulse frequency and cutting speed on the cutting quality are investigated. A mathematical model for the dross dimensions (height and diameter) is formulated and compared with the experimental results.

This study was presented in an article entitled "*Dross formation and process parameters analysis of fiber laser cutting of stainless steel thin sheets*", submitted to Optics and Lasers in Engineering in June 2013.

Dross formation and process parameters analysis of fiber laser cutting of stainless steel thin sheets

D. Teixidor[(1)], J. Ciurana[(1)], C. Rodríguez[(2)]

(1) Department of Mechanical Engineering and Industrial Construction, Universitat de Girona, Girona, Spain. daniel.teixidor@udg.edu
(2) Center for Innovation in Design and Technology, Tecnológico de Monterrey, Monterrey, Mexico.

ABSTRACT

The coronary stent fabrication requires high precision profile cut. Fiber lasers present a solution to accomplish these requirements. This paper presents an experimental study of fiber laser cutting of 316L stainless steel thin sheets. The effect of peak pulse power, pulse frequency and cutting speed on the cutting quality for fixed gas type and gas pressure were investigated. A mathematical model for the dross dimensions was formulated. The dross height and the dross diameter were analyzed and compared with the experimental results. This allows selecting the process parameters to reduce the dimensions of the dross deposited at the bottom of the workpiece.

Keywords: Laser cutting; fiber laser; cardiovascular stent, dross formation.

1. Introduction

The laser cutting process has developed significantly over the past few decades and has become routine in sheet metal fabrication as a result of the attractive cutting velocities, excellent cut quality, processing flexibility as well as the widespread application possibilities that it affords [1].

One of its growing applications is the manufacturing of coronary stents for medical application. A stent is a wire mesh tube, which is deployed in a diseased coronary artery to provide smooth blood circulation. Stents can be either balloon expandable or self-expanding (using shape memory alloys). Stents are typically made from biocompatible materials such as stainless steel, nitinol (Ni-Ti alloy), cobalt-chromium, titanium, tantalum alloys, platinum iridium alloy as well as polymer. The most commonly used is stainless steel. The laser key requirement for its fabrication is a small consistent kerf width and this demands constant beam quality and excellent laser power stability. The laser cut must have a good surface quality with a minimum amount of slag and burr to reduce post-processing similarly the heat affected zone (HAZ) and molten material recast needs to be small [2].

Fiber laser is seen as an efficient, reliable and compact solution for micro machining which heat affected zone, kerf width and dross could be diminished to a minimum. This is because its important advantages as the combination of high beam power with high beam quality, small spot sizes, higher efficiency and almost free maintenance.

There are several research works, which use a fiber laser to study how the process parameters of the laser cutting affect the quality of the resultant surfaces. Kleine et al. [2] presented micro-cutting results in stainless steel samples of 100 and 150 µm where the kerf width and the surface quality were analyzed. They studied also the laser conditions to minimize HAZ. They conclude that the fiber laser is capable to achieve very small diameters and small kerf widths presenting very similar features to those produced with a Nd:YAG laser. Muhammad et al. [3] investigate the basic characteristics of fiber laser cutting of stainless steel 316L tube and understand the effect of introducing water flow in the tubes on minimizing back wall damages and thermal effect. The influence of laser parameters upon cutting quality for fixed gas type and gas pressure was investigated. Wet cutting enabled significant improvement in cutting quality. It resulted in narrower kerf width, lower surface roughness, less dross, absence of back wall damages and smaller HAZ. Laser average power and pulse width play a significant role in controlling the cutting quality. Increasing the pulse width increased beam/material interaction time, which increased the kerf width and surface roughness. Meng et al. [4] designed a cardiovascular stent cutting system based on fiber laser where the kerf width size was studied for different cutting parameters including laser output power, pulse length, repeat frequency, cutting speed and assisting gas pressure. Baumeister et al. [5] presented laser micro-cutting results for stainless steel foils with the aid of a 100 W fiber laser. Different material thicknesses were evaluated (100um to 300um). Processing was carried out with cw operation, and with nitrogen and oxygen assisting gases. Besides the high processing rate of oxygen assisted

cutting, a better cutting performance in terms of a lower kerf width was obtained. Minimal kerf width of less 20µm was obtained with oxygen as the assisting gas. The kerf widths with nitrogen assisted gas were generally wider. Scintilla et al. [6] presented results of Ytterbium fiber laser cutting of Ti6Al4V sheets (1mm thick) performed with Argon as cutting assistance gas. The effect of cutting speed and shear gas pressure on the HAZ thickness, squareness, roughness and dross attachment was investigated. The results show that, with increasing the cutting speed and then decreasing the heat input from at 2 kW, an increase of HAZ and RL thickness occurs, up to 117 µm. Powell et al. [7] developed an experimental and theoretical investigation into the phenomenon of 'striation free cutting', which is a feature of fiber laser/oxygen cutting of thin section mild steel. The paper concludes that the creation of very low roughness edges is related to an optimization of the cut front geometry when the cut front is inclined at angles close to the Brewster angle for the laser– material combination. Yan et al. [8] carried out both experimental and 3D FE modeling studies to analyze the effects of process parameters on temperature fields, thermal-stress distribution and potential crack formation in high power fiber laser cutting of alumina. Based on the numerical and experimental results, the mechanism of crack formation in laser fusion cutting was revealed and crack- free cutting of thick-section alumina was demonstrated.

Other researchers studied the effect of process parameters on the fabrication of stents using different lasers on several materials like nitinol or stainless steel. Kathuria et al. [9] described the precision fabrication of metallic stent from stainless steel (SS 316L) by using short pulse Nd:YAG laser. They conclude that the processing of stent with desired taper and quality shall still be preferred by the short pulse and higher pulse repetition rate of the laser, which is desired to reduce further the heat affected zone as well as the wave depth of the cut section. Pfeifer et al. [10] Pulsed Nd:YAG laser cutting of 1mm thick NiTi shape memory alloys for medical applications (SMA-implants). They studied the influence of pulse energy, pulse width, and spot overlap on the cut geometry, roughness and HAZ. They generated small kerf width (k = 150–300 µm) in connection with a small angle of taper (θ<2º). Compared to short- and ultrashort-laser processing of SMA, high cutting speeds (v = 2–12 mm/s) along with a sufficient cut quality (Rz = 10–30 µm) were achieved. The drawbacks can be seen in the higher thermal impact of the laser–material processing on the SMA, resulting in a HAZ (dimension: 6–30 µm) which affects the material properties and the reduced accuracy of the cutting process. Shanjin et al. [11] presented Nd:YAG pulsed laser cutting of titanium alloy sheet to investigate the influences of different laser cutting parameters on the surface quality factors such as HAZ, surface morphology and corrosion resistance. The results presented show that medium pulse energy, high pulse rate, high cutting speed and argon gas at high pressure help to acquire thin HAZ layers. Also in comparison with air- and nitrogen-assisted laser cutting, argon-assisted laser cutting comes with unaffected surface quality. Yung et al. [12] performed a qualitative theoretical analysis and experimental investigations of the process parameters on the kerf profile and cutting quality. They micro-cut thin NiTi sheets with a thickness of 350 µm using a 355 nm Nd:YAG laser. The results showed that the kerf profile and cutting quality are significantly influenced by the process parameters, such as the single pulse energy, scan speed,

frequency, pass number and beam offset, with the single pulse energy and pass number having the most significant effects. They obtained debris-free kerf with narrow width (≈25 μm) and small taper (≈1º). And concluded that as the single pulse energy is increased and the laser beam velocity is decreased, the kerf width increases. Muhammad et al. [13] studied the capability of picoseconds laser micromachining of nitinol and platinum-iridium alloy in improving the cut quality. Process parameters used in the cutting process have achieved dross-free cut and minimum extent of heat-affected zone (HAZ). Li et al. [14] reported investigations of femtosecond laser processing of NiTi SMA using a fundamental wavelength of 775nm from Ti:Saphire laser and its second and third harmonic irradiations. They developed a thermal influence free optimal process to fabricate complex miniature SMA components. Huang et al. [15] studied the effect of a femtosecond laser machining on the surface and characteristics of Nitinol. The results have produced surface roughness of about 0.2 μm on Nitinol. SEM and microstructural analyses revealed a HAZ smaller than 70 μm in depth and a re-deposited layer of about 7 μm exists on the machined surface. Raval et al. [16] machined a coronary stent after Nd:YAG laser cutting of 316LVM tubing and an assessment of its surface characteristics after electrochemical polishing. Finally, Scintilla et al. [17] analyzed the influence of processing parameters and laser source type on cutting edge quality of AZ31 magnesium alloy sheets and differences in cutting efficiency between fiber and CO2 lasers were studied. They investigated the effect of processing parameters in a laser cutting of 1mm and 3.3 mm thick sheets on the cutting quality. Their results showed that productivity, process efficiency and cutting edges quality obtained using fiber lasers outperform CO2 laser performances.

Some authors studied the formation of the dross developing analytical models in order to predict the shape of this melt material attached to the cutting edge. Yilbas et al. [18] formulated a mathematical model to predict the melt thickness and the droplet diameter. They compared it with experimental results of a CO2 laser obtaining good fit. They found that the liquid layer thickness increases with increasing laser output power and reduces with increasing assisting gas velocity. Tani et al. [19] evaluated the 3D geometry of the cutting front of the melting film considering mass, force and energy balance in an analytical model. Schuöcker et al. [20] presented a model for the dynamic behavior of the liquid layer in laser cutting that predicts the melt ejection. They related the droplet ejection and the formation of periodic striations along the cut edges. Shuja et al. [21] simulated the temperature field and the phase change in the heated region. They examined the influence of laser power intensity and scanning speed on temperature field and melt depth.

The present work aims to investigate the characteristics of fiber laser cutting of stainless steel 316L-based cylindrical stents. The effect of laser cutting parameters on the cutting quality for fixed gas type and gas pressure was investigated. Therefore, machining stent geometries in stainless steel sheets, this work will contribute to understand the relation between the process parameters and the responses studied. The melt depth and dross size are mathematical modeled. The dross experimental values are compared with the predictions.

2. Methodology or Experimental Procedure

The laser source employed in this work was a Rofin FL x50 Fiber Laser. This is a multi-mode laser capable of delivering up to 500 W power at 1080 nm wavelength and a beam quality factor, M < 1.1. The output can be modulated with a pulse frequency up to 5 kHz. The shortest pulse duration is 26 µs. The process fiber used was 150 µm in diameter, which was mounted in a focusing optics consisted of a Precitec Fine Cutting head with a collimation lens of 50 mm length and a 50 mm focal length objective. The focused spot size was calculated to be 150 µm. The coaxial assist gas nozzle had an exit diameter of 0.5mm. The system is integrated in a Kondia CNC machine, which controls the movement of X, Y and Z stages for translating the work under the focused laser spot.

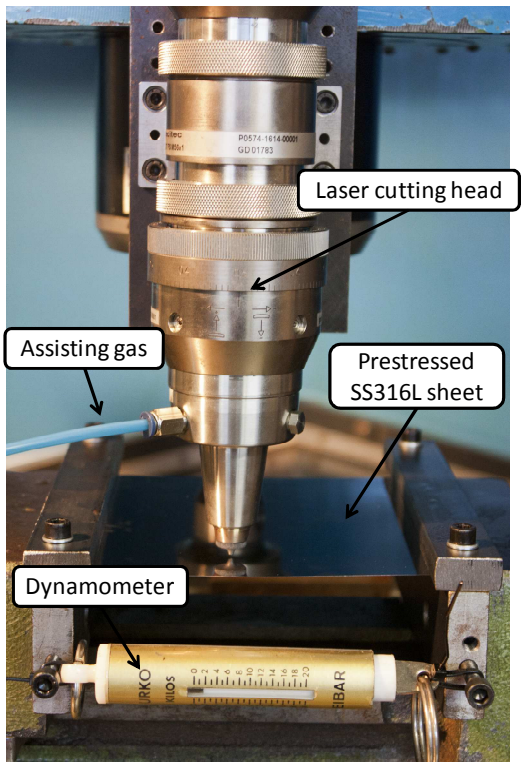

Figure 1 Set-up of the laser system.

In this work Stainless Steel 316L sheets of 100 µm thickness were used as a workpiece material. These sheets were clamped and prestressed, with an approximately 2 N tension, in order to avoid its deformation due the temperature. In this way the standoff distance is kept constant. Figure 1 presents the set-up of the system with the prestressed sheets and the laser cutting head in working position.

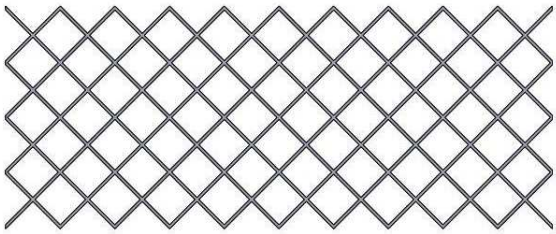

Figure 2 Stent geometry used on the laser cutting experiments.

Preliminary screening experiments were carried out to determine the appropriate processing parameters levels to be used for the design of experiments. A full factorial design was used to determine the effects of peak pulse power, cutting speed and pulse frequency on the resultant cutting quality. The factors and factor levels utilized in this work are summarized in Table 1Table 1.. These factor levels results in a total of 27 unique factor level combinations. Nitrogen was used as the assist gas to protect the optics and to remove the molten material from the cut kerf. The pressure was 6 bar, the stand-off distance between the nozzle tip and the workpiece surface was 0.2 mm and the pulse duration was 125 μs. These parameters were studied in the preliminary experiments and decided to keep constant for all the experiments. In order to investigate the effects of the process parameters on the cutting quality factors, stent simple geometry [9], as is presented in Figure 2, was used as a cutting shape for the experiments. The samples have dimensions of 20x8.5mm with strut width of 0.1mm. With this flat geometry a cylindrical structure could be formed by rolling and adhesive joining [22], but it is not the aim of this work. The cutting quality factors investigated were kerf width, surface roughness, dross deposition, and heat effects.

Table 1. Factors and factor levels of the design of experiments.

Peak pulse power	W	200	300	400
Pulse frequency	Hz	3000	4000	5000
Cutting Speed	mm/min	250	375	500

Characterization of the laser cut samples was conducted by confocal microscope Axio CSM 700 from Carl Zeiss. The kerf width is measured and the surface roughness is calculated by the microscope in conformity with the DIN EN ISO 4287 standard. The surfaces are also analyzed in 3D images from the top and the cut edges. The measurements of the dross area were performed with an optical microscope LEICA DMR-XA attached to NIKON F90 and RICOH X-RX3000 camera bodies and digital video with a SONY DXC950-P of 3CCD camera for the collection of digital images. These images were numerically processed using the Quartz PCI© software, version 5.

3. Results and Discussion

A total number of 27 stents were machined with laser cutting process by following the experimental plan discussed in previous section. Kerf width, surface roughness and dross deposition were measured as a quality factors. The surface roughness of four of the samples was not measured, and the dross deposition was just measured in 20 of the geometries machined. Some statistical analysis will be presented in order to identify the relations between the process parameters and the responses.

3.1 Kerf width

Figure 3 shows the influences of cutting parameters upon the kerf width. It presents how each process parameter affects the kerf width. The results clearly show that the kerf width increased as the peak pulse power, pulse frequency and cutting speed increased. As expected the increase of peak pulse power and pulse frequency results in bigger kerf width. During the cutting process, the average power is proportional to these parameters and the pulse width. Thus, higher average power results in bigger kerf width. On the other hand would be expected that the increasing of the cutting speed will lead to a reduction of the kerf width [3, 4]. As the cutting speed reduces, the interaction time between laser beam and material increases which creates a larger kerf. However, the results present the opposite trend. This happens because the range used (250 to 500 mm/min) is not big enough to see the real trend of the relation between cutting speed and kerf width. Muhammad et al. [3] pointed out that the relation between both parameters increased until 1000 mm/min where the kerf width started to decrease after this point. The kerf widths obtained in the experiments were within the range of 150 to 230 µm. Minimum kerf was obtained at lower peak pulse power, 200 W, lower pulse frequency, 3000 Hz and lower cutting speed, 250 mm/min. Although, the minimum achieved corresponds to the theoretical spot size calculated, it is clear that the experimental values obtained are bigger than this theoretic one. This was expected, Muhammad et al. [3] presented kerf width values 60% above the theoretic spot size when the pulse peak power or the pulse frequency is increased and Baumester et al. [5] showed that increasing the energy the kerf width become 200% higher than the focal diameter.

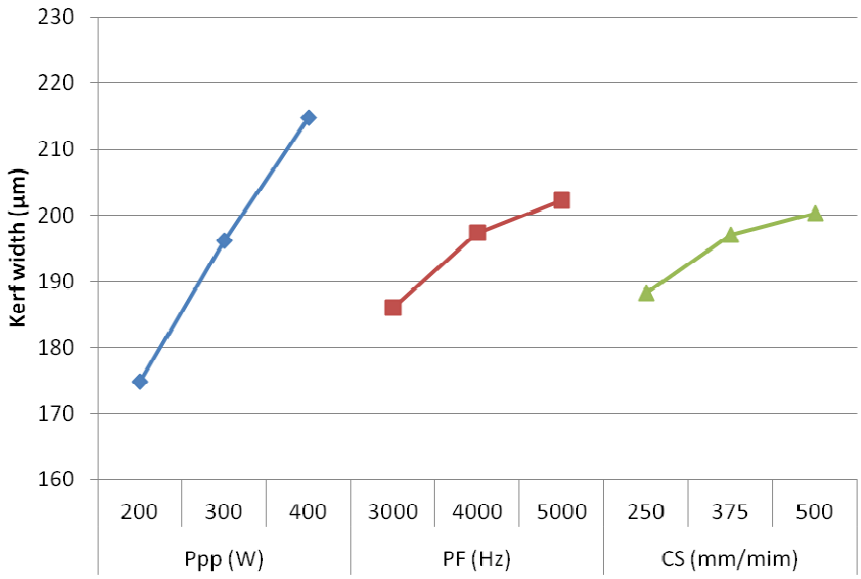

Figure 3. Kerf width as a function of laser cutting parameters: peak pulse power, pulse frequency, and cutting speed.

3.2 Surface roughness and Striation on the cut surface

Analysis was carried out to characterise the topography of the cut edges to determine the surface finish quality. The average roughness was measured in the mid section of the cut edge surface. Three measurements were taken in three different struts of each stent. The mean of these measures has been used as the experimental results for the surface roughness analysis. Figures 4 and 5 show the image of the cutting edge and the surface roughness profile obtained by the confocal microscope for two of the samples.

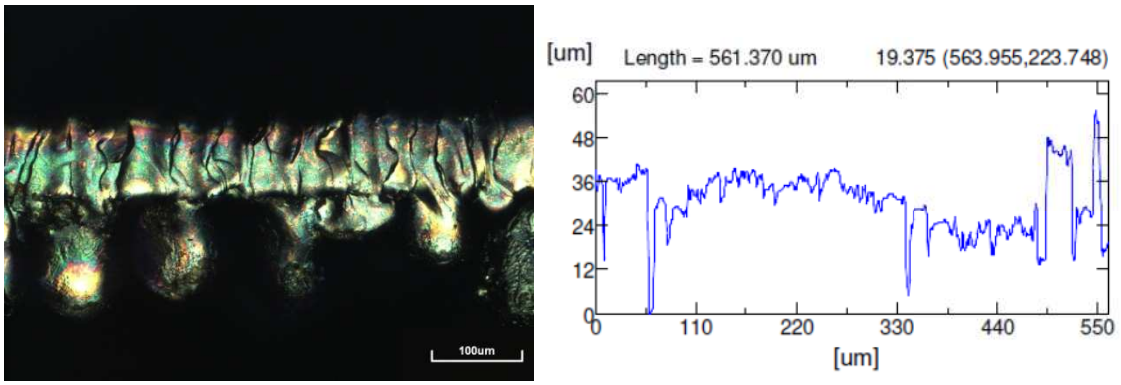

Figure 4. Surface roughness of the cut surface for pulse power 400 W, pulse frequency 3000 Hz and cutting speed 500 mm/min. a) Image of the cut surface from confocal microscope (219X). b) surface roughness profile across the cut edge. Where Ra = 1,447

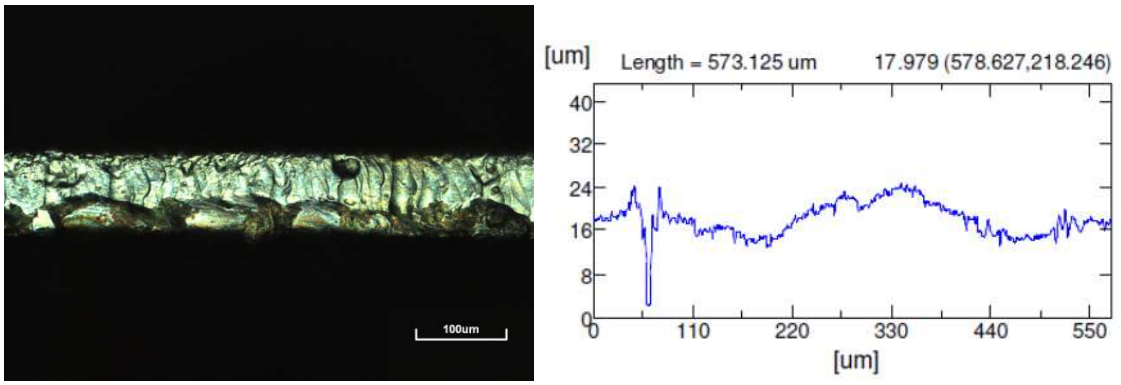

Figure 5. Surface roughness of the cut surface for peak pulse power 300 W, pulse frequency 3000 Hz and cutting speed 375 mm/min. a) Image of the cut surface from confocal microscope (219X), b) surface roughness profile across the cut edge. Where Ra = 0668,

Figure 6 shows the relationship between the surface roughness and the laser parameters. Thus the influence of the process parameters upon the surface roughness is presented. The surface roughness increased with the increasing peak pulse power. Although between the two levels seems to keep constant, clearly for the higher peak pulse power the surface roughness presents its higher values. Although, higher pulse frequency leads to higher average power, it results in better surface roughness due to high pulse overlapping. Lower cutting speed also increases the overlapping, thus higher cutting speed results in worst surface roughness as the results pointed out. The surface roughness obtained in the experiments was within the range of 0,547 to 1,447 µm. Although there are some parameters combinations with higher values of surface roughness, this range is similar to the ones presented in other works [2, 3]. Minimum Ra was obtained at medium peak pulse power, 300 W, medium pulse frequency, 4000 Hz and lower cutting speed, 250 mm/min.

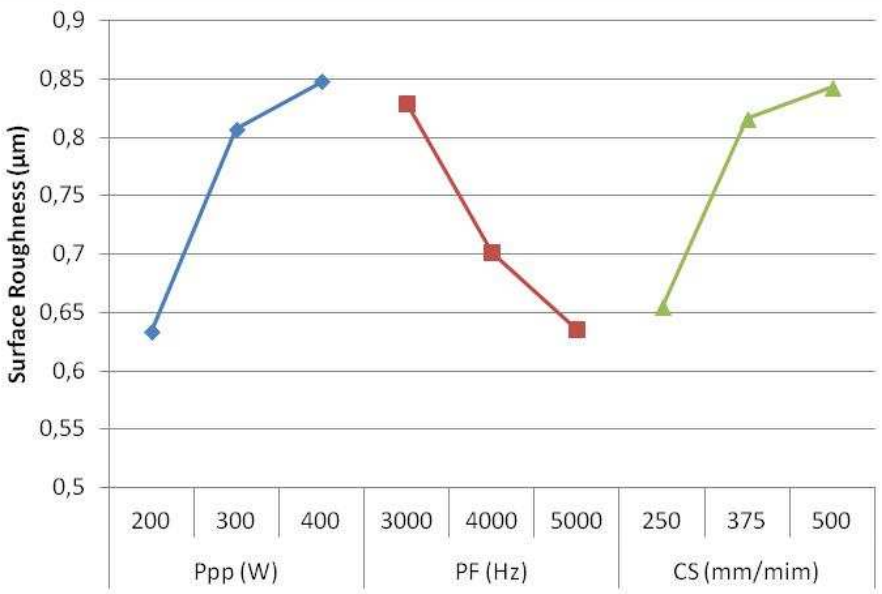

Figure 6. Surface roughness as a function of laser cutting parameters: peak pulse power, pulse frequency, and cutting speed.

The striation refers to periodic lines appeared on the cut surface. These periodic lines reflect the effect of the combination of the laser beam moving along the surface the pulse frequency and the pulse duration, generating pressure gradients across the cut kerf and varying vaporisation fronts. This phenomenon created regularly spaced striations and increased the surface roughness on the cut surface. Thus, striation is directly related to the surface roughness and mainly affects the surface quality of the cut zones. The profiles of the figures 4 and 5 indicate that striation occur, presenting different height depending on the parameters. However, looking at the images it is not easy to see a clear pattern related to the striations. It seems that the molten material is deposited on the cut surface modifying these striations generated from the laser beam movement.

3.3 Heat effects

Heat effect on the surrounding material is a critical factor in cutting thin materials especially in medical device application. Small and thin materials are very sensitive to thermal distortion. Experiment results show that low average power reduced the thermal distortion. Thus, when pulse peak power and pulse frequency are higher it resulted in a noticeable thermal effect and surface oxidation along the cut as clearly shows the figure 7.

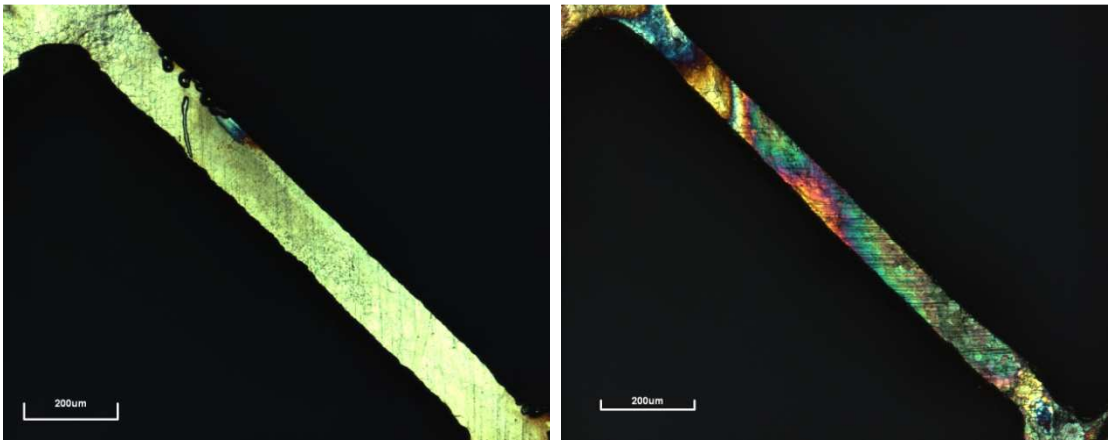

Figure 7 Comparison of the thermal effect along the strut; a) pulse peak power 200, pulse frequency 3000 Hz and cutting speed 250 mm/min, b) peak pulse power 400, pulse frequency 5000 Hz and cutting speed 500 mm/min.

3.4 Dross deposition

The images of the cut surface with the dross formed where obtained from destructive tests in which the specimens were embedded in resin. Figure 8 and 9 present images from the cut surface and from the bottom of the geometry with the dross deposited for two different samples. Clearly there is much dross deposited in the cut edges of the samples. Depending on the combination of the process parameters there is different amount of it. The area was measured from the cut surface images in order to establish a relation between the input parameters and the dross formation.

Figure 8. Dross deposition for peak pulse power 300 W, pulse frequency 3000 Hz and cutting speed 250 mm/min sample a) bottom image from optical microscope (50X), b) cut surface image from optical microscope (80X).

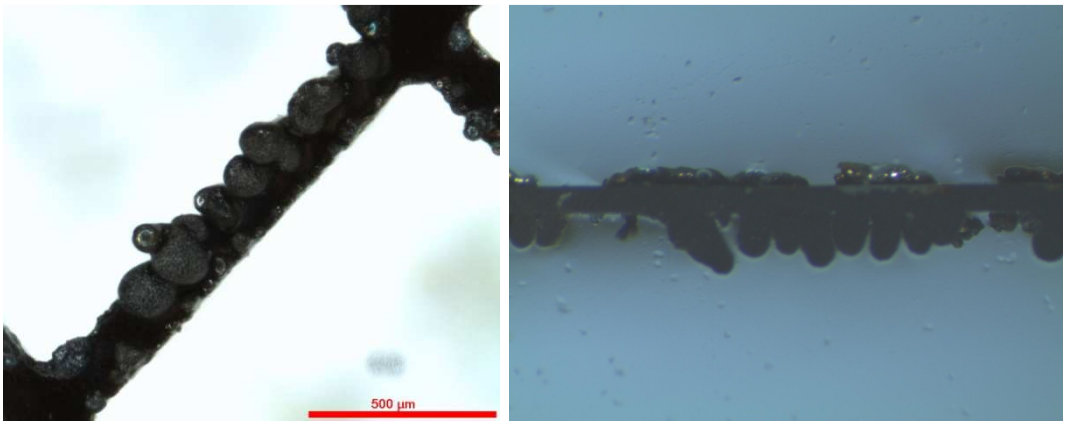

Figure 9. dross deposition for peak pulse power 300 W, pulse frequency 4000 Hz and cutting speed 500 mm/min sample a) bottom image from optical microscope (50X), b) cut surface image from optical microscope (80X).

The dross deposition has been measured for each stent in six different struts. The area of the dross has been taken from the upper part and lower part of the stent separately. The mean of the six measurements has been used as the value for the results analysis.

Figure 10 presents the dross deposition area as function of the laser cutting parameters. Clearly the samples processed were not free from dross. The molten material was not totally ejected out from the cut kerf and attached to the bottom side of the cut wall. The dross deposition area increased as the peak pulse power, pulse frequency and cutting speed increased. The relation presented is similar at the one for the kerf width. If the peak pulse power and the pulse frequency increase the average power increases leading to more molten material. More molten material means that is more difficult to remove by the assist gas. At the same time higher cutting speeds reduce the time the gas is working on the same area, thus the dross area gets bigger.

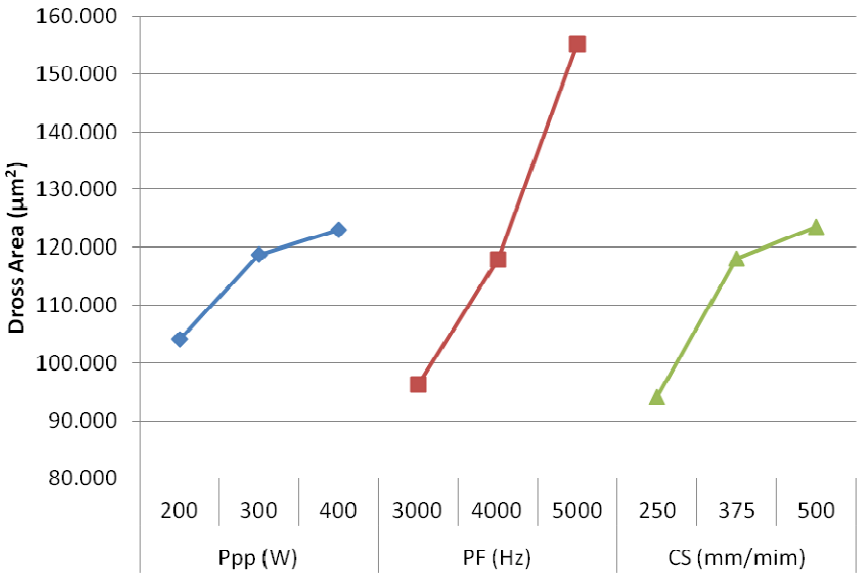

Figure 10. Dross deposition area as a function of laser cutting parameters: peak pulse power, pulse frequency, and cutting speed.

As can be seen in the figure 9b, there are some cases where the sample presents material formation on the top of the struts. This material rejected from the cutting zone, has been deposited on the sheet in droplets form. Thus, although these droplets are not always on the cut edge, the area of this material formed has been also measured following the same procedure described before.

Table 2. Workpiece and assisting gas properties used in the simulations.

Property	Value	Units
Boiling temperature	3133	K
Melting temperature	1648	K
Density of assisting gas	6.875 at 6bar	kgm^{-3}
Density of workpiece	7990	kgm^{-3}
Specific heat capacity	500	$Jkg^{-1}K^{-1}$
Latent heat of melting	$2.75x10^{5}$	Jkg^{-1}
Viscosity of melting material	$0.9x10^{-2}$	Nsm^{-2}
Viscosity of assisting gas	$61.77x10^{-6}$	Nsm^{-2}
Velocity of gas jet	417	ms^{-1}

4. Mathematical modelling

As shown in the results the dross deposition is quite important. Thus, a mathematic model is presented in order to predict the dimensions of this dross as function of some of the laser cutting parameters. In this way, we can select the proper laser conditions to reduce the amount of dross. The height and the diameter of the dross deposited on the experimental samples was measured and compared with the model predictions.

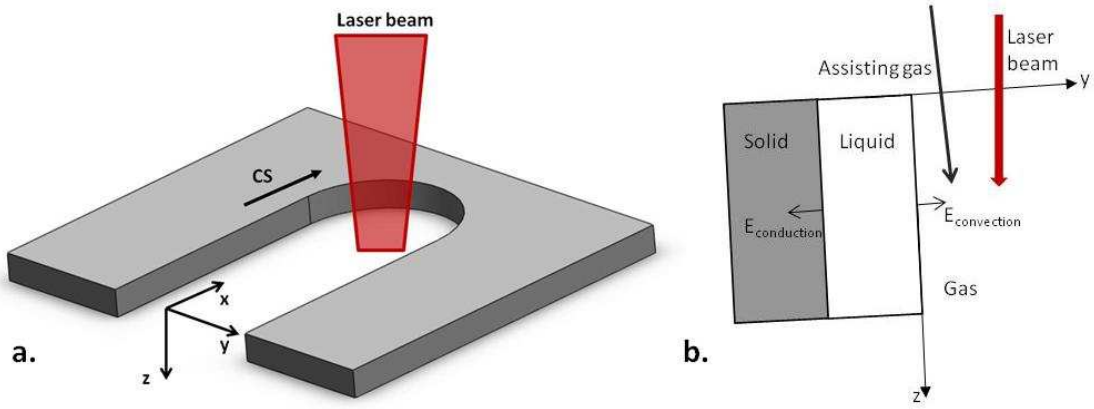

Figure 11. a) Schematic view of laser cutting process. b) Schematic view of melt section.

4.1 Dross height

Considering the laser cutting as a transient process where a Gaussian laser beam strikes the surface of a substrate, moving in the positive x direction with a uniform cutting speed. The laser beam intensity can be described by the Gaussian distribution as follows:

$$I(x,y,z) = \frac{P}{\pi R^2} e^{-[(x^2+y^2)/R^2]} \quad (1)$$

The process is considered continuous wave operation. The high repetition rates and the levels of cutting speed used during the experiments result in high overlapping between pulses (98.15-99.44%), calculated as presented in [23] making the assumption of the continuous wave acceptable. The convection and conduction are considered negligible.

Thus, the complex three dimensional kerf, as shown in Figure 11a, can be separated into finite surface elements described by x and y directions. For each element the energy balance can be described as follows; the laser input energy is equal to the energy necessary for the phase change of the surface.

$$E_{beam}\delta x\delta y = E_{melt}\delta x\delta y \quad (2)$$

The laser input energy is given by

$$E_{beam} = \int_{-\infty}^{\infty} I(x,y,z)\frac{\partial x}{CS} = \frac{aP}{CS\sqrt{\pi}R}e^{-(y^2/R^2)} \quad (3)$$

Where a is the absorptance of SS316L at the Nd:YAG laser wavelength 1.064 µm. The phase change energy is given by:

$$E_{melt} = \rho\left[C_{ps}(T_m - T_i) + L_m + C_{pm}(T_v - T_m)\right]d_H(y)\partial x\partial y \quad (4)$$

Where $d_H(y)$ is the dross height at y. Setting the energy balance yields

$$\frac{aP}{CS\sqrt{\pi}R}e^{-(y^2/R^2)}\partial x\partial y = \rho\left[C_{ps}(T_m - T_i) + L_m + C_{pm}(T_v - T_m)\right]d_H(y)\partial x\partial y \quad (5)$$

Then, the channel depth can be obtained as

$$d_H(y) = \frac{aP}{CS\sqrt{\pi}R\rho\left[C_{ps}(T_m - T_i) + L_m + C_{pm}(T_v - T_m)\right]}e^{-(y^2/R^2)} \quad (6)$$

4.2 Liquid layer thickness

Considering the melt layer generated at the solid surface during the steady laser heating process (Figure 11b). The influence of assisting gas on the cutting process needs to be modeled prior to dross diameter formulation. This is because the droplet diameter depends on the liquid layer. The rate of energy balance with the melting process is considered in order to determine the liquid layer thickness.

$$\dot{E}_{beam} + \dot{E}_{oxidation} = \dot{E}_{melt} + \dot{E}_{cond} + \dot{E}_{conv} \quad (7)$$

It is considered that the generated melt layer flows steadily in the direction of the assisting gas due to the drag force developed at the assisting gas-liquid interface. Because of the micrometric dimensions of the sheet thickness and the kerf width, it is assumed that the rate of energy convected (E_{conv}) from the surface to the assisting gas, and the rate of energy conducted (E_{cond}) from the melted material to the solid substrate are minimal compared with the incident beam energy. Also the use of nitrogen as an assisting gas reduces to a minimum the exothermic reaction which would contributed to the energy transport process at the interface ($E_{oxidation}$).

The energy of the melting or the phase change can be written as:

$$\dot{E}_{melt} = \dot{m}_L\left[C_{ps}(T_m - T_i) + L_m + C_{pm}(T_v - T_m)\right] \quad (8)$$

where C_{ps} and C_{pm} are the specific heat capacity of the material in the solid and the liquid state, respectively, T_i, T_m and T_v are the initial temperature, the melting temperature and the vaporization temperature of the material, respectively. $\dot{m}_L$ is the rate of mass generated from solid into liquid at the solid surface which in laser melting process, can be written as

$$\dot{m}_L = \frac{\partial}{\partial t}(\rho V) = \rho_L v_L A, \tag{9}$$

Where v_L is the velocity of the molten material, ρ_L is the density of the molten metal, A is the cross sectional area. Setting the rate of energy balance across the melt per unit area yields

$$\frac{\dot{E}_{beam}}{A} = \frac{\dot{E}_{melt}}{A} \tag{10}$$

Therefore,

$$v_L = \frac{P}{A\rho_L[C_{ps}(T_m - T_i) + L_m + C_{pm}(T_v - T_m)]} \tag{11}$$

Considering that the movement in the molten material towards the bottom of the workpiece is induced by a shear stress exerted by the assisting gas jet on the surface of the molten zone [20]. The melt's velocity is given by

$$v_L = \frac{s_L \cdot \tau}{\mu_L} \tag{12}$$

Where s_L is the liquid layer thickness, μL is the dynamic viscosity of the molten metal, and ζ is the shear stress which is given by the following equation.

$$\tau = \sqrt{\frac{\rho_G \mu_G v_G^3}{z}} \tag{13}$$

Where ρ_G is the density of the gas, μ_G is the dynamic viscosity of the gas, v_G is the gas velocity, and z is the sheet thickness. Introducing equations (6) and (7) into equation (4) yields

$$s_L = \frac{\mu_L P}{A\rho_L[C_{ps}(T_m - T_i) + L_m + C_{pm}(T_v - T_m)]} \left(\frac{\rho_G \mu_G v_G^3}{z}\right)^{-1/2} \tag{14}$$

4.3 Dross diameter

The dross formation depends on the liquid properties, such as viscosity, density and surface tension, as well as laser and cutting properties, such as assisting gas velocity, kerf size and liquid layer thickness. Moreover, a laminar flow of liquid film breaks up into droplets in an orderly and periodic manner. In practice small satellite droplets can also be formed in between the main droplets due to high aerodynamic forces and instabilities associated with the breakup process. The formulation of drop formation based on the ligament disintegration can be appropriate to a laser cutting process. Droplet diameter (d_D) formulated earlier is adopted herein [18]:

$$d_D = \left(\frac{3\pi}{\sqrt{2}}\right) s_L \left(1 + \frac{3\mu_L}{\sqrt{\rho_L s_L}}\right)^{1/6} \tag{15}$$

Equations (6) and (15) are used to compute the dross height and diameter in the cutting sections, respectively.

The dross height and diameter is analyzed and compared with the experimental results. Table 2 gives the material and assisting gas properties. The diameter and height of the dross presented as experimental results are obtained by taking the average diameter of the measures taken in 5 different struts of each sample. The diameter measures are taken from bottom images like figure 8a and the height measures are taken from cut edge front images like figure 8b.

Figure 11 presents the dross height predicted from equation 6 as a function of peak pulse power for different laser cutting speeds. As in the previous case, the height of the dross increases with the increasing of the pulse peak power. In this sense, the predicted height and the average measured show similar tendencies. The predicted lines show that the height of the dross reduces when the laser cutting speed increases and the experimental results present the opposite trend. In a laser milling process lower cutting speed results in higher material removal because the incident laser beam lasts longer in the same area. However, in the laser cutting process, the presence of the assisting gas changes the trend. As lower is the cutting speed more time is working the gas to eject the molten material, reducing the height dross. Although there is no much literature relating the dross dimension with the cutting speed, this is in the line with the results showed by Tani et al. [19]. Thus, the effect of the cutting speed in the model must be understood as the inverse of the reality. However further research is necessary to ensure this relation.

Figure 12 shows the dross diameter predicted from equation 15 with peak pulse power. Experimentally, obtained dross diameters are given for comparison. The higher pulse peak power results in bigger dross diameter. The Increasing of power intensity increases the liquid film thickness, which in turn enhances the dross diameter. On comparing the predictions with the average dross diameter measured both results agree quite well. However, both trend lines present different slopes. This may be associated to the assumptions made in the analysis.

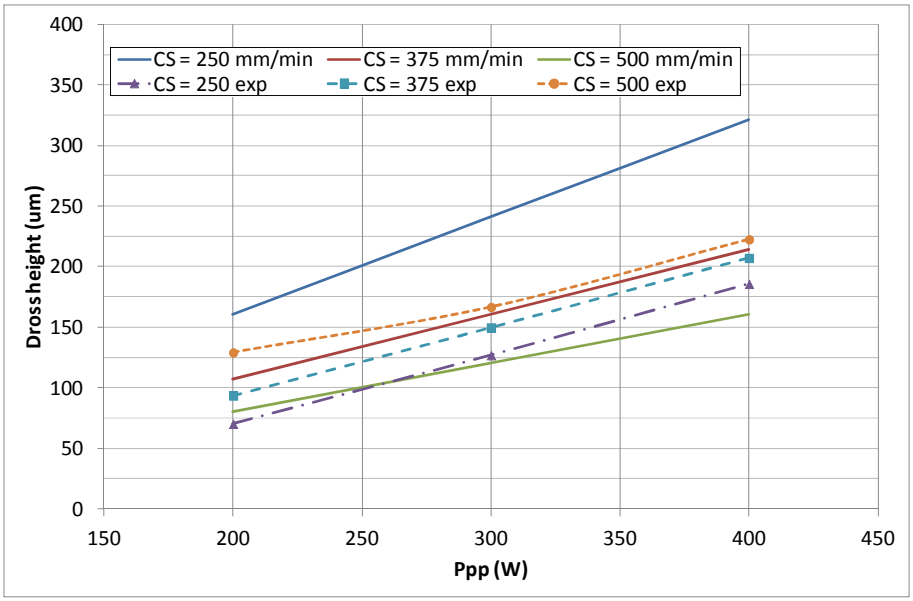

Figure 11. Predicted and experimental dross diameter as a function of peak pulse power for different laser cutting speeds.

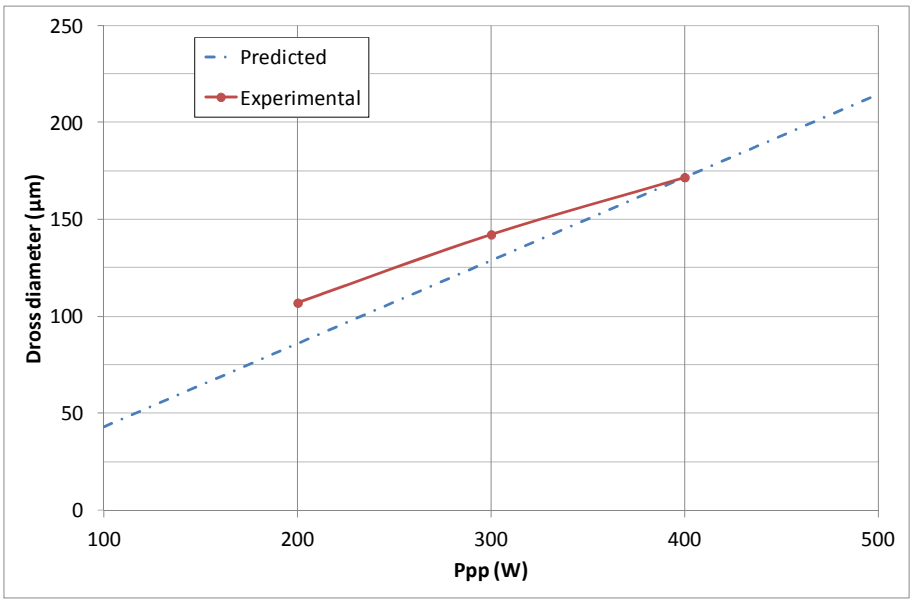

Figure 12. Predicted and experimental dross diameter as a function of peak pulse power.

5. Conclusions

In this study experimental results of fiber laser cutting of stainless steel 316L sheets were reported. The effect of peak pulse power, pulse frequency and cutting speed on the cutting quality for fixed gas type and gas pressure were investigated. The analysis showed that increasing the peak pulse power and the cutting speed increases the kerf width, surface roughness and dross deposition. However, the effect of the cutting speed needs further

research because with higher values the dross and the kerf width are expected to decrease. Higher pulse frequency values result in bigger kerf and dross but improves the surface roughness.

In order to reduce the amount of dross attached to the cutting edge, a mathematic model for the dross dimensions was formulated. The dross height and the dross diameter were analyzed and compared with the experimental results. Both dimensions increase with the increasing of the pulse peak power.

6. Acknowledgements

The authors would like to express their gratitude to the GREP research group from the UdG, the Tecnologico de Monterrey for the facilities provided during the experiments. This work was partially carried out with the grant supports from the European Commission project IREBID (FP7-PEOPLE-2009-IRSES-247476) and the Spanish Science and Innovation Minister project TECNIPLAD (DPI2009- 09852).

7. References

[1] G. Tawari, J.K. Sarin Sundar, G. Sundararajan, S.V. Joshi. Influence of process parameters during pulsed Nd:YAG laser cutting of nickel-base superalloys. Journal of Materials Processing Technology 170 (2005) 229–239.

[2] K.F. Kleine, B. Whitney, K.G. Watkins. Use of fiber lasers for micro cutting applications in medical device industry. 21st International Congress on Applications of Lasers and Electro-Optics, (2002).

[3] N. Muhammad, D. Whitehead, A. Boor, L. Li. Precision Machine Design. Comparison of dry and wet fiber laser profile cutting of thin 316L stainless steel tubes for medical device applications. Journal of Materials Processing Technology 210 (2010) 2261–2267.

[4] H. Meng, J. Liao, Y. Zhou, Q. Zhang. Laser micro-processing of cardiovascular stent with fiber laser cutting system. Optics & Laser Technology 41 (2009) 300– 302.

[5] M. Baumeister, K. Dickman, T. Hoult. Fiber laser micro-cutting of stainless steel sheets. Journal of Applied Physics. A 85, 121–124 (2006).

[6] L.D. Scintilla, D. Sorgente, L. Tricarico. Experimental Investigation On Fiber Laser Cutting Of Ti6Al4V Thin Sheet. Journal of Advanced Materials Research Vols. 264-265 (2011) pp 1281-1286.

[7] J. Powell, S.O. Al-Mashikhi, K.T.Voisey. Fibre laser cutting of thin section mild steel: An explanation of the ‘striation free’ effect. Optics and Lasers in Engineering 49 (2011) 1069–1075

[8] Y. Yan, L. Li, K. Sezer, D. Whitehead, L. Ji, Y. Bao, Y. Jiang. Experimental and theoretical investigation of fibre laser crack-free cutting of thick-section alumina. International Journal of Machine Tools & Manufacture 51 (2011) 859–870

[9] Y.P. Kathuria. Laser microprocessing of metallic stent for medical therapy. Journal of Materials Processing Technology 170 (2005) 545–550.

[10] R. Pfeifer, D. Herzog, M. Hustedt, S. Barcikowski. Pulsed Nd:YAG laser cutting of NiTi shape memory alloys—Influence of process parameters. Journal of Materials Processing Technology 210 (2010) 1918–1925.

[11] Lv. Shanjin, W. Yang. An investigation of pulsed laser cutting of titanium alloy sheet. Optics and Lasers in Engineering 44 (2006) 1067–1077.

[12] K.C. Yung, H.H. Zhu, T.M. Yue. Theoretical and experimental study on the kerf profile of the laser micro-cutting NiTi shape memory alloy using 355 nm Nd:YAG. Smart Materials and Structures 14 (2005) 337–342.

[13] N. Muhammad, D. Whitehead, A. Boor, W. Oppenlander, Z. Liu, L. Li. Picosecond laser micromachining of nitinol and platinum-iridium alloy for coronary stent applications. Applied Physics A (2012) 106:607–617.

[14] C. Lia, S. Nikumbb, F. Wong. An optimal process of femtosecond laser cutting of NiTi shape memory alloy for fabrication of miniature devices. Optics and Lasers in Engineering 44 (2006) 1078–1087.

[15] H. Huang, H.Y. Zheng, G.C. Lim. Femtosecond laser machining characteristics of Nitinol. Applied Surface Science 228 (2004) 201–206.

[16] A. Raval, A. Choubey, C. Engineer, D. Kothwala. Development and assessment of 316LVM cardiovascular stents. Materials Science and Engineering A 386 (2004) 331–343.

[17] L.D. Scintilla, L. Tricarico. Experimental investigation on fiber and CO2 inert gas fusion cutting of AZ31 magnesium alloy sheets. Optics & Laser Technology 46 (2013) 42–52.

[18] B.S. Yilbas, B.J. Abdul Aleem. Dross formation during laser cutting process. Journal of Physiscs D: Applied Physics 39 (2006) 1451–61.

[19] G. Tani, L. Tomesani, G. Campana, A. Fortunato. Quality factors assessed by analytical modelling in laser cutting. Thin Solid Films 453-454 (2004) 486-491.

[20] D. Schuöcker, J. Aichinger, R. Majer. Dynamic phenomena in laser cutting and process performance. Physics Procedia 39 (2012) 179–185.

[21] S.Z. Shuja, B.S. Yilbas, O. Momin. Laser heating of a moving slab: influence of laser intensity parameter and scanning speed on temperature field and melt size. Optics & Laser Technology 49 (2011) 265–272.

[22] M. Shikida, T. Yokota, J. Naito, K. Sato. Fabrication of a stent-type thermal flow sensor for measuring nasal respiration. Journal of Micromechanics and Microengineering 20 (2010) 055029.

[23] D. Teixidor, F. Orozco, T. Thepsonthi, J. Ciurana, C.A. Rodriguez, T. Özel. Effect of process parameters in nanosecond pulsed laser micromachining of PMMA-based microchannels at near-infrared and ultraviolet wavelengths. International Journal of Advanced Manufacturing Technology (2012) 170-012-4598-x

Chapter 8. Conclusions and outlook

Chapter 8 presents the conclusion of the Thesis, summarizes the main contributions presented and points out possible further works arising from the research exposed.

8.1 Conclusions

Laser milling is a very complex process. Thus, it is necessary to study the process and develop different tools for the optimal process parameters selection. In this way, the laser machining process planning conducted by operators and companies, will be more accurate and productive.

The Chapter 3 to Chapter 7 present studies and experiments of how the process parameters affect the final product characteristics. The use of different statistical and analytical tools established clear relations between inputs (pulse intensity, scanning speed and pulse frequency) and response variables (surface roughness, dimensional accuracy and productivity).

Moreover several AI models and GA are presented which provide intelligent selection of parameters for process planning. Multi-objective optimization models are used for selecting the proper process parameters combination for getting the best results in several responses. In Chapter 4, multi-criteria decision making for material and process parameter selection for

desired surface quality and dimensional accuracy is investigated using an evolutionary computation method based on particle swarm optimization. Chapter 6 adopted a model to find the optimal set of parameters to improve the dimensional accuracy reducing the error of the dimensions of micro-geometries.

Mathematical models are also presented in order to predict the effects of the laser and its parameters setting on the final part. In Chapter 5 a mathematical model is developed to calculate the depth of micro-channels machined in a single-pass of the laser beam. The same model, but adapted is used to predict the dross formation into a laser cutting process.

With the knowledge provided by these studies and the models developed will permit laser machine operators to optimize the parameters selection, maximizing productivity while ensuring quality requirements.

8.2 Main contributions

The main contributions of the work presented in this Thesis are summarized below:

- The effect of key process parameters (pulse intensity, pulse frequency and scanning speed) on the dimensional accuracy, surface roughness and material removal rate have been investigated for laser milling on tool steel.

- A novel multi-criteria ranking and parameter selection method which can find the best combination of those used to obtain results between established quality ranges.

- A multi-objective particle swarm optimizer in a 2.5D laser milling. It provides Pareto frontiers of non-dominated solution sets for optimum laser milling process parameters, providing decision makers with a resourceful and efficient means of achieving it.

- The microchannel geometry and MRR during a single pass laser micromachining process on PMMA polymer substrate as function of laser processing parameters. The effectiveness of using NIR wavelength nanosecond pulse laser ablation on PMMA polymer with comparison to UV wavelength laser ablation in fabricating microchannels is demonstrated.

- Mathematical modelling for microchannel depth profile was performed and validated with experimental microchannel depth profile images.

- A multi-objective optimization NSGA-II for a 3D laser milling process. Among the key process parameters, the geometry of the feature appears as an important input variable.
- A mathematic model for the dross dimensions was formulated for laser cutting process. In order to reduce the amount of dross attached to the cutting edge, the dross height and the dross diameter were analyzed and compared with the experimental results.
- Different tools for planning and selection of the process conditions are provided for the laser machining process.

8.3 Further work

Laser milling technology is far to be fully known. Further work could include study of machining of different materials. Several materials are being used in biomedical applications because of its biodegradable and biocompatible characteristics. Magnesium is one of these materials, but it presents a challenge for the laser technology. The magnesium in powdered form is extremely flammable. In contact with air and some heat reacts rapidly and produce hydrogen. At the same time the possibility to work with different laser types like ultrashort pulse lasers, with pulse lengths in the range of pico- and femtoseconds, would open a door into another research space.

Next step in the modelling of the process should be to develop FEM thermal based models to simulate the response of the process depending on the process parameters. This will provide a more visual tool to understand how the parameters selection affects the dimensions and the quality of the final part. This could provide information about the relation of the input parameters with the temperatures on the surface of the part and the final results. In this way, could be possible to control some response variables in function of the temperature provided by the laser beam. This kind of relation could be use to develop an in-process control system, which depending on the temperature on the workpiece surface (measured with sensors or infrared camera) could change the parameters of the laser in order to obtain better quality and dimensional accuracy.

8.4 Thesis results

Published articles

Teixidor, D.; Ferrer, I.; Ciurana, J.; Özel, T. (2012). Optimization of Process Parameters for Pulsed Laser Milling of Micro-channels on AISI H13 Tool Steel. Robotics and Computer-Integrated Manufacturing, 29; 1, 209-218

Teixidor, D.; Ferrer, I.; Ciurana, J. (2012). Experimental Analysis of Laser Micro-Machining Process Parameters. Materials Science Forum, 713, 67-73

Teixidor, D.; Ciurana, J.; Thepsonthi, T.; Ozel, T. (2012). Nanosecond pulsed laser micromachining of PMMA-based microfluidic channels. Journal of Manufacturing Processes, 14; 4, 435-442.

Teixidor, D.; Orozco, F.; Thepsonthi, T.; Ciurana, J.; Rodríguez, C.; Ozel, T. (2012). Effect of process parameters in nanosecond pulsed laser micromachining of PMMA based microchannels. International Journal of Advanced Manufacturing Technology, DOI:10.1007/s00170-012-4598-x

Conferences

Teixidor, D.; Ferrer, I.: Ciurana, J. (2011). An experimental analysis of process parameters to manufacture micro-channels in AISI H13 tempered steel by laser micro-milling. 4th Manufacturing Engineering Society International Conference (MESIC'11). Cadiz (Spain).

Teixidor, D.; Thepsonti, T.; Ciurana, J.; Özel, T. (2012). Laser micro-machining of PMMA-based micro-channels for microfluidics applications. 1st International Conference on Design and Processes for Medical Devices (PROMED). Brescia (ITALY).

Teixidor, D.; Ciurana, J.; Thepsonthi, T.; Ozel, T. (2012). Nanosecond Pulsed Laser Micro-Machining of PMMA-based Microfluidic Channels. 40th North American Manufacturing Research Conference (NAMRC). Indiana (USA).

Chapter 9. References

Aguilar, C. A., Lu, Y., Mao, S., & Chen, S. (2005). Direct-patterning of biodegradable polymers using ultraviolet and femtosecond lasers. Biomaterials 26: 7642-7649.

Amer, M. S., El-Ashry, M. a., Dosser, L. R., Hix, K. E., Maguire, J. F., & Irwin, B. (2005). Femtosecond versus nanosecond laser machining: comparison of induced stresses and structural changes in silicon wafers. Applied Surface Science, 242(1-2), 162–167.

ASCAMM. *ASCAMM centre tecnològic*. Retrieved the 12th of June, 2013, from: http://www.ascamm.com/

Ashkenasi, D., Kaszemeikat, T., Mueller, N., Dietrich, R., Eichler, H. J., & Illing, G. (2011). Laser Trepanning for Industrial Applications. Physics Procedia, 12, 323–331.

Bandyopadhyay, S., Gokhale, H., Sarin Sundar, J. K., Sundararajan, G., & Joshi, S. V. (2005). A statistical approach to determine process parameter impact in Nd:YAG laser drilling of IN718 and Ti-6Al-4V sheets. Optics and Lasers in Engineering, 43(2), 163–182.

Bartolo, P., Vasco, J., Silva, B., & Galo, C. (2006). Laser micromachining for mould manufacturing: I. The influence of operating parameters. Assembly Automation, 26(3), 227–234.

Baudach, S., Bonse, J., Krüger, J., & Kautek, W. (2000) Ultrashort pulse laser ablation of polycarbonate and polymethylmethacrylate. Applied Surface Science, 154/155: 555-560.

Baumeister, M., Dickman, K., & Hoult, T. (2006) Fiber laser micro-cutting of stainless steel sheets. Journal of Applied Physics. A 85, 121–124.

Ben-yakar, A., & Byerh, R. L. (2002). Femtosecond laser machining of fluidic microchannels for miniaturized bioanalytical systems, 4637, 212–217.

Benardos, P. G. & Vosniakos G.C. (2003). Predicting surface roughness in machining: a review. International Journal of Machining Tools and Manufacturing 43(8), 833–844.

Biswas, R., Kuar, a. S., Sarkar, S., & Mitra, S. (2010). A parametric study of pulsed Nd:YAG laser micro-drilling of gamma-titanium aluminide. Optics & Laser Technology, 42(1), 23–31.

Böhme, R., Hirsch, D., & Zimmer, K. (2006). Laser etching of transparent materials at a backside surface adsorbed layer. Applied Surface Science, 252(13), 4763–4767.

Bordatchev, E. V., & Nikumb, S. K. (2003). An Experimental Study and Statistical Analysis of the Effect of Laser Pulse Energy on the Geometric Quality During Laser Precision Machining. Machining Science and Technology, 7(1), 83–104.

Brousseau, E. & Eldukhri E. (2011). Recent advances on key technologies for innovative manufacturing. Journal of Intelligent Manufacturing, 22(5), 675-691.

Bustillo, A., Sedano, J., Villar, J. R., Curiel, L., & Corchado, E. (2008). AI for Modelling the Laser Milling of Copper Components, 498–507.

Bustillo, A., Díez-Pastor, J. F., Quintana, G., & García-Osorio C. (2011). Avoiding neural network fine tuning by using ensemble learning: application to ball-end milling operations. The International Journal of Advanced Manufacturing Technology, 57(5), 521-532.

Bustillo, A., Ukar, E., Rodriguez, J. J. & Lamikiz A. (2011). Modelling of process parameters in laser polishing of steel components using ensembles of regression trees. International Journal of Computer Integrated Manufacturing, 24(8), 735-747.

Bustillo A. & Correa M. (2012). Using artificial intelligence to predict surface roughness in deep drilling of Steel Components. Journal of Intelligent Manufacturing, 23(5), 1893-1902.

Butler-smith, P. W., Axinte, D. A., Pacella, M., & Fay, M. W. (2013). Journal of Materials Processing Technology Micro / nanometric investigations of the effects of laser ablation in the generation of micro-tools from solid CVD diamond structures, 213, 194–200.

Campanelli, S. L., Ludovico, A. D., Bonserio, C., Cavalluzzi, P. & Cinquepalmi, M. (2007). Experimental analysis of the laser milling process parameters. Journal of Materials Processing Technology, 8/1;191(1-3):220-223.

Campanelli, S. L., Casalino, G., Ludovico, A. D., & Bonserio, C. (2013). An artificial neural network approach for the control of the laser milling process. Journal of Advanced Manufacturing Technology, 66:1777–1784.

Campanelli, S. L., Casalino, G., Contuzzi, N. (2013). Multi-objective optimization of laser milling of 5754 aluminum alloy. Optics & Laser Technology, 52 48–56

Cai, W., & Piestun, R. (2007). Low pulse-energy micromachining in bulk glass with a short-cavity femtosecond oscillator. Optical Engineering, 46(12), 124301.

Chaitanya Vishnubhatla, K., Clark, J., Lanzani, G., Ramponi, R., Osellame, R., & Virgili, T. (2009). Femtosecond laser fabrication of microfluidic channels for organic photonic devices. Applied optics, 48(31), G114–8.

Chandrasekaran, M., Muralidhar, M., Krishna, C. & Dixit, U. (2010). Application of soft computing techniques in machining performance prediction and optimization: a literature review. International Journal of Advanced Manufacturing Technology, 46(5), 445–464.

Chen, S., Kancharla, V. V., & Lu, Y. (2003). Laser-based microscale patterning of biodegradable polymers for biomedical applications. International Journal of Material and Product Technology, 18:457-468.

Cheng, J-Y., Wei, C. W., Hsu, K-H., & Young T-H (2004). Direct-write laser micromachining and universal surface modification of PMMA for device development. Sensors & Actuators 99: 186-196.

Cheng, J., Perrie, W., Edwardson, S. P., Fearon, E., Dearden, G., & Watkins, K. G. (2009). Effects of laser operating parameters on metals micromachining with ultrafast lasers. Applied Surface Science, 256(5), 1514–1520.

Cheng, Y., Sugioka, K., Masuda, M., Toyoda, K., & Kawachi, M. (2003). 3D microstructuring inside Foturan glass by femtosecond laser, 50(50), 101–106.

Chichkov, B. N., Momma, C., Nolte, S., Alvensleben, F. Von, & Tu, A. (1996). Femtosecond , picosecond and nanosecond laser ablation of solids, 115, 109–115.

Choudhury, I. a., Chong, W. C., & Vahid, G. (2012). Hole qualities in laser trepanning of polymeric materials. Optics and Lasers in Engineering, 50(9), 1297–1305.

Cicală, E., Soveja, a., Sallamand, P., Grevey, D., & Jouvard, J. M. (2008). The application of the random balance method in laser machining of metals. Journal of Materials Processing Technology, 196(1-3), 393–401.

Ciurana, J., Arias, G., & Ozel, T. (2009). Neural Network Modeling and Particle Swarm Optimization (PSO) of Process Parameters in Pulsed Laser Micromachining of Hardened AISI H13 Steel. *Materials and Manufacturing Processes*, *24*(3), 358–368.

Coello Coello, C. A., & Becerra, R.L. (2009). Evolutionary Multiobjective Optimization in Materials Science and Engineering, Materials and Manufacturing Prcesses, 24 (2) 119 – 129.

Correa, M., Bielza, C., & Pamies-Teixeira, J. (2009). Comparison of Bayesian networks and artificial neural networks for quality detection in a machining process. Expert Systems with Applications, 36, 7270–7279.

Dahotre, N. B. & Harimkar, S. P. (2008). Laser fabrication and machining of materials. Springer.

Davis, K. M., Miura, K., Sugimoto, N., & Hirao, K. (1996). Writing waveguides in glass with a femtosecond laser. Optics letters, 21(21), 1729–31.

Day, D., & Gu, M. (2005). Microchannel fabrication in PMMA based on localized heating using high-repetition rate femtosecond pulses. Proceedings SPIE 6037: 24–31.

Deb, K., Pratap, A., Agarwal, S., & Meyarivan, T. (2002) A Fast Elitist Multiobjective Genetic Algorithm: NSGA-II, IEEE Transactions on Evolutionary Computation, 6;2, 182 – 197.

Deepak, K. L. N., Rao, D. N., Rao, S. V. (2010) Fabrication and optical characterization of microstructures in poly(methylmethacrylate) and poly(dimethylsiloxane) using femtosecond pulses for photonic and microfluidic applications. Applied Optics 49: 2475-2489.

Desai, C. K. & Shaikh A. (2012) Prediction of depth of cut for single-pass laser micro-milling process using semi-analytical, ANN and GP approaches. International Journal Of Advanced Manufacturing Technology, 60(9-12), 865-882.

Dhara, S. K., Kuar, a. S., & Mitra, S. (2007). An artificial neural network approach on parametric optimization of laser micro-machining of die-steel. The International Journal of Advanced Manufacturing Technology, 39(1-2), 39–46.

Dhupal, D., Doloi, B., & Bhattacharyya, B. (2007). Parametric analysis and optimization of Nd:YAG laser micro-grooving of aluminum titanate (Al2TiO5) ceramics. The International Journal of Advanced Manufacturing Technology, 36(9-10), 883–893.

Díez-Pastor, J. F., Bustillo, A., Quintana, G. & García-Osorio C. (2012). Boosting Projections to improve surface roughness prediction in high-torque milling operations. Soft Computing, 16(8), 1427-1437.

Dobrev, T., Dimov, S. S., & Thomas, a J. (2006). Laser milling: modelling crater and surface formation. Proceedings of the Institution of Mechanical Engineers, Part C: Journal of Mechanical Engineering Science, 220(11), 1685–1696.

Dubey, A. K., & Yadava, V. (2008). Optimization of kerf quality during pulsed laser cutting of aluminium alloy sheet. Journal of Materials Processing Technology, 204(1-3), 412–418.

Dubey, A. K., & Yadava, V. (2008), Laser beam machining-A review. International Journal of Machining Tools and Manufacturing, 5;48(6):609-628.

Dubey, A. K., & Yadava, V. (2008). Experimental study of Nd:YAG laser beam machining—An overview. J Mater Process Technol, 1/1;195(1-3):15-26.

Dumitru, G., Lüscher, B., Krack, M., Bruneau, S., Hermann, J., & Gerbig, Y. (2005). Laser processing of hardmetals: Physical basics and applications. International Journal of Refractory Metals and Hard Materials, 23(4-6), 278–286.

Dutta Majumdar, J. & Manna, I. (2010) Laser materials processing. International Materials Review, 56;5-6, 341-388.

Eaton, S., Zhang, H., Herman, P., Yoshino, F., Shah, L., Bovatsek, J., & Arai, A. (2005). Heat accumulation effects in femtosecond laser-written waveguides with variable repetition rate. Optics express, 13(12), 4708–16.

Florea, C., Winick, K. A., & Member, S. (2003). Fabrication and Characterization of Photonic Devices Directly Written in Glass Using Femtosecond Laser Pulses, 21(1), 246–253.

García-Ballesteros, J. J., Torres, I., Lauzurica, S., Canteli, D., Gandía, J. J., & Molpeceres, C. (2011). Influence of laser scribing in the electrical properties of a-Si:H thin film photovoltaic modules. Solar Energy Materials and Solar Cells, 95(3), 986–991.

Gečys, P., Račiukaitis, G., Miltenis, E., Braun, A., & Ragnow, S. (2011). Scribing of Thin-film Solar Cells with Picosecond Laser Pulses. Physics Procedia, 12, 141–148.

Garg, S., & Serruys, P. W. (2010). Coronary stents. Looking forward. Journal of American college of Cardiology, 56,10.

Gilbert, T., Krstic, V. D., & Zak, G. (2007). Machining of aluminium nitride with ultra-violet and near-infrared Nd:YAG lasers. Journal of Materials Processing Technology, 189(1-3), 409–417.

Giridhar, M. S., Seong, K., Schülzgen, A., Khulbe, P., Peyghambarian, N., & Mansuripur, M. (2004). Femtosecond pulsed laser micromachining of glass substrates with application to microfluidic devices. Applied optics, 43(23), 4584–9.

Gomez, D., Goenaga, I., Lizuain, I., & Ozaita, M. (2005). Femtosecond laser ablation for microfluidics. Optical Engineering, 44: 051105-8.

Gong, M. G. (2009) Research on Evolutionary Multi-Objective Optimization Algorithms. Journal of Software, 20(2): p. 271-289.

GREP. *GREP grup de recerca*. Retrieved the 12th of June, 2013, from: http://grep.udg.edu/

Greuters, J., & Rizvi, N. (2002). UV laser micromachining of silicon , indium phosphide and lithium niobate for telecommunications applications. *Proc. SPIE* 4876, Optics and Photonics Technologies and Applications, 479.

Grzenda, M., Bustillo, A. & Zawistowski P., (2012). A soft computing system using intelligent imputation strategies for roughness prediction in deep drilling. Journal of Intelligent Manufacturing, 23(5), 1733-1743.

Grzenda, M., Bustillo, A., Quintana, G. & Ciurana J. (2012). Improvement of surface roughness models for face milling operations through dimensionality reduction. Integrated Computer-Aided Engineering, 19(2), 179-197.

Hayden, C. J. (2010). A simple three-dimensional computer simulation tool for predicting femtosecond laser micromachining structures. Journal of Micromechanical and Microengineering 20: 025010-11.

Heyl, P., Olschewski, T., & Wijnaendts, R. W. (2001). Manufacturing of 3D structures for micro-tools using laser ablation. Microelectronic Engineering, 57-58, 775–780.

Hilton, P. A. (2002). In the beginning… the history of laser cutting. ICALEO Scottsdale, Arizona, USA.

Hu, X., & Eberhart, R. (2002). Multiobjective optimization using dynamic neighborhood particle swarm optimization. Proceeedings of IEEE Swarm Intelligence Symposium, 1404-1411.

Huang, H., Zheng, H. Y., & Lim, G. C. (2004). Femtosecond laser machining characteristics of Nitinol. Applied Surface Science, 228:201–206.

Jandeleit, J., Horn, a, Weichenhain, R., Kreutz, E. & Poprawe, R. (1998). Fundamental investigations of micromachining by nano- and picosecond laser radiation. Applied Surface Science, 127-129, 885–891.

Kaldos, A., Pieper, H. J., Wolf, E., & Krause, M. (2004). Laser machining in die making—a modern rapid tooling process. Journal of Materials Processing Technology, 155-156, 1815–1820.

Karazi, S. M., Issa A., & Brabazon, D. (2009). Comparision of ANN and DoE for the prediction of laser –machined micro-channel dimensions. Optics and Lasers in Engineering, 47:956-964.

Kancharla, V. V., & Chen, S. (2002). Fabrication of biodegradable polymeric devices using laser micromachining. Biomedical Microdevices 4: 105-109.

Karnakis, D., Rutterford, G., Knowles, M., Dobrev, T., Petkov, P., & Dimov, S. (2006). High quality laser milling of ceramics, dielectrics and metals using nanosecond and picosecond lasers. Proc. SPIE 6106, Photon Processing in Microelectronics and Photonics, 610604–610604–11.

Karpat, Y., & Özel, T. (2007). Multi-Objective Optimization For Turning Processes Using Neural Network Modeling And Dynamic-Neighborhood Particle Swarm Optimization. International Journal of Advanced Manufacturing Technology, 35 (3-4) 234-247.

Kathuria, Y. P. (2005). Laser microprocessing of metallic stent for medical therapy. Journal of Materials Processing Technology, 170(3), 545–550.

Khan Malek, C. G. (2006). Laser processing for bio-microfluidics applications (part II). Analytical and bioanalytical chemistry, 385(8), 1362–9.

Klank, H., Kutter, J. P., & Geschke, O. (2002). CO(2)-laser micromachining and back-end processing for rapid production of PMMA-based microfluidic systems. Lab on a chip, 2(4), 242–6.

Kleine, K. F., Whitney, B., & Watkins, K. F. (2002). Use of fiber lasers for micro cutting applications in medical device industry. 21st International Congress on Applications of Lasers and Electro-Optics.

Knowles, M. R. H., Rutterford, G., Karnakis, D., & Ferguson, a. (2007). Micro-machining of metals, ceramics and polymers using nanosecond lasers. The International Journal of Advanced Manufacturing Technology, 33(1-2), 95–102.

Koç, M., Özel, T. (2011). Micro-manufacturing: Design and Manufacturing of Micro-Products. John Wiley & Sons, Inc.

Komlenok, M. S., Kononenko, V. V., Ralchenko, V. G., Pimenov, S. M., & Konov, V. I. (2011). Laser Induced Nanoablation of Diamond Materials. Physics Procedia, 12, 37–45.

Kononenko, T. V., Komlenok, M. S., Pashinin, V. P., Pimenov, S. M., Konov, V. I., Neff, M., Romano, V., et al. (2009). Femtosecond laser microstructuring in the bulk of diamond. Diamond and Related Materials, 18(2-3), 196–199.

Kononenko, T. V., Kononenko, V. V., Pimenov, S. M., Zavedeev, E. V., Konov, V. I., Romano, V., & Dumitru, G. (2005). Effects of pulse duration in laser processing of diamond-like carbon films. Diamond and Related Materials, 14(8), 1368–1376.

Kumar, A., & Gupta, M. C. (2010). Laser machining of micro-notches for fatigue life. Optics and Lasers in Engineering, 48(6), 690–697.

Lauzurica, S., García-Ballesteros, J. J., Colina, M., Sánchez-Aniorte, I., & Molpeceres, C. (2011). Selective ablation with UV lasers of a-Si:H thin film solar cells in direct scribing configuration. Applied Surface Science, 257(12), 5230–5236.

Lee, W.-H., & Ozel, T. (2007). Laser Micro-Machining of Spherical and Elliptical 3-D Objects Using Hole Area Modulation Method. *ASME 2007 International Manufacturing Science and Engineering Conference*, 235–242.

Li, B., Schwarz, T., & Sharon, A. (2006). Implementation of microfluidic devices at a transparency. Journal of Micromechanical and Microengineering, 16: 2649-2645.

Li, C., Nikumb, S., & Wong, F. (2006). An optimal process of femtosecond laser cutting of NiTi shape memory alloy for fabrication of miniature devices. Optics and Lasers in Engineering, 44(10), 1078–1087.

Li, Z L, Chu, P. L., Zheng, H. Y., Lim, G. C., & Simtech, T. (2009). Process Development of Laser Machining of Carbon Fibre Reinforced Plastic Composites. SIMTech technical reports 10, 1.

Li, Z.L., Zheng, H. Y., Lim, G. C., Chu, P. L., & Li, L. (2010). Study on UV laser machining quality of carbon fibre reinforced composites. Composites Part A: Applied Science and Manufacturing, 41(10), 1403–1408.

Lia, C., Nikumbb, S., & Wong, F. (2006). An optimal process of femtosecond laser cutting of NiTi shape memory alloy for fabrication of miniature devices. Optics and Lasers in Engineering, 44, 1078–1087.

Mahdavinejad, R. A., Khani, N., & Fakhrabadi, M. M.S. (2012). Optimization of milling parameters using artificial neural network and artificial immune system. Journal of Mechanical Science and Technology, 26 (12), 4097-4104 .

Marco, C. De, Eaton, S. M., Suriano, R., Turri, S., Levi, M., Ramponi, R., Cerullo, G., et al. (2010). Surface properties of femtosecond laser ablated PMMA. ACS applied materials & interfaces, 2(8), 2377–84.

Malek, C.G.K. (2006). Laser processing for bio-microfluidics applications (part I). Analytical and Bioanalytical Chemistry, 385: 1351-1361.

Malek, C. G. K. (2006). Laser processing for bio-microfluidics applications (part II). Analytical and Bioanalytical Chemistry, 385: 1362-1369.

Mark, D., Haeberle, S., Roth, G., von Stetten, F., & Zengerle, R. (2010). Microfluidic lab-on-a-chip platforms: requirements, characteristics and applications. Chemical Society Reviews, 39(3): 1153-1182.

Martin, D. M., Boyle, F. (2011) Drug-eluting stents for coronary artery disease: A review. Medical Engineering & Physics, 33 148-163

Meng, H., Liao, J., Zhou, Y., & Zhang, Q. (2009). Laser micro-processing of cardiovascular stent with fiber laser cutting system. Optics & Laser Technology, 41(3), 300–302.

Mishra, S., & Yadava, V. (2013). Modeling and optimization of laser beam percussion drilling of thin aluminum sheet. Optics & Laser Technology, 48, 461–474.

Muhammad, N., Whitehead, D., Boor, a., & Li, L. (2010). Comparison of dry and wet fibre laser profile cutting of thin 316L stainless steel tubes for medical device applications. Journal of Materials Processing Technology, 210(15), 2261–2267.

Muhammad, N., Whitehead, D., Boor, a., Oppenlander, W., Liu, Z., & Li, L. (2011). Picosecond laser micromachining of nitinol and platinum–iridium alloy for coronary stent applications. Applied Physics A, 106(3), 607–617.

Nedialkov, N. N., Imamova, S. E., Atanasov, P. a., Berger, P., & Dausinger, F. (2005). Mechanism of ultrashort laser ablation of metals: molecular dynamics simulation. Applied Surface Science, 247(1-4), 243–248.

Nayak, N. C., Lam, Y. C., Yue, C. Y. & Sinha, A. T. (2008). CO2 laser micromachining of PMMA: the effect of polymer molecular weight. Journal of Micromechanical and Microengineering, 18:095020-7.

Ngoi, B. K. ., Venkatakrishnan, K., Lim, E. N. ., Tan, B., & Koh, L. H. . (2001). Effect of energy above laser-induced damage thresholds in the micromachining of silicon by femtosecond pulse laser. Optics and Lasers in Engineering, 35(6), 361–369.

Niino, H., Kawaguchi, Y., Sato, T., Narazaki, A., Ding, X., & Kurosaki, R. (2004). Surface microfabrication of fused silica glass by UV laser irradiation. Photon Processing in Microelectronics and Photonics III, 5339, 112–117.

Nikumb, S., Chen, Q., Li, C., Reshef, H., Zheng, H. Y., Qiu, H., & Low, D. (2005). Precision glass machining, drilling and profile cutting by short pulse lasers. Thin Solid Films, 477(1-2), 216–221.

Petkov, P. V, Dimov, S. S., Minev, R. M., & Pham, D. T. (2008). Laser milling: pulse duration effects on surface integrity. Proceedings of the Institution of Mechanical Engineers, Part B: Journal of Engineering Manufacture, 222(1), 35–45.

Pfeifer, R., Herzog, D., Hustedt, M., & Barcikowski, S. (2010). Pulsed Nd:YAG laser cutting of NiTi shape memory alloys—Influence of process parameters. Journal of Materials Processing Technology, 210(14), 1918–1925.

Pfleging, W., Boehm, J., Finke, S., Gaganidze, E., Hanemann, T., Heidinger, R., & Litfin, K. (2003). Direct laser-assisted processing of polymers for microfluidic and micro-optical applications. Proceedings SPIE, 4977: 346-356.

Pham, D. T., Dimov, S. S., Ji, C., Petkov, P.V., & Dobrev, T. (2004). Laser milling as a 'rapid' micromanufacturing process. Proc Inst Mech Eng Pt B: Journal Engineering Manufacture, 218(1):1-7.

Pham, D. T., Dimov, S. S., & Petkov, P. V. (2007). Laser milling of ceramic components. International Journal of Machine Tools and Manufacture, 47(3-4), 618–626.

Powell, J., Al-Mashikhi, S. O., & Voisey, K. T. (2011). Fibre laser cutting of thin section mild steel: An explanation of the 'striation free' effect. Optics and Lasers in Engineering, 49 1069–1075

Pugmire, D. L., Waddell, E. A., Haasch, R., Tarlov, M. J., & Locascio, L. E. (2002). Surface characterization of laser-ablated polymers used for microfluidics. Analytical Chemistry, 74: 871-878.

Quintana, G., Bustillo, A., & Ciurana, J. (2012). Prediction, monitoring and control of surface roughness in high-torque milling machine operations, International Journal of Computer Integrated Manufacturing, 25(12), 1129-1138.

Raval, A., Choubey, A., Engineer, C., & Kothwala, D. (2004). Development and assessment of 316LVM cardiovascular stents. Materials Science and Engineering A, 386 331–343.

Riveiro, a., Quintero, F., Lusquiños, F., Del Val, J., Comesaña, R., Boutinguiza, M., & Pou, J. (2012). Experimental study on the CO2 laser cutting of carbon fiber reinforced plastic composite. Composites Part A: Applied Science and Manufacturing, 43(8), 1400–1409.

Rizvi, N. H., & Apte, P. (2002) Developments in laser micro-machining techniques. J Mater Process Technol, 127(2):206-210.

Roberts, M. a, Rossier, J. S., Bercier, P., & Girault, H. (1997). UV Laser Machined Polymer Substrates for the Development of Microdiagnostic Systems. Analytical chemistry, 69(11), 2035–42.

Romoli, L., Tantussi, G., & Dini, G. (2011). Experimental approach to the laser machining of PMMA substrates for the fabrication of microfluidic devices. Optics and Lasers in Engineering, 49(3), 419–427.

Saklakoglou, I. E., & Kasman, S. (2011). Investigation of micro-milling process parameters for surface roughness and milling depth. Journal of Advanced Manufacturing Technology, 54:567–578

Samant, A. N., & Dahotre, N. B. (2009). An integrated computational approach to single-dimensional laser machining of magnesia. Optics and Lasers in Engineering, 5;47(5):570-577.

Samant, A. N., & Dahotre, N. B. (2009). Physical Effects of Multipass Two-Dimensional Laser Machining of Structural Ceramics. Advanced Engineering Materials, 11(7), 579–585.

Samant, A. N., Du, B., & Dahotre, N. B. (2009). In-situ surface absorptivity prediction during 1.06 μm wavelength laser low aspect ratio machining of structural ceramics. Physica Status Solidi (a), 206(7), 1433–1439.

Samant, A. N., & Dahotre, N. B. (2010). Three-dimensional laser machining of structural ceramics. Journal of Manufacturing Processes, 12(1), 1–7.

Schuöcker, D., Aichinger, J., & Majer, R. (2012). Dynamic phenomena in laser cutting and process performance. Physics Procedia, 39 179–185.

Scintilla, L. D., Sorgente, D., & Tricarico, L. (2011). Experimental Investigation On Fiber Laser Cutting Of Ti6Al4V Thin Sheet. Journal of Advanced Materials Research, Vols. 264-265 pp 1281-1286.

Scintilla, L. D., & Tricarico, D. (2013). Experimental investigation on fiber and CO2 inert gas fusion cutting of AZ31 magnesium alloy sheets. Optics & Laser Technology, 46 42–52.

Semaltianos, N. G., Perrie, W., Cheng, J., French, P., Sharp, M., Dearden, G., et al. (2010). Picosecond laser ablation of nickel-based superalloy C263. Applied Physics A: Materials Science and Processing, 98(2):345-355.

Shanjin, L., & Yang, W. (2006). An investigation of pulsed laser cutting of titanium alloy sheet. Optics and Lasers in Engineering, 44 1067–1077.

Shikida, M., Yokota, T., Naito, J. & Sato K. (2010). Fabrication of a stent-type thermal flow sensor for measuring nasal respiration. Journal of Micromechanics and Microengineering, 20 055029.

Shuja, S. Z., Yilbas, B. S., & Momin, O. (2011). Laser heating of a moving slab: influence of laser intensity parameter and scanning speed on temperature field and melt size. Optics & Laser Technology, 49 265–272.

Sowa, S., Watanabe, W., Tamaki, T., Nishii, J., & Itoh, K. (2004). Symmetric waveguides in polymethyl methacrylate fabricated by femtosecond laser pulses. Optical Express, 14: 291-297.

Snakenborg, D., Klank, H., & Kutter, J. P. (2004). Microstructure fabrication with a CO 2 laser system. Journal of Micromechanics and Microengineering, 14(2), 182–189.

Srinivas, N., & Deb, K. (1994). Multiobjective Optimization Using Nondominated Sorting in Genetic Algorithms, Evolutionary Computation 2, 3, 221 – 248.

Steen, W. M., & Mazumder, J. (2010). Laser material processing. Springer.

Streltsov, A. M., & Borrelli, N. F. (2002). Study of femtosecond-laser-written waveguides in glasses. Journal of the Optical Society of America B, 19(10), 2496.

Sugioka, K., Meunier, M., & Piqué, A. (2010). Laser precision microfabrication. Springer.

Sullivan, A. B. J. & Houldcroft, P. T. (1967). Gas-jet laser cutting. British Welding Journal, August 443.

Suriano, R., Kuznetsov, A., Eaton, S. M., Kiyan, R., Cerullo, G., Osellame, R., Chichkov, B. N., et al. (2011). Femtosecond laser ablation of polymeric substrates for the fabrication of microfluidic channels. Applied Surface Science, 257(14), 6243–6250.

Suriyage, N. U., Ghantasala, M. K., Iovenitti, P., & Harvey, E. C. (2004). Fabrication, measurement, and modeling of electro-osmotic flow in micromachined polymer microchannels. *Proc. SPIE* 5275, BioMEMS and Nanotechnology, 5275, 149–160.

Tani, G., Tomesani, L., Campana, G., & Fortunato, A. (2004). Quality factors assessed by analytical modelling in laser cutting. Thin Solid Films, 453-454 486-491.

Tawari, G., Sarin Sundar, J.K., Sundararajan, G. & Joshi, S. V. (2005). Influence of process parameters during pulsed Nd:YAG laser cutting of nickel-base superalloys. Journal of Materials Processing Technology, 170 229–239.

Teixidor, D., Ferrer, I., Ciurana, J., & Özel, T. (2013). Optimization of process parameters for pulsed laser milling of micro-channels on AISI H13 tool steel. Robotics and Computer-Integrated Manufacturing, 29(1), 209–218.

Teixidor, D., Orozco, F., Thepsonthi, T., Ciurana, J., Rodríguez, C. a., & Özel, T. (2013). Effect of process parameters in nanosecond pulsed laser micromachining of PMMA-based microchannels at near-infrared and ultraviolet wavelengths. The International Journal of Advanced Manufacturing Technology , 67(5-8), 1651-1664.

Tsai, C.-H., & Chen, H.-W. (2003). Laser milling of cavity in ceramic substrate by fracture-machining element technique. Journal of Materials Processing Technology, 136(1-3), 158–165.

Uriarte, L., Herrero, A., Ivanov, A., Oosterling, H., Staemmler, L., Tang, P. T., et al. (2006) Comparison between microfabrication technologies for metal tooling. Proc Inst Mech Eng Part C, 220(11):1665-1676.

Vázquez, E., Ciurana, J., Rodríguez, C. A., Thepsonthi, T., & Özel, T. (2011) Swarm Intelligent Selection and Optimization of Machining System Parameters for Micro-channel Fabrication in Medical Devices. Materials and Manufacturing Processes, Vol. 26.

Waddell, E. A., Locascio, L.E., & Kramer, G. W. (2002) UV laser micromachining of polymers for microfluidic applications. Journal Association Lab Automation, 7: 78-82.

Waddell, E. A. (2006). Laser ablation as a fabrication technique for microfluidic devices. Methods in molecular biology, 321(1), 27–38.

Wang, C., & Zeng, X. (2007). Study of laser carving three-dimensional structures on ceramics: Quality controlling and mechanisms. Optics & Laser Technology, 39(7), 1400–1405.

Wang, C., Zhang, L., Liu, Y., Cheng, G., Zhang, Q., & Hua, K. (2012). Ultra-short pulse laser deep drilling of C/SiC composites in air. Applied Physics A, 1–7.

Wang, X. C., Zheng, H. Y., Chu, P. L., Tan, J. L., Teh, K. M., Liu, T., Ang, B. C. Y., et al. (2010). High quality femtosecond laser cutting of alumina substrates. Optics and Lasers in Engineering, 48(6), 657–663.

Will, M., Nolte, S., Chichkov, B. N., & Tünnermann, A. (2002). Optical properties of waveguides fabricated in fused silica by femtosecond laser pulses. Applied optics, 41(21), 4360–4.

Yan, Y., Li, L., Sezer, K., Whitehead, D., Ji, L., Bao, Y., & Jiang, Y. (2012). Nano-second pulsed DPSS Nd:YAG laser striation-free cutting of alumina sheets. International Journal of Machine Tools and Manufacture, 53(1), 15–26.

Yilbas, B. S., Akhtar, S. S., & Karatas, C. (2011). Laser trepanning of a small diameter hole in titanium alloy: Temperature and stress fields. Journal of Materials Processing Technology, 211(7), 1296–1304.

Yilbas, B.S., & Abdul Aleem, B. J. (2006). Dross formation during laser cutting process. Journal of Physiscs D: Applied Physics, 39 1451–61.

Yilbas, B. S., Arif, a F. M., & Abdul Aleen, B. J. (2009). Laser cutting of large-aspect-ratio rectangular blanks in thick sheet metal: thermal stress analysis. Proceedings of the

Institution of Mechanical Engineers, Part B: Journal of Engineering Manufacture, 223(1), 063–071.

Yousef, B. F., Knopf, G. K., Bordatchev, E. V., & Nikumb, S. K. (2003). Neural network modeling and analysis of the material removal process during laser machining. The International Journal of Advanced Manufacturing Technology, 22(1-2), 41–53.

Yuan, D., & Das, S. (2007). Experimental and theoretical analysis of direct-write laser micromachining of polymethylmethacrylate by CO2 laser ablation. Journal of Applied Physics, 101:024901-6.

Yung, K. C., Mei, S. M., & Yue, T. M. (2002). A study of the heat-affected zone in the UV YAG laser drilling of GFRP materials. Journal of Materials Processing Technology, 122(2-3), 278–285.

Yung, K. C., Zhu, H. H., & Yue, T. M. (2005). Theoretical and experimental study on the kerf profile of the laser micro-cutting NiTi shape memory alloy using 355 nm Nd:YAG. Smart Materials and Structures, 14(2), 337–342.